The vascular bone marrow niche influences outcome in chronic myeloid leukaemia via the E-selectin - SCL/TAL1 - CD44 axis

Dissertation
Zur Erlangung des Doktorgrades
der Naturwissenschaften

vorgelegt am Fachbereich 14
der Johann Wolfgang Goethe-Universitat
in Frankfurt am Main

von
Parimala Sonika Godavarthy
aus Kakinada, India

Frankfurt (2019)
(D30)

vom Fachbereich Biochem, Chemie und Pharmazie (FB14) der
Johann Wolfgang Goethe-Universität als Dissertation angenommen.

Dekan: Prof. Dr. Clemens Glaubitz

Gutachter: Prof. Dr. Rolf Marschalek
Prof. Dr. Daniela S. Krause

Datum der Disputation:

Die Ergebnisse dieser Arbeit wurden bereits teilweise in folgenden Publikationen veroffentlicht:

Godavarthy PS, Kumar R, Herkt SC, Pereira RS, Hayduk N, Weissenberger ES, Aggoune D, Manavski Y, Lucas T, Pan KT, Voutsinas JM, Wu Q, Müller MC, Saussele S, Oellerich T, Oehler VG, Lausen J, Krause DS. "The vascular bone marrow niche influences outcome in chronic myeloid leukemia via the E-selectin - SCL/TAL1 - CD44 axis". *Haematologica. 2019 Apr 24*. PMID:31018977.

Die Veröffentlichtung in gedruckter und elektronischer Form aller in dieser Dissertation verwendeten Abbildungen erfolgt mit Genehmigung der jeweiligen Rechteinhaber.

DECLARATION

I herewith declare that I have not previously participated in any doctoral examination procedure in mathematics or natural science discipline.

Frankfurt am Main, (Date)
(Signature)

Authors' declaration

I hereby declare that I produced my doctoral dissertation on the topic of

"The vascular bone marrow niche influences outcome in chronic myeloid leukaemia via the E-selectin - SCL/TAL1 - CD44 axis"

independently and using only the tools indicated. In particular, all references borrowed from external sources are clearly acknowledged and identified.

I confirm that I have respected the principles of good scientific practise and have not made use of the services of any commercial agency in respect of my doctorate.

Frankfurt am Main, (Date)
(Signature)

Table of Contents

Zusammenfassung **1**
Summary 6

Introduction **8**
1. Haematopoiesis 9
2. Bone marrow microenvironment 10
3. Leukaemia 12
    - Acute myeloid leukaemia (AML) 13
    - Acute lymphoblastic leukaemia (ALL) 14
    - Chronic lymphoblastic leukaemia (CLL) 14
4. Chronic myeloid leukaemia (CML) 14
    - Phosphoinositide 3-kinase (PI3K) 16
5. Bone marrow microenvironment in leukaemia 17
    - Alterations in BMM leading to haematological malignancies 17
    - Chemo-resistance 19
6. E-selectin 19
7. CD44 21
8. SCL/TAL1 23
9. Targeting of bone marrow microenvironment 24

Hypothesis **27**

Materials and Methods **28**
1. Mice and genotyping 28
2. Drug treatment 30
3. *In vivo* microscopy 30
4. Transplantation 32
    - Primary transplant 32
    - Secondary transplant 34
5. Homing 34
6. Analysis of diseased mice and tumour burden 34
7. Virus production 35
8. Southern Blot 35
9. Maintenance of cell lines 36
10. Immunoprecipitation 36
11. qPCR 37
12. Mass spectrometry 37
13. Chromatin Immunoprecipitaion 38
14. Western Blot 39
    - Preparation of nuclear extracts 39
    - Preparation of whole cell lysate 40
15. *In vitro* adhesion assays 41
16. Immunofluorescence 42
17. Methylcellulose 44
18. FACS 44
    - Membrane molecules 44
    - Cell cycle 44
19. Luciferase assay 45
20. Isolation of hCD34^{+} cells 45

21. Gene expression profiling data and statistical analysis of CML patients 46
22. Analysis and Statistics 47

Results 48
1. GMI-1271 decreases the adhesion of leukaemic cell line to endothelium *in vivo* 48
2. GMI-1271 decreases the adhesion of primary CML cells to endothelium *in vivo* 49
3. Combination therapy of an E-selectin inhibitor with imatinib prolongs survival 51
4. Inhibition of E-selectin leads to decrease in homing and engraftment of LIC 53
5. Inhibition of E-selectin alters the localisation of leukemic cells to endothelium 54
6. Inhibition of E-selectin reduces the adhesion of leukaemia cells and increases *Scl/Tal1* expression 57
7. *SCL/TAL1* regulates the expression of CD44 62
8. *SCL/TAL1* regulates the *CD44* expression at a transcriptional level 64
9. Imatinib increases the binding of SCL/TAL1 to the CD44 regulatory element 66
10. Overexpression of *Scl/Tal1* leads to prolongation of survival in murine CML 68
11. Binding of CD44 to E-selectin might play a role in cell cycle regulation 70
12. Inhibition of E-selectin leads to an increase in cell cycle 72
13. Inhibition of E-selectin changes expression of cell cycle regulators 74
14. A synergistic effect of GMI-1271 and imatinib leads to decreased expression of CD44 77
15. BCR-ABL1 indirectly phosphorylates SCL/TAL1 78
16. Molecular changes in the non-adherent and adherent fractions of the cells to E-selectin 81
17. Secondary transplantation of CML-initiating cells from a GMI-1271 or imatinib treated microenvironment increases aggressiveness of the disease 82
18. Expression of *SCL/TAL1* can act as a prognostic factor in human patients with CML 87
19. Significance of *SCL/TAL1* and *CD44* expression in the different phases of CML 88
20. Dual inhibition of CXCR4 and E-selectin 90

Discussion 92
1. The vascular niche offers chemo-protection to cancer stem cells 92
2. Targeting the vascular niche in haematological malignancies and solid tumours 93
3. Targeting the BMM alters the localisation of CML stem cells in the BMM and influences the cell cycle status 93
4. SCL/TAL1 regulates expression of CD44 94
5. BCR-ABL1 phosphorylates SCL/TAL1 via pAKT 96
6. Exposure of leukaemia cells treated with GMI-1271 and imatinib to a new microenvironment increases the aggressiveness of the disease 97
7. Targeting E-selectin and CXCR4 in combination with BCR-ABL1 inhibition may provide a better targeting strategy for CML 98
8. Correlation between *SCL/TAL1* and *CD44* in human patients 99

Conclusion 100

List of abbreviations 101

References 103

Acknowledgements 112

Curriculum Vitae 113

Zusammenfassung

Das Knochenmarksmikromilieu (KMM) besteht aus unterschiedlichsten Nischenzellen, darunter mesenchymale Stromazellen (MSZ), Osteoblasten, Zellen des Nervensystems, persivaskuläre und endotheliale Zellen, Adipozyten und viele weitere. Diese liefern unter anderem Signale zur Regulation und Unterstützung der Produktion und Differenzierung von verschiedenen Blutzellen und stellen damit die Aufrechterhaltung der Homöostase sicher. Veränderungen in der Interaktion zwischen hämatopoetischen Zellen und dem Mikromilieu kann die Entstehung von hämatologischen Erkrankungen befördern und verursachen. Es ist daher bedeutsam, die komplexen Veränderungen im Progress von gesunder zu maligner Nische zu verstehen und diese Erkenntnisse zur Entwicklung neuartiger Therapien zu verwenden. Im Fall von Leukämien bietet das Knochenmarksmikromilieu, insbesondere die enossale Nische, einen Zufluchtsort für leukämische Zellen, wodurch leukämische Stammzellen (LSZ) vor Chemotherapie geschützt werden. Bei Erkrankungen an CML führt Imatinibmesilat als Standardmedikament in der Chemotherapie dieser Leukämieform in den meiste Fällen zu einer Remission der Erkrankung. Allerdings entwickeln manche Patienten ein Rezidiv, möglicherweise durch ein von dem KMM unterstützten Fortbestehen leukämischer Stammzellen.

In der vaskulären Nische exprimieren endotheliale Zellen E-Selectin, welches bekanntermaßen mit Liganden auf leukämischen Zellen interagiert. So interagiert E-Selectin unter anderen mit CD44, einem Adhäsionsmolekül, welches üblicherweise in CML-LSZ überexprimiert wird. Experimente an Mäusen konnten die wichtige Rolle von E-Selectin und CD44 für das Auffinden der Knochenmarksnische („Homing“) und Einnisten von LSZ bei CML *in vivo* zeigen; die Abwesenheit von CD44 oder E-Selectin verlängerte das Überleben

der Mäuse. Es ist bekannt, dass E-Selectin eine Rolle in der Metastasierung von Brutkrebsspielt und im Fall von multiplem Myelom und AML auf maligne Zellen *in vivo* protektiv wirkt. In verschiedenen Pathologien wie dem multiplen Myelom bot E-Selectin Resistenz gegen multiple Myelomzellen, und die Hemmung des E-Selectin-Rezeptors und des Liganden verbesserte das Überleben von Mäusen. Andererseits ist auch bekannt, dass Brustkrebszellen von E-Selectin abhängen, um zum Knochen zu gelangen.

Unserer Hypothese nach kann das gezielte Eingreifen in das Mikromilieu durch die Blockade der Interaktion von CML-initiierenden Zellen mit E-Selectin zusätzlich zur Therapie mit Imatinib das Überleben verbessern. Die Behandlung mit GMI-1271, einem niedermolekularen Antagonisten von E-Selectin führte zur verringerten Adhäsion von CML-Zelllinien und primären humanen CML-Zellen an E-Selectin *in vivo* und *in vitro*. Die Behandlung von an CML erkrankten Mäusen mit GMI-1271 in Kombination mit Imatinib verlängerte das Überleben der Mäuse, verglichen zur alleinigen Standardtherapie mit Imatinib, und senkte deren Tumorlast. Wir konnten beobachten, dass sich CML-initiierende Zellen in größerem Abstand vom Endothel aufhalten, wenn eine Therapie mit GMI-1271 gemeinsam mit Imatinib, im Gegensatz zur alleinigen Therapie mit Imatinib, gewählt wurde. Dies legt nahe, dass die Lokalisation der CML-initiierenden Zellen im Knochenmarksmikromilieu durch die Kombinationsbehandlung beeinflusst wurde. Es wurde zuvor gezeigt, dass Endothelzellen Ruhe induzieren können, und da Imatinib nur auf die zyklischen Zellen abzielen kann, deuten unsere Daten darauf hin, dass eine Nichtbindung an Endothel und daher eine Lokalisierung von Leukämiezellen weiter vom Endothel entfernt möglicherweise zu einer besseren Zielausrichtung von LIC mit Imatinib geführt hat. Verschiedene *in vitro* Adhäsionsuntersuchungen bestätigten, dass die Unterdrückung der Interaktion von CML-Zellen mit E-Selectin durch GMI-1271 zu einer erhöhten Expression des hämatopoetischen Transkriptionsfaktors Scl/Tal1 auf mRNA- und Proteinebene führte.

Die erhöhte Scl/Tal1-Expression war spezifisch für die Nicht-Adhäsion an E-Selectin. CD44, ein Adhäsionsmolekül, wird bekanntermaßen in BCR-ABL1+ Zellen überexprimiert. Dieser Zusammenhang brachte uns zu unserer Hypothese, dass Scl/Tal1 eine Rolle in der Kontrolle der CD44-Expression spielen könnte. Diverse Knockdown-Experimente an SCL/TAL1 in K562, einer CML-Zelllinie, führten zu einer erhöhten Expression von CD44. Massenspektrometrische Analysen bestätigten, dass der Knockdown von SCL/TAL1 zur Hochregulation von CD44 führte. Unsere Daten zeigen eine negative Korrelation von SCL/TAL1 und CD44. Darüber hinaus zeigten ChIP-Experimente, dass Scl/Tal1 an das regulatorische Element von CD44 bindet und dadurch dessen Expression negativ beeinflusst. Die Behandlung mit Imatinib verstärkt diese Bindung an das regulatorische Element. Eine Überexpression *in vivo* von SCL/TAL1 in BCR-ABL1-Zellen führte zu einer Verlängerung des Überlebens der untersuchten Mäuse. Unsere Daten legen darüber hinaus nahe, dass die Kombinationstherapie durch GMI-1271 und Imatinib, im Vergleich zur alleinigen Therapie mit GMI-1271 oder Imatinib, die Expression von CD44 reduziert. Folglich verändert die Unterdrückung der Interaktion von E-Selectin und CML-LSZ durch GMI-1271 und Imatinib die Lokalisation der CML-initiierenden Zellen relativ zum Endothel und verlängert das Überleben *in vivo*. Die Behandlung mit GMI-1271 löst molekulare Veränderungen aus, erhöht Scl/Tal1 und damit die Scl1/Tal1-abhängige CD44-Regulation.

Darüber hinaus ist bekannt, dass E-Selectin den Zellzyklus von HSZ beeinflusst, indem es die Proliferation während der Hämatopoese auch im gesunden Organismus unterstützt. Daher erhöht die sowohl die alleinige Behandlung mit GMI-1271 als auch die Kombinationstherapie von Imatinib und GMI-1271 die G2-S-M-Phase im Zellzyklus nicht-adhärenter Zellen *in vitro* und *in viv*o. Dies legt nahe, dass die Blockade der Interaktion mit E-Selectin den Zellzyklus bei CML im Gegensatz zu HSZ erhöht. Dieser beschleunigte Zellzyklus war mit Veränderungen an Zellzyklusregulatoren verbunden, so wurde sowohl

eine erhöhte Aktivität von CDK4 als auch eine verringerte Expression von p16 beobachtet. Wir konnten Veränderungen in sowohl non-adhärenten als auch adhärenten Zellen nach Bindung an E-Selectin aufdecken, während Veränderungen des Zellzyklus und der CD44-Expression hauptsächlich in non-adhärenten Zellen zu sehen sind. Diese Daten liefern vorläufige Ergebnisse, dass sich nicht adhärente Zellen und adhärente Zellen mechanistisch unterscheiden können und dass die Adhäsion zwischen Leukämie-Stammzellen und der Nische eine Rolle bei der Chemoprotektion spielen kann.

BCR-ABL1 ist eine konstitutiv aktives Tyrosinkinase, die diverse nachgelagerte Zielproteine phosphoryliert. Wir konnten zeigen, dass die Phosphorylierung von SCL/TAL1 durch BCR-ABL1 über den Phosphoinositid-3-Kinase-Signalweg gesteuert wird. Zusammen betrachtet, reduziert die Blockade von BCR-ABL1 durch Imatinib die Phophorylierung von AKT und damit von Phospho-SCL/TAL1, steigert dessen Aktivität und lässt damit SCL/TAL1 vermehrt an das regulatorische Element von CD44 binden, wodurch dessen Aktivität wiederum negativ beeinflusst wird. Diese Erkenntnis stellt somit eine Verbindung zum bisher unbekannten Mechanismus der Phosphorylierung von SCL/TAL1 durch BCR-ABL1 da.

Wie E-Selectin wurde der Chemokinrezeptor CXCR4 vorwiegend in HSCs und auch in CML untersucht. CML-Zellen, die CXCR4 exprimieren, weisen eine bessere Migration und Adhäsion an der Nische auf. CML Studien, in denen CXCR4 durch AMD3100 inhibiert wurde, haben erfolgreich gezeigt, dass diese Inhibition die protektive Natur des Stromas überwindet Es ist bekannt, dass GMI-1359, ein Nachfolger von GMI-1271, E-Selectin und CXCR4 in Kombination angreift. Die zweifache Blockade von sowohl E-Selectin als auch CXCR4, einem mit CML-LSZ in Verbindung stehenden Chemokin-Rezeptor, durch GMI-1359 zeigte einen Trend in Richtung verlängerten Überlebens *in vivo*. Humane Patientendaten zeigen eine negative Korrelation von SCL/TAL1 und CD44 in Fällen von

CML. Patienten mit einer hohen Expression von SCL/TAL1 zeigen ein besseres Rezidiv-freies Überleben.

Zusammenfassend lässt sich zeigen, dass E-Selectin in der vaskulären Nische den Verbleib von LSZ in der Ruhephase ermöglicht und daher eine Behandlung mit GMI-1271 die Dislokation aus dieser Nische und einen beschleunigten Zellzyklus bewirkt. Dies erhöht die Anfälligkeit gegenüber Imatinib. Die Regulation der CD44-Expression durch SCL/TAL1, den AKT-Signalweg und ein Onkogen lassen molekulare Veränderungen in leukämischen Stammzellen vermuten, die eine Loslösung aus der Nische bewirken. Unsere Arbeit konnte molekulare Signale, welche die Interaktion zwischen leukämischen Zellen und dem Mikromilieu regulieren, aufzeigen und Erkenntnisse liefern, wie eine Beeinflussung der Nische sowohl die Entstehung als auch die Therapie von malignen Erkrankungen unterstützen kann.

Summary

The bone marrow microenvironment comprises of niche cells namely mesenchymal stromal cells (MSCs), osteoblasts, neuronal cells, adipocytes, and perivascular stromal cells, endothelial cells etc. which provide signals regulating and supporting the production of the blood cells necessary to maintain homeostasis[1]. Alteration in interaction between hematopoietic cells and microenvironment can give rise to haematological malignancies. In leukaemia, including chronic myeloid leukaemia (CML), the bone marrow microenvironment provides sanctuaries to leukaemia cells, thereby protecting the leukaemia stem cells (LSCs) from chemotherapy[2]. In CML, imatinib mesylate a standard chemotherapeutic drug used for treatment majorly results in remission of disease [3]. However, some patients may develop relapse possibly due to persistence of LSCs, partially protected by BMM. In vascular niche, endothelial cells express E-selectin molecule, which is known to interact with ligands present on leukaemia cells [4]. For example, E-selectin interacts with CD44, an adhesion molecule commonly overexpressed on CML LSCs. Studies have reported the essential role of E-selectin and CD44 in homing and engraftment of LSCs in CML *in vivo* [5,6].

We hypothesized that targeting the microenvironment by inhibiting the interaction of CML initiating cells to E-selectin and treatment with tyrosine kinase inhibitor can improve the survival. Treatment with GMI-1271, a small molecule antagonist to E-selectin resulted in reduced adhesion of murine and human CML cells to E-selectin *in vivo* and *in vitro.* Treatment of CML mice with GMI-1271 in combination with the tyrosine kinase inhibitor imatinib prolonged survival of mice compared to treatment with imatinib with a decrease in tumor burden. Several *in vitro* adhesion assays confirmed inhibition of interaction of CML cells to E-selectin by GMI-1271, which led to an increased expression in haematopoietic transcription factor *Scl/Tal1* in leukaemia initiating cells. The increase in *Scl/Tal1* expression

was specific to non-adhesion to E-selectin. These data led us to hypothesize that *Scl/Tal1* might be playing role in controlling expression of CD44. Several knockdown experiments of SCL/TAL1 in CML cell lines increased the expression of CD44. In addition, ChIP experiments revealed that SCL/TAL1 can bind to CD44 regulatory element thus negatively regulating its expression. Moreover, E-selectin is known to regulate HSC cell cycle by maintaining its proliferation in normal haematopoiesis[7]. However, in our study, treatment with GMI-1271 alone or with imatinib increased G2-S-M phase of cell cycle in non-adherent cells *in vitro* and *in vivo* suggesting inhibition of interaction with E-selectin increases cell cycle in CML cells, in contrast to HSCs. Furthermore, BCR-ABL1 is constitutively active tyrosine kinase enzyme which phosphorylates several downstream targets. We have revealed phosphorylation of SCL/TAL1 is regulated by BCR-ABL1 via PI3K kinase pathway. Taken together, inhibition of BCR-ABL1 activity by imatinib reduces phosphorylation of AKT and thus phospho SCL/TAL1, which increases its activity and hence SCL/TAL1 can bind to CD44 regulatory element negatively regulating its expression. The human patient data also suggests a negative correlation between *SCL/TAL1* and *CD44* in CML. Additionally, patients expressing high *SCL/TAL1* have better relapse free survival. Our studies implicate negative correlation between SCL/TAL1 and CD44.

In summary, it suggests that the vascular niche, E-selectin can maintain quiescence of LSC and dislocation from the niche by treatment with GMI-1271 and can increase cell cycle status of LSC and alter localization in the niche making it vulnerable for imatinib. Our work demonstrates molecular signals that govern the interaction between leukaemia cells and the microenvironment and how modulating the niche can improve development and treatment of malignancies.

Keywords: Bone marrow microenvironment, vascular niche, E-selectin, SCL/TAL1, CD44, PI3K pathway, GMI-1271, imatinib.

Introduction

1. Haematopoiesis

Haematopoiesis is the process of production of all cellular components of blood cells. Initial haematopoiesis termed primitive haematopoiesis occurs in the yolk sac in embryos which is considered a primitive site [8]. The main function of primitive haematopoiesis is to supply red blood cells (RBC) helping tissue oxygenation during growth of the embryo. Primitive haematopoiesis is a transient process that later becomes definitive or adult haematopoiesis [9]. In mammals, the next site is the aorta gonad mesonephros (AGM) and placenta [10,11]. Subsequent colonisation by HSC occurs in fetal liver, thymus and bone marrow.

In the human and murine system, the origin of all blood cells in the hematopoietic system is believed to lie in haematopoietic stem cells (HSC) that have self-renewal capacity and give rise to multipotent progenitors (MPPs) which ultimately lose self-renewal potential and differentiate into cells of the various lineages. [12,13]. In broadly classified terms, MPPs further give rise to oligo-potent progenitors which are called common lymphoid and myeloid progenitors (CLPs and CMPs, resp.). All progenitor populations have restricted lineage commitment: CMPs give rise to megakaryocyte/erythrocyte progenitors (MEPs), granulocyte/macrophage progenitors (GMPs), and dendritic cell (DC) progenitors, CLPs give rise to T cell progenitors, B cell progenitors, natural killer (NK) cell progenitors and DC progenitors. Notably, DC progenitors could be derived from both CMPs and CLPs. This phenomenon is called the hematopoietic hierarchy [14 15]. The hematopoietic hierarchy is known to exist within a system where there is tight regulation, mediated by growth factors, transcription factors (TF) or cytokines controlling the fate of cells. TFs like Runt-related transcription factor 1 (RUNX1), GATA binding protein 1 (GATA1), MLL, PU.1, CCAAT enhancer binding protein alpha (CEBP α), T-cell acute leukemia 1/ Stem cell leukemia (TAL1/SCL) and LIM domain only 1 (LMO2), Ikaros and several growth factors like

Granulocyte colony stimulating factor (G-CSF), erythropoietin (EPO), thrombopoietin (TPO) and Interleukin (IL3) regulate self-renewal and differentiation of HSCs and progenitors [15,16]. Transcription factors like SCL/TAL1, RUNX1, GATA1, MLL are involved to regulate the self-renewal capacity of HSC [17,18]. TFs play an important role in lineage priming, a process by which HSCs maintain a low level of lineage-associated genes [19]. However, in committed progenitors, the surface expression of certain markers are consistent and defined.

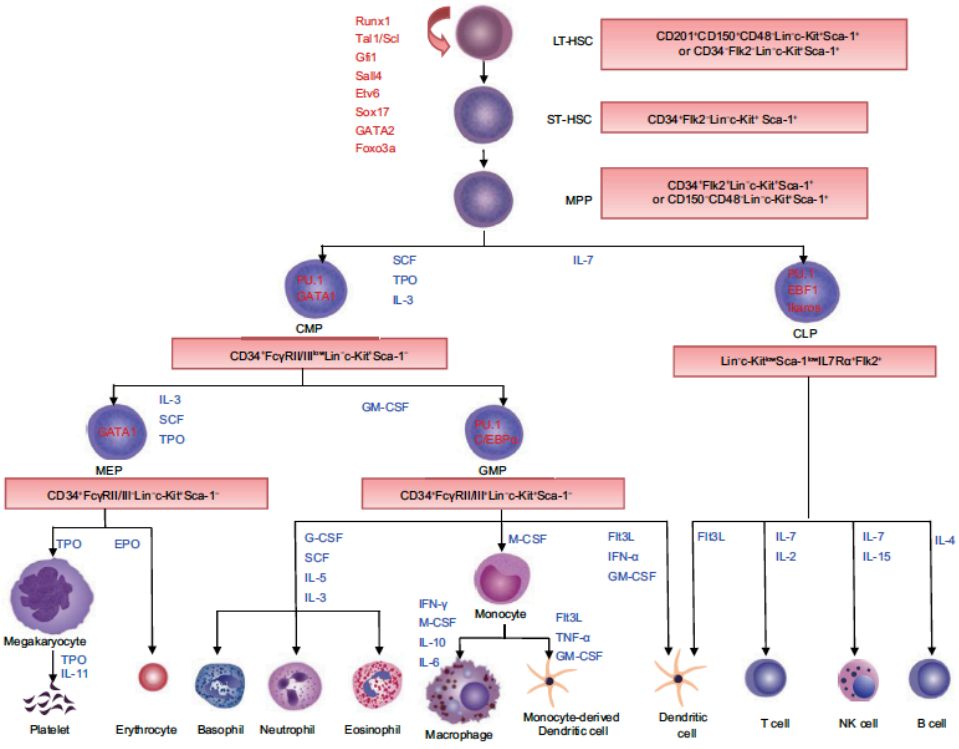

Figure 1: The classical model of the hematopoietic hierarchy showing differentiation of HSC to committed progenitors and mature cells [20]

Although the classical model of haematopoiesis is useful for understanding the differentiation of HSCs, this model is simplified and based on surface markers and bulk transplantation studies [20]. Recent technological advances and genetic mouse models have challenged this concept in past years and new types of HSPCs have been studied due to their lineage bias. For example, studies have shown that MPPs can be divided into MPP1, MPP2,

MPP3, MPP4 according to immune phenotype, lineage bias and abundance in bone marrow [21,22]. MPP1 is more similar to ST-HSCs known to have multi-lineage potential, but MPP2 is megakaryocyte biased, MPP3 is myeloid biased whereas MPP4 is lymphoid primed. HSC generate all three MPPs but no MPPs generate other MPPs *in vivo*. Thus, MPPs are heterogeneous populations with different lineage potential. Single cell RNA sequencing and bioinformatics on human HSPCs suggests a model in which acquisition of lineage specific fates is a continuous process and uni-lineage restricted cells come from low primed undifferentiated HSPCs without any major multi- or bi-potent stages [23].

Another study suggested that a continuum of progenitors executes myeloid and lymphoid differentiation rather than uni-lineage progenitors being present downstream of stem cells [24]. Indeed, various studies support the idea that the hematopoietic hierarchy is more complicated than in the classical model and new approaches are being developed to re-design a new hierarchy of haematopoiesis [20].

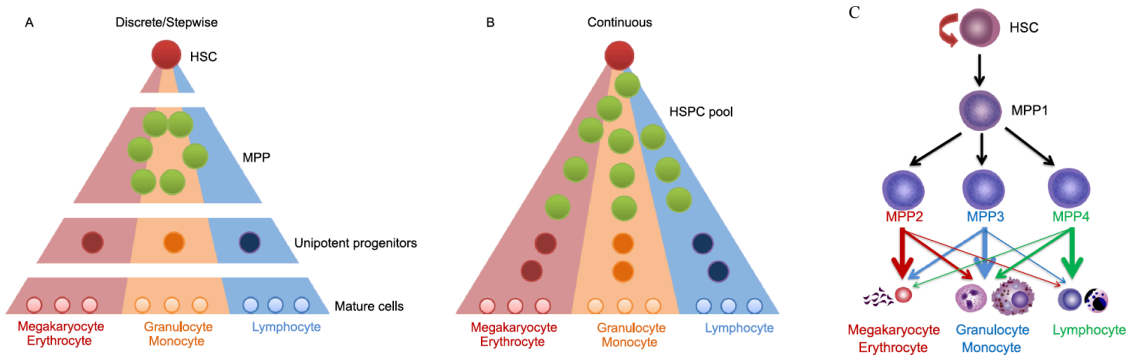

Figure 2: The discrete (A) and continuous (B) hematopoietic differentiation model. C) Revised model of differentiation of MPPs into lineage committed cells [20]

2. Bone marrow microenvironment

The bone marrow microenvironment (BMM) is the 'domicile' of normal hematopoietic stem cells and their malignant counterparts [1]. The BMM comprises of various cell types such as osteolineage cells, osteoblasts, osteoclasts, mesenchymal stem cells (MSC), arteriolar and sinusoidal endothelial cells, adipocytes, CXCL-12 abundant reticular cells (CAR),

macrophages, neurons, as well as the extracellular matrix (ECM), cytokines and other factors, such as the oxygen tension and shear forces. The interplay between these various factors control the fate of HSC [25]. The niches can be categorised formally and broadly into a vascular and an endosteal niche which are important for different functions of HSC.

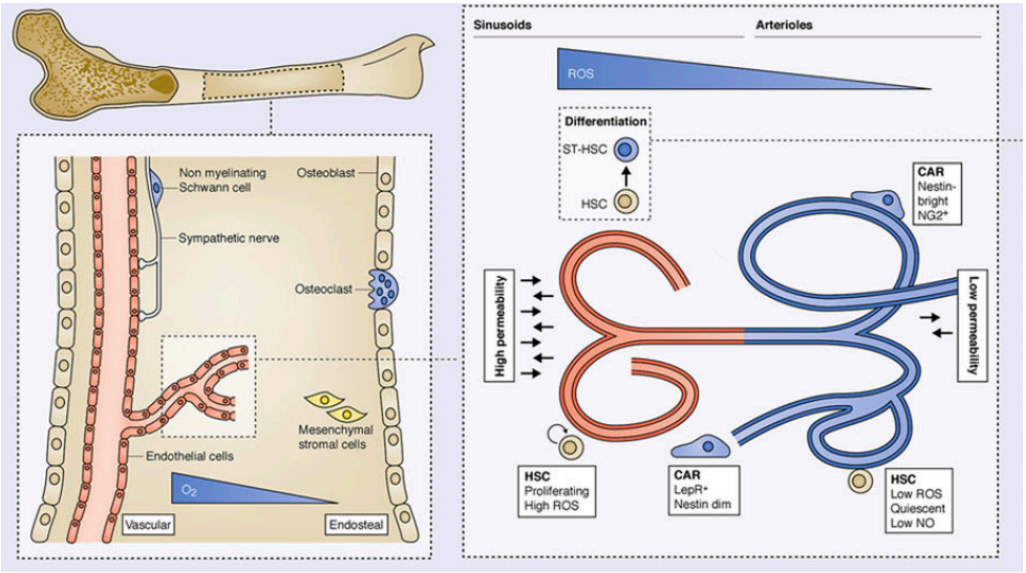

Figure 3: Components of bone marrow microenvironment [1].

However, controversies in the field continue to challenge the existence of distinct niches or their classification [26–29]. Hematopoietic stem and progenitor cells (HSPCs) reside inside the bone marrow, with their location in the niche appearing to be dependent on their maturation state [30] and/or their activity [31]. HSC are known to be located closer to arterioles maintaining their quiescence, and in response to stress HSCs move away from arterioles and induce HSC proliferation [32]. Furthermore, low permeability of arterioles and low reactive oxygen species (ROS) appear to result in maintenance of HSC quiescence and high permeability of sinusoids and higher levels of ROS correspond to differentiation of HSC [33,34]. Similarly, increased nitric oxide (NO) in the bone marrow vasculature leads to HSC mobility and lower levels of NO mediating decreased mobility [35].

Studies indicate that endothelial cells support HSC maintenance by providing factors like C-X-C ligand (CXCL12), stem cell factor (SCF), angiopoietin, fibroblast growth factor (FGF2). E-selectin, a receptor expressed on endothelial cells supports HSC function as deletion of E selectin leads to quiescence of HSC [7]. Several *in vitro* and *in vivo* models support the concept that sinusoidal endothelial cells regulate haematopoiesis, in part by release of soluble factors and anatomic proximity of $CD150^+$ $CD244^-$ $CD48^-$ Lin^- HSC to BM sinusoidal vessels [29].

Mesenchymal stromal cells (MSCs) are a heterogeneous self-renewing population of cells defined by a set of markers, like nestin [36], neural-glial antigen (NG)-2 [32] or leptin receptor [37] and are enriched closer to the vasculature. MSC give rise to different lineages including osteoblasts, the bone forming cells, adipocytes, the fat cells, or chondrocytes, which are cartilage forming cells [38]. $Nestin^+$ MSCs are spatially associated with HSCs and express HSC maintenance genes whereby deletion of $Nestin^+$ MSC was associated with a reduction of HSCs [36].

The endosteum lies between bone and bone marrow comprising of osteoblasts and osteoclasts affecting haematopoiesis. Another important component is the extracellular matrix which is consists of various structural proteins, non-collagenous proteins and growth factors. For example, fibronectin, a key component in the ECM is known to be important for cellular adhesion and proliferation of hematopoietic progenitors [39].

3. Leukaemia

Leukaemia is a malignancy found in children and adults that occurs when alterations in normal cell regulatory processes cause uncontrolled proliferation of hematopoietic stem cells or specific precursors in the bone marrow. The four major types based on whether the disease is of the myeloid or lymphoid lineage, and whether the course is acute or chronic are: acute lymphoblastic leukaemia (ALL), chronic lymphocytic leukaemia (CLL), acute myeloid

leukaemia (AML) or chronic myeloid leukaemia (CML). Notably, ALL occurs more often in children, whereas other subtypes are more common in adults [40].

- **Acute myeloid leukaemia (AML)**

AML is a heterogeneous disorder defined by clonal expansion of myeloid progenitors (blasts) in the bone marrow and peripheral blood and possibly other organs. Its incidence is highest in elderly patients where treatment of patients above age 60 remains poor [41]. Recent reports have revealed that the disorder arises from a series of recurrent alterations in hematopoietic stem cells or progenitor cells which occur with increase in age. This phenomenon called clonal evolution has been found to originate in both founding clones and novel sub-clones [42]. Chromosomal abnormalities (deletions, translocations) are identified in 52% of AML patients [43]. Notably, about 40-50% cases are cytogenetically normal (CN-AML) when assessed by conventional analysis [44]. A deep study of gene expression is currently used to classify AML subtypes. The genetic landscape of AML is defined due to driver mutations which are responsible for the initiation of the abnormality together with passenger mutations turning the abnormality into a disorder [45]. *Nucleophosmin 1 (NPM1)* mutations are the most frequent. The expression of this protein is cytoplasmic rather than nuclear, stimulating leukaemia development [46,47]. Mutations in the *DNA methyltansferase 3A (DNMT3A)* gene occurs in 18–22% of all AML cases and about 34% of CN-AML. The most common are the arginine codon 882 (R882-DNMT3A) mutations causing a defect in normal haematopoiesis and methylation [48,49]. Recently, DNMT3A mutations have been identified as pre-leukemic mutations in the clonal evolution of AML, arising early during AML evolution and persisting in times of remission [50]. Mutations in the gene encoding the tyrosine kinase *FLT3*, i.e. internal tandem duplications (ITD) in the juxta-membrane (JM) domain or in the second tyrosine kinase domain (TKD) of the gene have been found in 20% of all AML cases [51]. Both types of mutations are responsible for activation of FLT3

signalling, promoting blast proliferation. Other mutations of importance include mutations in the *isocitrate dehydrogenase (IDH)* 1 and 2 gene, which are gain-of-function/oncogenic mutations causing loss of physiologic enzyme function, and mutations in *ten–eleven translocation oncogene family member 2 (TET2)* representing loss of function mutations [52,53].

- **Acute lymphoblastic leukaemia (ALL)**

Acute lymphoblastic leukaemia (ALL) is a malignant transformation and proliferation of lymphoid progenitor cells in the bone marrow or blood. The incidence of B cell-ALL is higher in children than adults. In paediatric patients, several syndromes such as Down syndrome or Fanconi anaemia have been associated with ALL [54,55]. In the majority of cases, the leukaemia is due to chromosomal aberrations like ETV6-RUNX1, TCF3-PBX1, BCR-ABL1 and rearrangement of MLL or hyperploidy [56].

- **Chronic lymphoblastic leukaemia (CLL)**

Chronic lymphocytic leukaemia (CLL) is a leukaemia affecting adults which is characterised by an accumulation of small mature B lymphocytes in blood, bone marrow and lymph nodes. It occurs most commonly due to mutations in oncogenes and tumour suppressors such as TP53 due to chromosomal aberrations, and hypermutation of heavy chain genes (IGHV) [57].

4. Chronic myeloid leukaemia (CML)

Chronic myeloid leukaemia is a clonal haematopoietic stem cell disorder characterised by a reciprocal translocation between the long arms of chromosomes 9 (ch9) and 22 (ch22) giving rise to the fusion gene *BCR-ABL1*, the Philadelphia chromosome. The translocation results in an oncogenic BCR-ABL1 protein which is a consecutively active tyrosine kinase protein [58,59]. The discovery of the Philadelphia (Ph) chromosome in the 1960s was the first chromosomal abnormality detected which was a breakthrough in cancer biology. The *ABL*

gene located is on chromosome 9, the human homologue of the v-abl oncogene carried by the Abelson murine leukemia virus (A-MuLV), and it behaves as a non-receptor tyrosine kinase [60]. ABL protein has a complex role in integrating signals from various extracellular and intracellular sources and this influences decisions regarding cell cycle and apoptosis [61,62]. The 160 kDa BCR protein on chromosome 22 is ubiquitously expressed [60]. The first N-terminal exon is known to encode a serine–threonine kinase. The breakpoints within the *ABL* gene at 9q34 can occur anywhere at its 5' end, either upstream of the first alternative exon Ib or downstream of the second alternative exon Ia. Break- points within BCR localize to 1 of 3 so-called breakpoint cluster regions (bcr). This fusion gene is transcribed into *BCR-ABL1* mRNA, and translated into the BCR-ABL1 protein. Depending on the precise location of fusion, the molecular weight of the protein can range from 185 to 210 kDa [63].

The *BCR-ABL1* gene codes for a constitutively active protein. Due to its auto-phosphorylation ability, there is a marked increase of phosphorylation on tyrosines in BCR-ABL1 itself, which generates binding sites for the SH2 domains of other proteins. Generally, substrates of BCR-ABL1 can be categorised according to their physiologic role into adapter molecules (such as CRKL and $p62^{DOK}$), proteins associated with the organization of the cytoskeleton and the cell membrane and proteins with catalytic function. Interestingly, CRKL is the major tyrosine-phosphorylated protein in CML neutrophils, whereas phosphorylated $p62^{DOK}$ is predominantly found in early progenitor cells [64,65].

To target the constitutively active tyrosine kinase, synthetic compounds were developed with chemical structures capable of competing with adenosine triphosphate (ATP) or proteins for binding in the catalytic site [66]. One of the major advancements in chemotherapy and targeted therapy is development of STI571 -2-phenlyaminopyrimidine, commonly known as imatinib mesylate [67].

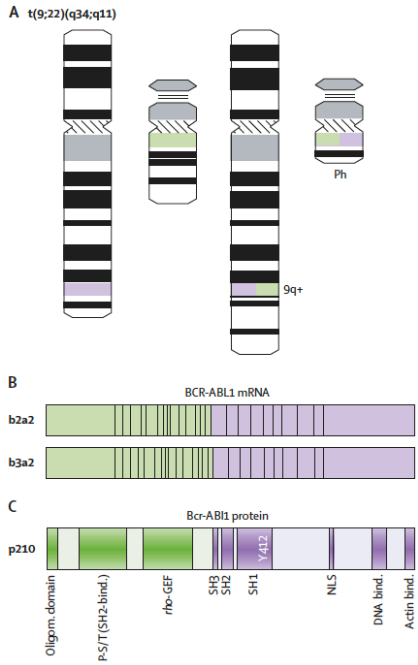

Figure 4: Pathophysiology of CML [68]

In theory, binding of ATP to its pocket allows BCR-ABL1 to phosphorylate tyrosine residues on its substrates. The synthetic ATP mimic STI571 fits the pocket by competing with ATP and not allowing the transfer of the phosphate group to its substrate.

Three BCR-ABL1 driven major mechanisms have been implicated in the malignant transformation by BCR-ABL1, like constitutively active mitogenic signalling (Ras and the MAP kinase, JAK-STAT pathway, PI3 kinase pathway, Myc pathway), altered adhesion molecules and extracellular matrix and reduced apoptosis [3].

- **Phosphoinositide 3- kinase (PI3K)**

The presence of BCR-ABL1 protein enhances cell proliferation. One of its downstream pathways includes PI3 kinase whose activity is required for the proliferation of BCR-ABL–positive cells [69].

BCR-ABL1 protein forms complexes with PI3 kinase, CBL, and the adapter molecules CRK and Crk like protein (CRKL), which activate PI3 kinase [70]. The next downstream substrate in this cascade appears to be the serine–threonine kinase AKT [71].

Studies showed that AKT lies downstream of the IL-3 receptor and identified the pro-apoptotic protein phosphorylated BCL-2 associated agonist of cell death (BAD) as a key

substrate of AKT [72]. BAD is inactive due to its inability to bind anti-apoptotic proteins such as B-cell lymphoma (BCL_{XL}) and it is trapped by cytoplasmic 14-3-3 proteins. This underlines the role of BCR-ABL1 in promoting anti-apoptosis.

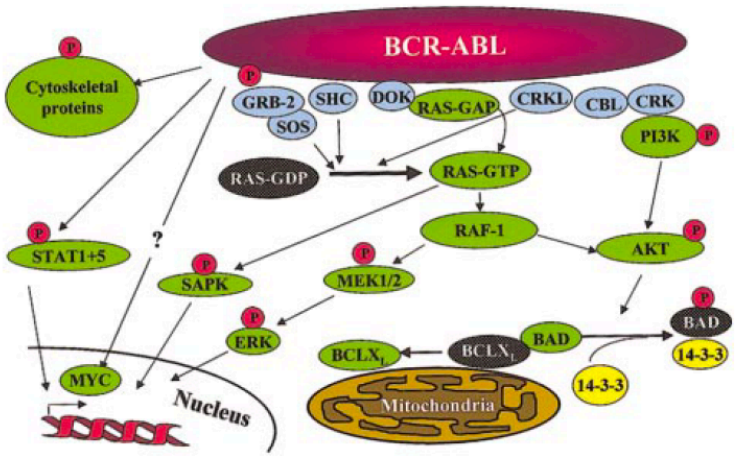

Figure 5: Signalling of BCR-ABL1[3]

5. The bone marrow microenvironment (BMM) in leukaemia

Several studies provided evidence for the support of malignant haematopoiesis and chemotherapy resistance by the BMM. Leukaemia cells or leukaemia stem cells (LSCs) not only impact the BMM but are also, reciprocally, influenced by the BMM, although in a different way from HSCs. LSCs can influence the BMM making it more hospitable for leukaemia and less for HSC [73–75]. It can also serve as an origin for leukaemia relapse due to protection of LSC [2].

- **Alterations in BMM leading to haematological abnormalities**

Pioneering studies demonstrated that mice deficient for retinoic acid receptor gamma (RAR gamma), a receptor for a nuclear hormone, had a myeloproliferative phenotype [76]. Furthermore, loss of retinoblastoma (Rb) gene in the niche led to myeloproliferation [77]. Also, absence of Dicer1, an mRNA processing enzyme, in osteoprogenitor cells led to

myelodysplastic syndrome (MDS) developing later to AML in few mice [78] . *Ptpn11* mutations exclusively in MSC and osteoprogenitor cells led to MPN in children and adults with increased levels of C-C motif chemokine ligand (CCL3) [79]. MSC-specific expression of *Cxcl12* is known to control quiescent treatment-resistant leukaemia stem cells [80]. E-selectin expressed on endothelial cells is known to mediate engraftment of LIC in CML and is upregulated in AML providing chemo-resistance in vascular niche [6,81]. Moreover, rapid remodelling of the endosteal niche leads to depletion of osteoblastic cells and impairment of normal HSC in T-ALL [82].

Several adhesion molecules expressed on leukaemia cells have been shown to regulate specific interactions with the niche promoting the development of disease. For example, CD44 is a cell surface glycoprotein interacting with ECM proteins such as hyaluronan, osteopontin and the endothelial receptor E-selectin [83]. In CML, CD44 expression on leukaemia cells is required for efficient homing and engraftment, but it is not required for B-ALL [5]. Similarly, in AML CD44 is known to interact with the niche and to be required for homing of leukaemia stem cell to their supportive niches [84]. Integrin β3 has been shown to enhance Wnt signalling in AML cells by mediating resistance to chemotherapy [85]. CD98, another adhesion molecule, promotes AML proliferation and maintenance of leukaemia stem cells by increasing their engraftment [86]. In CML, integrin β 1 is also involved in adhesion of CML cells to fibronectin and decreased proliferation of leukaemia cells [87].

Several cytokines, chemokines or secreted molecules are known to be secreted by leukaemic cells or niche cells affecting the progression of the disease. Vascular endothelial growth factor (VEGF) and angiopoietin secreted by leukaemia cells are known to control proliferation of leukaemia and endothelial cells in B-ALL [88] and AML [89].

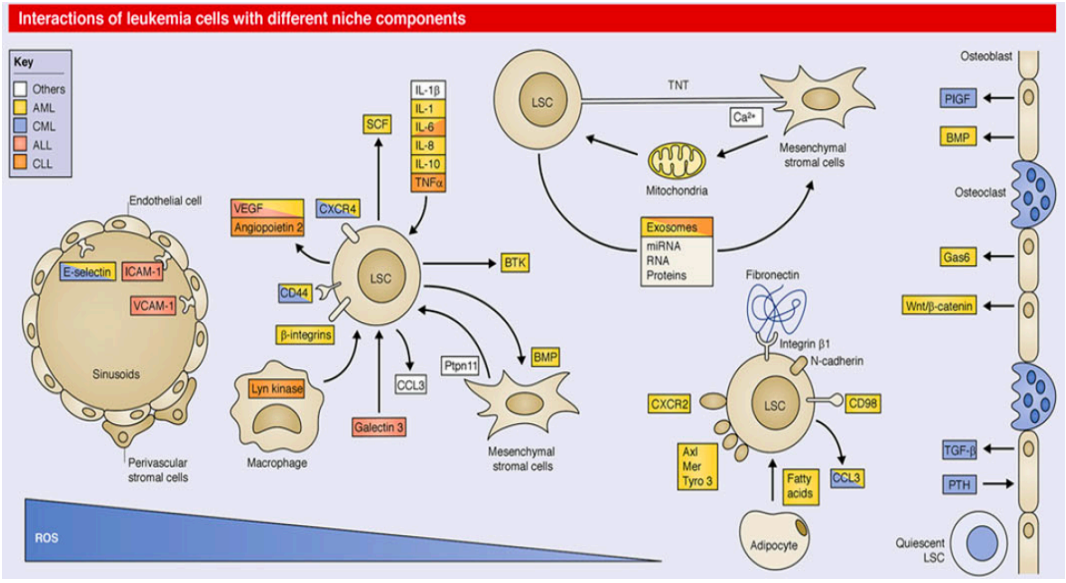

Figure 6: The bone marrow microenvironment in leukaemia [1]

- **Chemo-resistance**

Previously, chemo-resistance was primarily associated with LSCs. However, the contributions of the BMM recently became evident. N-cadherin, an adhesion molecule, has been shown to mediate adhesion of CML cells to MSCs through an increase in N-cadherin-β catenin complexes and Wnt signalling mediating resistance against tyrosine kinase inhibitors [90]. Leukaemia cells also interact with vascular cell adhesion molecule (VCAM-1) on stromal cells via integrin α β1 leading to activation of the NF-kB pathway and chemo-resistance [91]. Other examples include soluble galectin- 3 which can be taken up by B-ALL cells leading to their protection from chemotherapeutic agents. Furthermore, expression of galectin 3 in CML cell lines induced proliferation and drug resistance [92,93].

6. E- selectin

E selectin belongs to a family of selectins together with P- and L-selectin. Selectins are transmembrane receptors present on the cell membrane of endothelial cells (E-selectin), lymphocytes (L-selectin) or platelets (P-selectin). All three members of the selectin family share a similar structure: The extracellular part I is composed of 3 domains: The N-terminal domain which is dependent on calcium, the epidermal growth factor domain which helps in

ligand interactions and the complementary regulatory protein (CRP) domain consisting of repeats of approximately 60 amino acids [94]. The CRP domain serves as a spacer between the other two domains. The number of CRP repeats defines each selectin molecule, and E-selectin is known to consist of 6 CRP repeats. It is followed by a single helicoidal transmembrane chain and a cytoplasmic tail connected to the actin cytoskeleton inside the cell.

E-selectin is vastly and exclusively expressed on endothelial cells. In physiological conditions, the role of E-selectin is to mediate the adhesion of leukocytes and neutrophils to endothelium, whereas in pathological conditions, cancer cells interact with E-selectin to promote their invasion [95–97]. The known ligands of E-selectin are E-selectin ligand-1 (ESL-1), P- selectin glycoprotein ligand-1 (PSGL-1), β2 integrin, L-selectin, CD43 CD44, lysosomal-associated membrane protein-1/2 (LAMP-1/2) and death receptor-3 (DR3) [98]. E-selectin recognises sialyl Lewis-a/x tetra saccharides present on glycoproteins and glycolipids on the surface of leukocytes and tumour cells.

The expression of E selectin is trigged by pro-inflammatory signals or molecules such as tumour necrosis factor α (TNFα), interleukin 1b (IL-1b), endothelial monocyte activating polypeptide II (EMAPII), and bacterial lipopolysaccharide (LPS) [99]. During inflammation, E-selectin is important for recruiting leukocytes to the site of injury. The release of cytokines induces expression of E-selectin on endothelial cells at the site of injury. In such conditions, the expression of E- selectin reaches its maximum after 2-6 hours [99]. Studies report that susceptibility to infection is increased in the absence of E-selectin and P-selectin [100]. In haematopoiesis, E-selectin was shown to be essential to promote HSC proliferation demonstrating it is crucial component of vascular niche [7].

The interaction between E-selectin and its ligands triggers signalling in both endothelial cells bearing E- selectin and cells bearing the ligand. In the normal condition: E-selectin binding to PSGL-1 on neutrophils activates β2 integrin through the Syk-Src pathway. Simultaneously, E-selectin transduces signals into endothelial cells through p38 and p42/p44 MAP kinase pathways [101]. In case of cancer, the sequence is: The extracellular domains of E-selectin bind to ligands on cancer cells. The initial adhesion is weak which allows the rolling of cancer cells on the surface of endothelial cells. After primary adhesion, chemokines are released by the endothelial cells which activate integrins on the cancer cells [102]. These integrins are capable of binding to ICAM/VCAM on endothelial cells allowing extravasation and transmigration of cancer cells.

In chronic myeloid leukaemia (CML), deficiency of E-selectin in the recipient bone marrow endothelium significantly reduced engraftment by BCR-ABL1-expressing leukaemia stem cells. These results also suggest that BCR-ABL1$^+$ leukaemia initiating cells (LIC) rely to a greater extent on selectins for homing and engraftment [6].

Rivipansel (GMI-1070), a pan selectin inhibitor was developed to target selectins in sickle cell anaemia. Uproleselan (GMI-1271), a specific E-selectin inhibitor has been used in AML and multiple myeloma studies [81,103]. GMI-1271 is currently in clinical trials for treatment of AML in combination of chemotherapy [104].

7. CD44

CD44 is a glycoprotein existing in approximately 20 isoforms encoded by a single gene [105]. CD44 molecules differ in size due to post-translational modifications like N- and O-glycosylation and insertion of alternatively spliced exons giving rise to isoforms [106,107]. The smallest and most common hematopoietic isoform (CD44s) is present on the membrane of most cells [108]. CD44 has seven extracellular domains, a transmembrane, and a cytoplasmic

domain. In the extracellular domain, between domains 5 and 6, variant exon products can be inserted by alternative splicing giving rise to CD44 splice variants [106,109]. The N terminal on the extracellular domain is known to form a globular structure and has binding sites for ECM proteins such as fibronectin, collagen, laminin and cell surface receptors like E selectin [110–112]. Interestingly, one of the major receptor for CD44 binding is hyaluronic acid (HA) [113]. HA binding depends on CD44 cross linking or conformation changes and redistribution in the cell membrane. The cytoplasmic tail of CD44 contains binding sites for cytoskeletal proteins like ezrin, radixin and moesin (ERM). ERM proteins link CD44 to the actin cytoskeleton [114,115]

One of the functions of CD44 is to serve in anti-apoptosis [116]. In resting cells, CD44-associated merlin signals through yes associated protein (YAP) downregulation which promotes caspase3 activation and apoptosis. When CD44 becomes activated by HA interactions, merlin is phosphorylated and dissociated from CD44. Hence, CD44 attenuates the activation of Hippo signalling leading to anti-apoptosis [117,118].

CD44 also participates in the localisation of leukaemia initiating cells in the bone marrow protecting them from chemotherapy. In AML, CD44 is required for the transport of LIC to the HSC niche, and anti-CD44 antibodies alter the fate of the LIC by inducing differentiation [119]. CD44 plays an essential role in homing and engraftment of LIC in CML. In a mouse model of CML, BCR-ABL1-transduced progenitors from CD44-deficient donors were defective in BM homing and decreased in engraftment [5]. These studies provided additional evidence that LIC may be more dependent on CD44 for homing to the bone marrow. In AML, a CD44-specific blocking antibody decreased leukaemia cell homing and led to reduced proliferation in murine models [120].

8. SCL/TAL1

The basic helix-loop-helix (bHLH) protein stem cell leukemia (SCL)/T-cell acute lymphoblastic leukemia (T-ALL) (TAL1) is a pivotal haematopoietic transcriptional regulator [121]. In adult haematopoiesis, SCL/TAL1 is expressed at higher levels in the HSC compartment, myeloid progenitors, and mature myeloid cells (red cells, megakaryocytes, mast cells and basophils) and at lower levels in lymphoid progenitors.

The importance of SCL/TAL1 was initially demonstrated when in *in vivo* murine models, deletion of SCL/TAL1 led to embryonic death at embryonic day 9.5 due to the absence of primitive erythropoiesis and myelopoiesis in the yolk sac [122,123]. Further studies in murine models suggested the essential role of SCL/TAL1 in endothelial and blood development.

In adult Lin^- $Sca1^+$ $cKit^+$ (LSK) $CD150^+$ $CD48^+$ HSCs, SCL/TAL1 controls expression of the genes encoding transcription factors inhibitor of DNA binding 1 (ID1) and cyclin-dependent kinase (CDK) inhibitor P21/ CDK inhibitor 1A (CDKN1A) thus maintaining G0 phase [124] playing a role in quiescence and self-renewal of cells. However, opposite effects were observed in cord blood HSCs where it is supposed to maintain proliferation [125].

ChIP sequencing data from multipotent hematopoietic progenitors, proliferative lineage-specific primed precursors, and terminally differentiated erythroid and megakaryocytic cells revealed changes in the occupancy of SCL/TAL1 binding sites during differentiation of HSC [126]. SCL/TAL1 binds to the genome through a complex of proteins. Importantly, SCL/TAL1 binds the consensus Ebox DNA motif, CANNTG, as a heterodimer with ubiquitously expressed bHLH E-proteins (E12/E47, HEB, E2-2) [127]. Further, non-DNA-binding proteins (LMO and LIM domain binding protein (LDB)) are recruited to form the SCL core complex: SCL: E-protein: LMO1/2: LDB1. This complex later recruits all other transcriptional factors and co-factors.

In normal conditions, SCL/TAL1 expression is downregulated during T-cell differentiation. However, SCL/TAL1 expression can be activated in T cells through chromosomal translocations (interstitial deletions in the SIL-SCL locus) and mono/ biallelic transcriptional mechanisms [128]. This ectopic thymic expression is seen in 60% of childhood and adult T-ALL cases [129]. Overexpression of SCL/TAL1 alone is, however, insufficient to induce leukaemia. Additional hits by oncogenic events are required for full leukaemic transformation with short latency periods. In 45% of SCL/TAL1 T-ALL cases, the cooperating genetic event is ectopic expression of LMO1 or LMO2 through chromosomal rearrangement [130]. Murine transgenic models have shown that SCL and LMO1/2 co-expression confers aberrant self-renewal to pre- leukaemic thymocytes. This self-renewal capacity is acquired due to the enhancement of the NOTCH pathway [131,132].

9. Targeting of the bone marrow microenvironment

As described above, the BMM provides a protective environment for leukaemia and it is of utmost importance to find the connecting mechanisms between the BMM and leukemic stem cells in order to develop therapies targeting the microenvironment [1]. The majority of therapies are targeted towards LSCs. However, the persistence of LSCs in the BMM make it important to target the interactions between LSCs and their microenvironment hopefully leading to eradication of leukaemia cells.

For example, granulocyte colony forming factor (G-CSF), an HSC mobilization agent, induces HSC mobilization [133] and G-CSF in combination with chemotherapy improved disease-free survival in CML patients in a randomized clinical trial [134]. Additionally, antibodies against CXCR4 inhibited chemotaxis of AML cells towards CXCL12 and reduced the tumour burden in a xenotransplantation model of AML [135]. The CXCR4 inhibitor AMD3100 combined with chemotherapy led to prolonged survival in acute promyelocytic leukaemia [136]. Clinical trials employing antibody or peptide inhibitors against

CXCR4 in AML and CML are currently ongoing. A neutralizing agent for CXCL12 named NOX-A12 led to reduced chemotaxis of leukaemic cells and increased sensitivity to chemotherapy in CLL [137]. In the vascular niche, targeting of E selectin led to improved survival of mice in multiple myeloma and AML [81,103]. In AML, a clinical trial is ongoing with GMI-1271, a small molecule inhibitor of E-selectin, in combination with chemotherapy [104]. Likewise, the inhibition of the interaction between AXL receptor and growth specific arrest 6 (GAS6) secreted by stromal cells with MYD1-72 led to disruption of the chemoprotective niche in AML [138]. The inhibition of Bruton tyrosine kinase (BTK) by PCI-32765 inhibited migration and integrin-mediated adhesion to fibronectin in CLL [139].

Other forms of targeting the BMM include inhibition of exosome formation with carboxyamidotrizole/orotate (OTC) or blocking tunnelling nanotubes resulting in inhibition of transport of material to leukemic cells or stromal cells [140]. Recently, in a xenotransplantation model of AML it was shown that vascular damage in AML is induced due to increased levels of ROS or NO in endothelial cells, and this could be targeted by inhibitors of NO production [141]. In CML, an increase of bone remodelling by osteoblast specific activation of the receptor for parathyroid hormone (PTH) attenuated CML due to release of TGF-β1 from the bone matrix, but not AML [142]. Hence, targeting the BMM might be a useful approach to complement existing therapies, hopefully increasing current success rate of therapies.

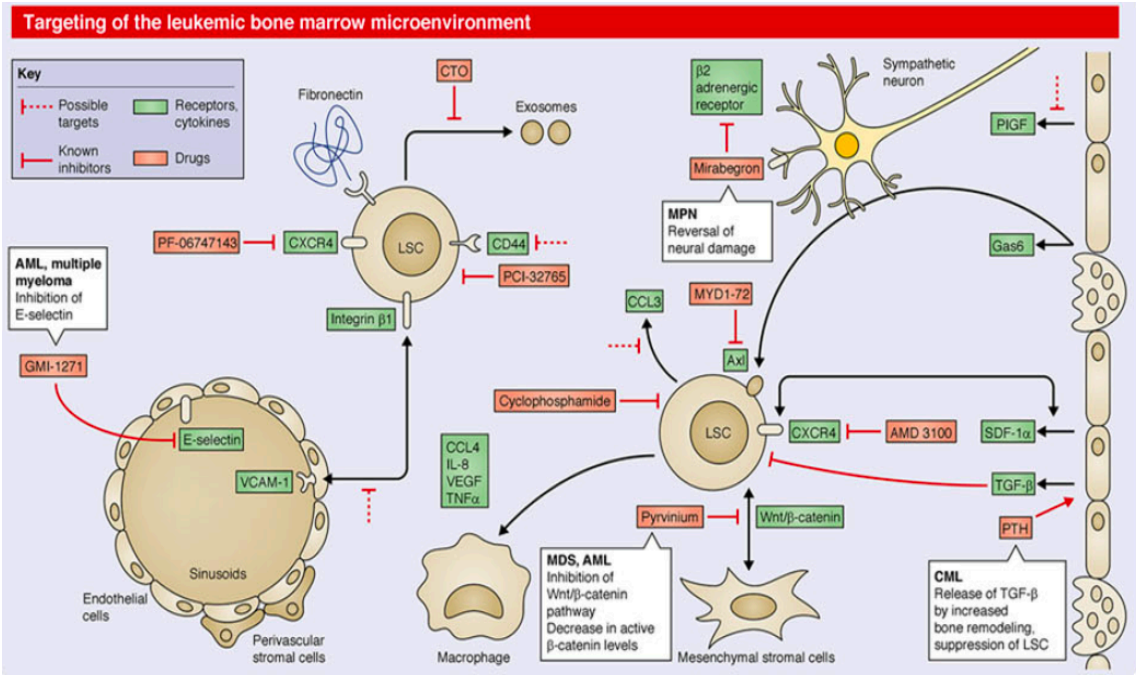

Figure 7: Targeting of bone marrow microenvironment [1]

Hypothesis

Based on the discussed information, we hypothesised the following:

- Inhibition of interaction of leukaemia cells to E-selectin, with GMI-1271 and treatment with chemotherapy can prolong the survival of mice and thereby can act as potential therapeutic strategy.
- Treatment with GMI-1271 can increase *Scl/Tal1* expression in leukaemia cells and affect the expression of CD44.

Materials and Methods

1. Mice and genotyping

BALB/c mice were purchased from Charles River Laboratories (Wilmington, MA). Rag-2 -/- IL2R γ -/- CD47 -/- knockout and Tie2-GFP mice were bred in Georg-Speyer-Haus. All murine studies were approved by the local animal care committee (Regierungspräsidium Darmstadt).

- **Rag2/CD47/Il2rg**

***Recombinant activating gene 2 (RAG2)* Allele:**

Primer Name	Sequence 5' --> 3'
Wild type Forward	ATC AAT GGT TCA CCC CTT TG
Wild type Reverse	TCA TGT GAA AGC AGT TCA GGA C
Mutant Reverse	CCG CCA TAT GCA TCC AAC
Mutant Forward	CAG CGC TCC TCC TGA TAC TC

Table 1: Rag2 primers

Results: Mutant = 291 basepairs (bp)
Heterozygote = 291 bp and 441 bp
Wildtype = 441 bp

***CD47* Allele:**

Primer Name	Sequence 5' --> 3'
Wild type Reverse	CAC CTT ACA GCA CTC CCA CA
Mutant Reverse	TGG GCT CTA TGG CTT CTG AG
Common Common	GAA GTG GAA GTT GAA CAA ATC G

Table 2: CD47 primers

Results: Mutant = 199 bp
Heterozygote = 199 bp and 300 bp
Wildtype = 300 bp

***Interleukin 2receptor gamma (IL2RG)* Allele:**

Primer Name	Sequence 5' --> 3'
Common	AAG AGA TTA CTT CTG GCT GTC AG
Wild type Reverse	CTC TGG GGT TTC TGG GG
Mutant Reverse	ATG CTC CAG ACT GCC TTG

Table 3:IL2RG primers

Results: Mutant = 130 bp
Wildtype = 94 bp

PCR: *RAG2* and *CD47*

Step #	**Temp °C**	**Time**	**Note**
1	94	2 min	
2	94	20sec	
3	65	15sec	-0.5 C per cycle decrease
4	68	10sec	
5			repeat steps 2-4 for 10 cycles (Touchdown)
6	94	15sec	
7	60	15sec	
8	72	10sec	
9			repeat steps 6-8 for 28 cycles
10	72	2min	
11	10		hold

Table 4: PCR for RAG2 and CD47

- ***IL2RG* Allele:**

Step #	Temp °C	Time	Note
1	95	3min	
2	95	5sec	
3	60	30sec	
4			repeat steps 2-3 for 40 cycles
5	4		Hold

Table 5: PCR for IL2RG

2. Drug treatment

Mice were treated twice a day with vehicle (normal saline) or GMI-1271 or GMI-1359 (GlycoMimetics Inc., Maryland, USA) by intraperitoneal injection at 20 mg/kg/dose from day 10 to 30 after transplantation. Imatinib was administered via oral gavage once a day at 100 mg/kg (Enzo Life Sciences, ALX-270-492, Farmingdale, NY).

For the *in vitro* assays, K562 cells were treated for 8 hours with different compounds that inhibit signalling pathways downstream of BCR-ABL1 at the following concentrations: Imatinib (Enzo Life Sciences, ALX-270-492, Farmingdale, NY) at 10μM [143,144], wortmannin (PI3K inhibitor, Selleckchem, S2758) at 20μM [145] and MK-2206 (inhibitor of AKT1/2/3, Selleckchem, S1078) at 20μM [146]. For the *in vitro* adhesion assays, BCR-ABL1$^+$ BaF3 or BCR-ABL1$^+$ BaF3 cells overexpressing CD44 were treated with GMI-1271 at 20μM [7] and imatinib at 10μM.

3. *In vivo* microscopy (IVM)

Unirradiated Tie2-GFP reporter mice (GFP expression is under the control of the Tie2 promoter labelling endothelial cells) pre-treated with vehicle or GMI-1271 were intravenously injected with 500,000 BaF3$^+$ BCR-ABL1 or BaF3 BCR-ABL1 CD44$^+$ cells.

The cells had been pre-labelled with the Cell Tracker orange CMTMR dye (C2927, Thermo Fisher Scientific, Darmstadt) at a 1:1000 dilution for 30 minutes at 37° C in water bath. After 2-4 hours, the mice were anesthetised by injection of xylene/ketamine and the scalp was removed by making a fine incision on the skin and flapping the skin on the sides. The skull surface was cleaned several times with PBS until no residual fur was found. A drop of Methocell was applied to the skull to avoid drying and to provide a tight seal between the skull and the coverslip, which was placed on the skull in a holder. The mouse was kept in a warm chamber and the calvarium was visualized under a 2-photon microscope (LaVision Biotech, Bielefeld) using a 40x objective. A well-defined area containing a vessel and cells was selected and movies were recorded at 1 frame/second using the Inspector Pro software. Each video was taken for a minimum of 900 frames (15 minutes). The videos were analysed frame by frame by measuring the time of contact of cells with the GFP^+ endothelial cells lining the vessels.

100,000 peripheral blood or bone marrow cells from CML patients were labelled with 1 μM CMTMR dye (C2927, Invitrogen, Germany) as described above and intravenously injected into non-irradiated Rag-2 -/- interleukin-2 receptor γ gamma -/- CD47 -/- knockout mice (cat. no. 025730, The Jackson Laboratory, Bar Harbor, Maine). The mice had been pre-treated with GMI-1271 or vehicle 2 hours before injection. Dextran FITC (1 mg/mouse) (46945, Sigma, Taufkirchen, Germany) to visualise vessels was injected intravenously at the time of injection of cells. 2-4 hours after injection, the injected cells were visualized by 2-photon microscopy and recordings were performed as described above. The videos were analysed frame by frame by measuring the time of contact of cells with the endothelium.

In order to measure the distance between leukaemia cells labelled with CMTMR to bone or endothelium, 100,000 BCR-$ABL1^+$ BaF3 cells or Lin $^-$ BCR-$ABL1^+$ cells from mice with established CML were injected into unirradiated Tie2GFP mice. The Tie2GFP mice were

treated with GMI-1271 2 hours before injection of cells, at the time of injection and 18 and 20 hours after injection of leukaemia cells. Similarly, Tie2GFP mice were treated with imatinib at the time of injection and 18 and 20 hours after injection of leukaemia cells. Mice were anaesthetised and prepared for intravital microscopy as described above. Z-stacks with 2 μm distance were recorded starting from a point below a cell until coverage of the cell by bone. As described above, an area with cells and vessels was chosen and Z-stacks of 2 μm distance were recorded from a point below the cell surface until coverage by the bone. Approximately 20 cells were recorded for each condition. Shortest distance to bone/endothelium was calculated using the Fiji program. [147,148]

4. Transplantation

- **Primary Transplant**

Male 5-6 week old Balb/c mice were injected with 200 mg/kg 5-fluorouracil (5-FU) by tail vein injection. On day 4 post 5-FU, mice were sacrificed by CO2 asphyxiation. Both tibiae and femora were harvested and placed in sterile cold PBS. After harvesting, further steps were performed under sterile conditions. The edges of the bones were chopped and the bone marrow was flushed with media (DMEM + 10% FCS + 1% penicillin streptomycin, 1% L-glutamine). The pellet was lysed with ACK lysing buffer and the cells were resuspended in a pre-stimulation media and incubated overnight in a 10 cm dish. The next day, approximately 30 million cells were resuspended in 2 ml of spinfection media in a 6 well plate and transduced with 2 ml cryopreserved retrovirus expressing MSCV IRES GFP BCR-ABL1. During transduction the plate was sealed with parafilm and centrifuged for 90 minutes at 32 C at 2500 rpm. After centrifugation, the cells were resuspended, placed in an incubator for 2-4 hours and later resuspended in incubation media. The next day, 2 ml virus was again added back to the well and the spinfection procedure was followed as described above (Van Etten, 2001; Wolff & Ilaria, 2001).

After the centrifugation, the cells were resuspended and incubated for 2-4 hours. Simultaneously, recipient 5-6 week old female mice were sublethally irradiated twice with 375 cGy. The cells were counted, and the irradiated mice were transplanted at a dose of $3x10^5$ cells per mouse in Hanks balanced salt solution (HBSS) solution. The mice were monitored daily and any abnormalities in their posture and behaviour were noted.

For the *Scl/Tal1* overexpression experiment, 5-FU–treated BM cells, as described for the primary transplant, were transduced with MSCV IRES RFP BCR-ABL1 retrovirus alone or doubly transduced with MSCV IRES RFP BCR-ABL1 retrovirus and SiEW empty vector or *Scl/Tal1* overexpressing lentivirus [151] in a similar way as described above. After 2 spinfections, BM cells were transplanted into sublethally irradiated recipient Balb/c mice (750cGy) at a dose of 2.5×10^5.

Pre-stimulation		**Spinfection media**		**Incubation media**	
DMEM	7.7ml	DMEM	5.3ml	DMEM	12.5ml
FCS	1.5ml	FCS	1.3ml	FCS	12.4ml
WEHI	0.5ml	WEHI	0.8ml	WEHI	0.8ml
P/S	100µl	P/S	160µl	P/S	160µl
L-Glu	100µl	L-Glu	160µl	L-Glu	160µl
Cipro	10µl	Cipro	16µl	Cipro	16µl
IL3	10µl	IL3	16µl	IL3	16µl
IL6	20µl	IL6	32µl	IL6	32µl
SCF	50µl	SCF	80µl	SCF	80µl
		PB	40µl		
		Hepes	160µl		

Table 6: Composition of the prestimulation, spinfection and incubation media for bone marrow transplantation.

- **Secondary transplantation:**

Primary mice with established CML-like myeloproliferative neoplasia (MPN) treated with vehicle, imatinib, GMI-1271 or imatinib + GMI-1271 were sacrificed on day 15 or day 17. The bones and spleen of each mouse were collected and kept in sterile PBS. Bone marrow and spleen were crushed, and all the samples were filtered. Either bone marrow or spleen cells from each individual donor mouse were transplanted by injecting 1.5×10^6 cells into two sub-lethally irradiated secondary recipients per donor. The mice were monitored daily and any abnormalities in their function and posture were noted.

5. Homing assay

In the homing assay, male 5-6 week-old Balb/c mice were injected with 200 mg/kg 5-FU by tail vein injection. On day 4 post 5-FU, mice were sacrificed by CO2 asphyxiation. Both tibiae, femora, radii and ulnae were harvested and placed in sterile PBS. The bone marrow was flushed with sterile medium containing fetal bovine serum, as described previously. The spinfection was performed as previously described. 2.5×10^6 cells per mouse were intravenously injected into irradiated Balb/c mice treated with vehicle or GMI-1271. 18 hours later, BM and spleen of the recipient mice were harvested and stained for lineage, Sca-1, c-Kit markers and the cells analysed by flow cytometry [5,6].

6. Analysis of diseased mice and tumour burden

The leukaemic burden in the peripheral blood of diseased animals was assessed by weekly analysis by a Scil Vet animal blood counter (Scil Animal Care Company, Viernheim, Germany) after day 12 of transplantation and by staining leukocytes from peripheral blood with a phycoerythrin (PE)-conjugated antibody to CD11b (myeloid cells) (clone M1/70, Biolegend, San Diego, CA) and analysis of GFP/RFP expression (leukemic cells are $CD11b^+$ GFP/RFP^+) by flow cytometry. Spleens were weighed and pathological report was created at death. Leukaemia-initiating cells were analysed by staining for GFP, c-Kit, lineage (B220,

CD5, Gr-1 and Ter119 cocktail), and Sca-1 (BD Biosciences, Franklin lakes, NJ).

7. Virus production

293T cells were seeded at 3×10^6 per 6 cm plate 18 hours before transfection. After 18 hours, media was replaced with fresh media containing chloroquine (25 μm).

Mastermix for 2 plates:

Lentivirus		Retrovirus	
Constructs	**Concentration**	**Constructs**	**Concentration**
DNA(plasmid)	10 μg	DNA(plasmid)	10 μg
VSV	1.5 μg	Ecopak	5 μg
Delta 8.9	3.75 μg		
CaCl2	62 μl	CaCl2	62 μl
H20	Up to 500 μl	H20	Up to 500 μl

Table 7: Production of lentivirus and retrovirus production

500 μl of 2 X HBS was added dropwise to the master mix while vortexing. 1000 μl of mastermix was added to each plate. After 8 hours and 24 hours, the medium was replaced with fresh medium. After 48 hours, the virus was harvested and filtered through a 0.2 μm filter and stored in aliquots at -80 C. **Titration :** 3T3 cells were seeded at 3×10^6 per 6 cm plate. After 18 hours, the 3T3 cells were transduced with the virus in a 1:3 and 1:30 dilution. Then the plates were incubated for 48 hours. After 48 hours, 3T3 cells were trypsinised and washed and analysed by flow cytometry [152]. The percentage of GFP or RFP positivity was analysed by FlowJo.

8. Southern blot

Genomic DNA from spleen was digested with the restriction enzyme BglII, run on an agarose gel and transferred onto a nylon membrane. The blot was then hybridized with a

radioactively labelled probe targeting the GFP gene, in order to detect distinct proviral integration sites, as described [142,152]. The blot hybridized with an RFP probe was generated by the non-radioactive Digoxigenin-11-dUTP (DIG) method according to the manufacturer's instructions (Roche, Mannheim, Germany).

9. Maintenance of cell lines

BCR-ABL1^{+} BaF3 cells were maintained in RPMI 1640 (Thermo Fisher Scientific, Darmstadt) supplemented with 10 % FCS, 1% Glutamine, 1% penicillin-streptomycin. K562 cells were maintained in RPMI supplemented with 10 % FCS, 2 % L-glutamine, 1% penicillin-streptomycin. 293T cells were maintained in DMEM supplemented with 10 % FCS, 2 % L-glutamine, 1% penicillin-streptomycin, 1% non-essential amino acids. 3T3 cells were grown in DMEM supplemented with 10 % FCS, 1 % L-glutamine, 1% penicillin-streptomycin.

10. Immunoprecipitation (IP)

K562 cells treated with imatinib or the AKT inhibitor were resuspended in RIPA buffer (50mM Tris-HCL (pH-8.0), 150 mM NaCl, 2mM EDTA (pH-8.0), 1% NP-40, 0.5% sodium deoxycholate) and incubated on ice for 1 hour followed by centrifugation at 14.000 x g at 4° C for 20 minutes. 10 µl of the supernatant was used as control input. The supernatant was probed with Protein G Dynabeads (10003D, Thermo Fisher Scientific, Darmstadt, Germany) and 3 µg of an anti-SCL/TAL1 antibody (TA590662, Origene, Rockville, MD) and incubated at 4° C overnight. The beads were then washed with RIPA buffer and blocked with Rotiblock diluted in RIPA buffer for 60 minutes. The beads were washed three times with RIPA buffer and, finally, with PBST on a magnetic stand. The elution was performed with 25 µl 4x SDS loading dye added to the beads and incubated for 5 minutes at 95° C. The input and final eluted lysate were analysed by Western blotting.

11.qPCR

The cell pellet was resuspended in trizol, and RNA extraction was performed using the Qiagen kit protocol (74034, Qiagen, Germany). 250-500 ng of RNA was converted to cDNA according to the instructions (E6560, New England Biolabs, USA). A mastermix was prepared with Power SyBR Green (A25742, Thermo Fisher Scientific, Darmstadt) with 10μM forward and reverse primers in triplicates with the RNA concentration being 20 ng or higher. The average of triplicate Ct value was calculated and normalized to the Ct values of GAPDH. Delta Ct and Delta Delta Ct values were calculated and represented as either Delta Ct or as relative expression.

	Forward primer	**Reverse primer**
hScl/Tal1	TCGGCAGCGGGTTCTTTGGG	CCATCGCTCCCGGCTGTTGG
mScl/Tal1	GCATGGTAGGTTGGCTTAAC	AGGAGAAGGGTCTGCTTTAC
hCD44	GACAGCAACCAAGAGGCAAG	AGACGTACCAGCCATTTGTG
mCD44	CCACAGCCTCCTTTCAATAACC	GGAGTCTTCGCTTGGGGTA
hMyc	CGGATTCTCTGCTCTCCTCG	TTCCTCCTCAGAGTCGCTGC
hGATA1	GACACTCCCCAGTCTTTCAGG	CAGTTGAGGCAGGGTAGAGC
hRUNX1	TCGACTCTCAACGGCACCCGA	TGACCGGCGTCGGGGAGTAG
hKLF1	GTGATAGCCGAGACCGCGCC	TTCTCCCCTGTGTGCGTGCG
hPU.1	CAGCTCTACCGCCACATGGA	TAGGAGACCTGGTGGCCAAGA
GAPDH	AGGTCGGTGTGAACGGATTTG	GGGGTCGTTGATGGCAACA

Table 8: qPCR primers (h=human, m=mouse)

12.Mass spectrometry

Quantitative mass spectrometry was performed by using triple SILAC-labelling (SILAC medium, Thermo Scientific, Rockford, USA). K562 cells treated with DMSO as control or 10 μM imatinib or 20 μM MK-2206 for 2 or 4-hours labelled with light, medium or heavy

SILAC medium. The cells were then harvested, immunoprecipitation was performed as described with an anti-SCL/TAL1 antibody and the lysates were analysed by mass spectrometry, as described [153].

13. Chromatin immunoprecipitation (ChIP)

K562 cells were treated with imatinib (10 μM) for 8 hours *in vitro*. After treatment, cells were crosslinked with formaldehyde dropwise and incubated for 15 minutes at room temperature. Then the reaction was quenched using glycine. After washing the pellet in cold PBS three times, the pellet was resuspended in ChIP lysis buffer (50mM HEPES KOH, 140 mM NaCl, 1% Triton X-100, mM EDTA pH 8, 0.1% sodium deoxycholate, 0.1% SDS) containing a protease inhibitor. Cells were incubated for 1 hour at 4°C. Lysates were sonicated to shear DNA to an average fragment length of 500-1000 bp for 7 minutes with 30 seconds on and off amplitude. The sonicated fragments and the unfractionated fraction were visualized on a 1.5% agarose gel. The cell debris was pelleted for 4 minutes at 8000g at 4C, and the supernatant was harvested, aliquoted (20-25 μg) in new tubes, snap-frozen in liquid nitrogen and finally stored at -80°C before further analysis. For immunoprecipitation, protein G beads (10003D, Thermo Fisher Scientific, Darmstadt, Germany) were washed with RIPA buffer (50 mM Tris-HCl pH8, 150 mM NaCl, 1% NP-40, 2 mM EDTA pH 8, 0.5% sodium deoxycholate) together with salmon sperm DNA followed by blocking in Rotiblock. 20-25 μg of chromatin (lysate) was incubated with 7.5 μg anti-SCL/TAL1 antibody (Origene, TA590662, Rockville) and pre-blocked protein G beads overnight in a rotator at 4C. A rabbit IgG antibody was used as a control (sc-2027, Santa Cruz Biotechnology, Dallas) and incubated in a similar way. Another chromatin (lysate) was used as input and was incubated at 4C without rotation. After 6 washing steps with wash buffer (20mM Tris-Hcl pH8, 150 mM NaCl, 1% Triton X 100, 2 mM EDTA pH8, 0.1 % SDS) and final wash buffers (20mM Tris-Hcl pH8, 500 mM NaCl, 1% Triton X 100, 2 mM EDTA pH8, 0.1 % SDS) on a

magnetic rack, the DNA was eluted in an elution buffer (100mM NaHCO3) and placed on a shaker for 30 minutes at 30C. Proteinase K was added to all the samples along with the input sample and incubated for 30 minutes at 30 C to reverse cross-linking. Finally, the ChIP DNA was purified using the ChIP DNA Clean and Concentrator kit (Zymo Research, USA, Irvine). The DNA was eluted with 40 µl, and the qPCR analysis was performed using 2 µl of chromatin with four different primer sets specific for four different regions where SCL/TAL1 binds on the *CD44* regulatory element. DNA recovery was calculated as percent of the input [154].

	Forward primer	**Reverse primer**
CD44 pair 1	TGGAGAAGGCAAGGTTTTTG	AGCCCCCAAAAGATAGTGCT
CD44 pair 2	CTCACTCATGTGGCTGTTGG	CCAGTTGCTCTGGTGTGTGT
CD44 pair 3	GAGCAAGCAAGCAGGAGAGT	GGCAAAAATGAAGGGATGTC
CD44 pair 4	CTGAGGGCATTTACTGCAGA	CTTTGCACATGGAATACGCA
Chromosome 18	ACTCCCCTTTCATGCTTCTG	AGGTCCCAGGACATATCCATT

Table 9: ChIP primers

14. Western blots

- **Preparation of nuclear extracts:**

K562 cells were treated *in vitro*, harvested and washed 2 times with cold PBS. Similarly, BCR-ABL1$^+$ BaF3, BCR-ABL1 CD44$^+$ BaF3, BCR-ABL1$^+$ BaF3 overexpressing *Scl/Tal1* and BCR-ABL1$^+$ BaF3 cells co-transduced with sh*Tal1* were also washed 2 times with cold PBS. The pellet was then re-suspended in buffer A (10mM HEPES, 1.5 mM $MgCl_2$, 10mM KCl, 0.05% NP40, 0.5 mM DTT, protease and phosphatase inhibitors) and incubated on ice for 10 min. After fractionation, the cells were centrifuged at 4°C at 14000 rpm for 10 min.

The collected supernatant represents the cytosolic fraction and were stored at -80° C. The pellet was resuspended in buffer B (5mM HEPES, 1.5 mM $MgCl_2$, 0.2 mM EDTA, 26% glycerol, 0.5mM DTT, 300mM NaCl, protease and phosphatase inhibitors) and sonication was performed for 15 seconds on and off three times. The samples were incubated for 30 minutes on ice and centrifuged at 4°C at 14000 rpm for 20 min. The supernatant corresponds to the nuclear fraction and was stored at -80° C.

- **Preparation of whole cell lysates:**

After treatment *in vitro* the BCR-ABL1$^+$ BaF3 cells were harvested and washed with 1X PBS. Lysates were prepared by resuspending the pellets in 30-100 µl RIPA buffer (50 mM Tris HCl, pH 7.4, 150 mM NaCl, 1% Triton X-100, 1% NaDOC, 0.1% SDS and 1 mM EDTA, 50 mM NaF, 1 mM Na_3VO_4, aprotinin, protease and phosphatase inhibitors). The cells were incubated on ice for 20 minutes and centrifuged at 4°C at 14000 rpm for 20 min. The supernatant representing the protein lysate was stored at -80°C.

The protein concentrations of RIPA lysates or nuclear fractions were measured using the BCA colorimetric quantification method (Cat No.5000006, Bio-Rad, Hercules, CA) and Bradford protein assay (Bio-Rad, Hercules, CA). The absorption was measured at 595 nm. A standard curve was calculated and the concentration of the protein was obtained according to the standard curve. Equal concentrations of samples 40µg for nuclear extracts or 20 µg of whole cell lysates) were mixed with the SDS running buffer Roti-load at 4X (K929.1, Carl Roth, Karlsruhe, Germany), boiled at 95°C for 5 minutes and loaded on 4-12% NuPAGE Bis-Tris Gel (NP0321BOX, Thermo Fischer Scientific, Darmstadt). The running was performed for 90 minutes at 120 V.

The proteins were then blotted on nitrocellulose (88018, Thermo Fisher Scientific, Darmstadt) or activated PVDF (Poly-vinylidene difluoride) membranes (LC2002, Thermo

Fisher Scientific, Darmstadt), and blotting was carried out for 90 minutes at 200 V. The membranes were blocked with 5% milk in TBST or Roti-block (A151.1, Carl Roth) for 30 minutes at room temperature. The membranes were probed with antibodies to SCL/TAL1 (sc12984, Santa Cruz Biotechnology, Dallas) for human cell lines, SCL/TAL1 (ab236520, Abcam, Cambridge, UK), SCL/TAL1 , pTAL1 S122 (ab138646, Abcam, Cambridge, UK), pSCL/TAL1 T90 (SA0807221, Aviva Systems Biology, San Diego), AKT (9272, Cell Signalling, Danvers), pAKT Ser473 (9271, Cell Signalling, Danvers), CD44 (PA5-21419, Invitrogen, Darmstadt), vinculin (company) or the nuclear membrane marker Lamin B1 (ab16048, Abcam). The membranes were incubated overnight at 4C. The membranes were washed with TBST (0.1% tween) three times for 10 minutes. Later, membranes were incubated with the secondary antibodies anti-rabbit HRP (70748, Cell Signalling, Danvers), anti-goat HRP (ab97110, Abcam) and anti-mouse HRP (7076, Cell Signalling, Danvers) at room temperature for 1 hour followed by washing with TBST. The membranes were incubated with ECL mixture (34094, Thermo Fisher Scientific, Darmstadt), and the films were developed.

15. *In vitro* adhesion assays

48-well plates were coated with 1 μg recombinant murine or human E-selectin–IgG1 Fc fusion protein (575-ES, R&D Systems, Minneapolis) in 20 mM PBS (pH 7.4) with 1 mM $CaCl_2$ per well or 1ug BSA as control for 16 hours at 4°C. Unbound selectin was removed, wells were washed gently with PBS and blocked with 1% bovine serum albumin (BSA) dissolved in IMDM (Iscove modified Dulbecco medium) for 1 hour at room temperature. 20,000 murine Lin^- c-Kit^+ BCR-$ABL1^+$ cells from diseased mice in triplicate or 50,000 human CML cells were added to control or E-selectin-coated wells. The cells were treated with vehicle, imatinib (10 μM), GMI-1271 (20 μM) or imatinib plus GMI-1271. The plates were gently spun down at 500 rpm for 1 minute. After incubation at 4°C for 6 hours the

plates were washed gently 4 times, and adherent cells were counted. For the adhesion experiments, BaF3 cells, BCR-ABL1$^+$ BaF3, BaF3 transduced with empty vector or BCR-ABL1$^+$ BaF3 cells overexpressing CD44 were serum-starved for 12 hours, and, later, 70,000 cells were added in duplicate to E-selectin-coated or control plates. The four drugs were then added to the cells before the plates were carefully centrifuged. Plates were then incubated at 37 C for 6 hours. After incubation, non - adherent and adherent cells were harvested and stained for CD44 (103011, Biolegend, San Diego) or plated in the methylcellulose assay.

- **Cell cycle and Western blot:**

70,000 serum-starved BCR-ABL1$^+$ BaF3 cells were treated with vehicle, imatinib (5 μM), GMI-1271 (20 μM) or imatinib + GMI-1271, added on wells pre-coated with E-selectin and incubated at 37°C for 6 hours. After incubation, non-adherent and adherent cells were separated and either cell cycle staining or preparation of protein lysates was performed as described.

In order to investigate the expression of genes involved in the cell cycling, all cells from each well were harvested after the adhesion assay, and RNA was prepared.

For the "soluble E-selectin experiment", BCR-ABL1$^+$ BaF3 cells were added to E-selectin-coated 48-well plates, which were centrifuged at low speed and kept in an incubator at 37 °C for one hour. Thereafter, BSA, 0.05 μg or 0.1 μg E-selectin plus GMI-1271 (20 μM) in each condition were added to the cells. Consequently, the plate was incubated at 37 °C for 6 hours and then washed 4 times. Adherent cells were counted, while non-adherent cells were removed for RNA preparation.

16. Immunofluorescence (IF)

Non-adherent and adherent cells from the adhesion assay, as described above, were harvested and cytospins were performed with 70,000 cells per slide on slides pre-coated with

poly - L-lysine. The slides were air dried, and the area of interest was encircled with a PAP pen. The cells were fixed with 4 % paraformaldehyde (PFA), a commonly used fixation agent, for 20 minutes at room temperature and permeabilized with 0.25 % Triton X-100 for 10 minutes. The cells were then blocked with 2% BSA for 15 minutes at room temperature. The primary antibodies to CDK4 (sc-23896, Santa Cruz Biotechnology, Dallas), CDK6 (sc-796, Santa Cruz Biotechnology, Dallas), p21 (sc-6246, Santa Cruz Biotechnology, Dallas) or p16 (10883-1-AP, Proteintech UK) were used at a 1:50 dilution in 2% BSA and incubated in a humid chamber overnight at 4 °C. The slides were washed gently with PBS three times and incubated with the secondary antibodies anti-rabbit or anti-goat Alexa Fluor 488/ Alexa Fluor 555 (Invitrogen, Grand Island, NY) at a 1:500 dilution for one hour at room temperature. The slides were washed gently with PBS three times and incubated with 4',6-diamidino-2-phenylindole (DAPI) at a dilution of 1:2500 for 10 minutes. Following this, the slides were mounted using mounting media consisting of glycerol and DAPCO (1,4 – diazabicyclo (2.2.2) octane) (290734, Sigma, Taufkirchen, Germany) and air-dried overnight at room temperature. 10-15 images counterstained with DAPI were acquired on a confocal laser scanning microscope (CSLM) using a 20X objective. The intensity of the fluorescence in the nucleus and cytoplasm were measured. Quantitative analysis was performed by using ImageJ. An area of interest (nucleus) was marked, and area and integrated density were measured. The fluorescence of the adjacent background near the cells was also recorded. The corrected total cell fluorescence (CTCF) was calculated by measuring the integrated density of the nucleus for all the protein targets by using the formula CTCF = Integrated Density – (Area of selected cell x mean fluorescence of background readings) [155,156].

17.Methylcellulose

6×10^4 total BM or 6×10^5 total spleen cells from treated mice with CML were added to 3.2 ml of pre-aliquoted methylcellulose (M3231, Stem Cell Technologies, Vancouver, Canada) supplemented with 100 pg/ml IL-3 (Peprotech, Rocky Hill, NJ). The tubes were vortexed and incubated at room temperature. 1.1 ml was aliquoted in triplicate onto tissue culture dishes with grids. The plates were incubated, and after 10 days, colonies were counted.

3,600 BCR-ABL1$^+$ BaF3 cells from the non-adherent and adherent fractions plated in an adhesion assay, as described above, were plated in 3.2 ml methylcellulose (Cat. no. 03814, ClonaCell-TCS medium, Stem Cell Technologies, Canada). 1.1 ml was aliquoted in triplicate onto tissue culture dishes with grids. The plates were incubated and after 10 days, colonies were counted.

18.FACS

- **Membrane molecules:**

Cells were pelleted were resuspended in PBS antibodies (Lin cocktail, Sca1, c-Kit, CD44 (103020, Biolegend, San Diego, CA) at a 1:50 dilution. The samples were incubated for 30 minutes at 4°C in the dark. The samples were washed with PBS, and the cell pellet was dissolved in 200 µl PBS and acquired on a BD LSR Fortessa (BD Biosciences, Franklin Lakes, NJ).

- **Cell Cycle:**

Non-adherent and adherent cells from the adhesion assay, as described above, were harvested, fixed and permeabilised for 15 minutes in fixation/permeabilisation buffer (554714, BD Biosciences) and stained overnight with an antibody to Ki67 (652403, Biolegend, San Diego) at a 1:100 dilution. The cells were washed and incubated with DAPI (5 mg/ml) at a 1:200 dilution for 30 minutes on ice. The stained cells were acquired on a BD

LSR Fortessa (BD Biosciences, Franklin Lakes, NJ).

19. Luciferase assay

The human *CD44* regulatory element, a 700 bp fragment containing SCL/TAL1 binding sites, was cloned into the luciferase vector pGL4.23 (Promega, Mannheim, Germany) via NheI and HindIII restriction sites. K562 cells or K562 cells transduced with lentivirus overexpressing *SCL/TAL1* or expressing sh*SCL/TAL1* were seeded in a 24-well plate (250,000 cells/well) 4 hours before transfection. The transfection was carried out by pipetting 125 ng of the reporter plasmid and a vector expressing β-galactosidase as control per well in serum-free media, to which 3 µl Metafectene (T040, Biontech, Germany) had been added. The transfected cells were incubated at 37° C for 48 hours. After incubation the cells were harvested for the luciferase and β-galactosidase activity assays. The cells were lysed by using lysis buffer (50 mM Tris-pH 7.4, 1% Triton X-100, 50 mM NaCl) for 20 minutes on ice. Lysates were prepared by centrifugation at 15000 rpm for 10 min at 4C. 10 µl of lysate was added to 100 µl luciferase assay reagent (E1500, Promega, Mannheim) in a 96 well plate, and measurements were carried out. At the same time, 10 µl of lysate was added to the β-galactosidase reagent and incubated for 30 minutes at 37C. The reaction was stopped by adding β-galactosidase assay stop solution (75707, Thermo Fisher Scientific, Darmstadt, Germany), and the absorbance was measured at 405 nm. To control for transfection efficiency, the firefly luciferase activity was normalized to β-galactosidase [151].

20. Isolation of human $CD34^+$ cells

Human $CD34^+$ cells were isolated from healthy, allogeneic bone marrow donors which had undergone bone marrow aspiration or from donors whose HSC had been mobilized into peripheral blood (Permit #329-10 from the local ethics committee), as performed by the Blutspendedienst Baden Württemberg-Hessen. The peripheral blood mononuclear cells (PBMC) were isolated by using Ficoll gradient. The blood was slowly layered on top of the

Ficoll. The gradient was centrifuged for 40 minutes at 1500 rpm at 20 °C without brake. After centrifugation, the PBMC fraction, which was found in the layer in the middle of the gradient, was carefully removed and washed twice with PBS. The cells were immunomagnetically enriched by incubating PBMCs with anti-human CD34 microbeads (130-046-702, Miltenyi Biotec, Germany) according to the manufacturer's instructions and separated by magnetic enrichment using a manual MACS magnetic separator. The isolated human $CD34^+$ cells were grown in the serum-free expansion medium Stem Span (SFEMI, Stemcell Technologies, Cologne, Germany) supplemented with 100 ng/ml FLT-3, 100 ng/ml SCF, 20 ng/ml IL-3 and 20 ng/ml IL-6 [157].

21. Gene expression profiling data and statistical analysis of CML patients

To correlate expression of *SCL*/*TAL1* and *CD44* in CML patient samples we examined two published data sets (Radich et al., 2006; McWeeney et al., 2010). The first data set included 90 samples [158] from patients in various phases of CML (42 chronic phase, 17 accelerated phase and 31 blast crisis samples), and also included sorted $CD34^+$ samples from 5 healthy individuals (Rosetta Inpharmatics DNA microarray platform). The log10 ratio of expression of each individual patient sample was shown relative to expression in a pool of CP samples. Of 42 CP CML patient samples, 37 were drawn prior to allogeneic transplantation. These samples had available outcomes to assess the impact of *SCL*/*TAL1* expression on outcomes after allogeneic transplantation. Patients had not been treated with tyrosine kinase inhibitor therapy prior to transplantation. For the analysis of relapse and mortality data, two outcomes were examined: Relapse (n = 10) and a combination of death or relapse to assess relapse free survival (n = 20), calculating the time in the study by subtracting the date of transplant from the date of relapse, or the date of relapse or death, respectively. For patients without event, time was calculated as the number of days between transplant and last contact. We estimated

hazard ratios (HRs) and 95% confidence intervals (CIs) associated with each outcome using Cox proportional hazards regression models. We modeled *SCL/TAL1* expression levels by splitting patients into high and low groups at the third quartile, and also as a continuous measurement. HRs and CIs reported for continuous *SCL/TAL1* represent a 0.25 increase in *SCL/TAL1* expression levels. We created Kaplan-Meier curves and used the Log-rank test to detect differences between high and low *SCL/TAL1* expression groups, splitting at the third quartile, as mentioned.

The second data set [159] included 59 available sorted $CD34^+$ samples from CP CML patients prior to treatment with imatinib mesylate (HG-U133 Plus 2.0 GeneChip arrays, Affymetrix). For these analyses the average expression of multiple probe sets for *SCL/TAL1* (1561651_s_at, 206283_s_at, 216925_s_at) and *CD44* (1557905_s_at, 1565868_at, 204489_s_at, 204490_s_at, 209835_x_at, 210916_s_at, 212014_x_at, 212063_at, 217523_at, 229221_at) were used.

For the third data set we obtained CML blood samples from our colleagues in France. RNA was extracted from leukocytes from peripheral blood of patients with CML in CP and healthy individuals and qPCR for *SCL*/*TAL1* and *CD44* was performed. Consequently, delta Ct values for *SCL*/*TAL1* and *CD44* were compared.

22. Analysis and Statistics

Statistical significance between two different treatment groups was assessed by Student's t-test. If more than two treatment groups were compared, an ANOVA test and a Tukey test as post hoc test were employed using Prism Version 6 software (GraphPad, La Jolla, CA). Differences in survival were assessed by Kaplan-Meier nonparametric tests (Log-rank or Wilcoxon tests). Data were presented as mean ± s.e.m and differences were considered significant when P values ≤ 0.05.

Results

1. GMI-1271 decreases the adhesion of leukaemic cell line to endothelium *in vivo*

GMI-1271 is a small molecule antagonist that targets the E-selectin molecule, exclusively expressed on endothelial cells. As a preliminary experiment to confirm *in vivo,* the inhibitory role of GMI-1271 for adhesion of leukaemia cells to endothelium, we injected BaF3 cells stably transduced with the *BCR-ABL1* oncogene (BCR-ABL1^{+} BaF3) into un-irradiated Tie2-GFP mice. The Tie2-GFP mice were pre-treated with vehicle or GMI-1271 before the injection of cells, which had been labelled with the dye CMTMR. After homing, we performed intravital microscopy (IVM) on live anaesthetized mice and visualized the endothelium (GFP^{+}) in the calvarium (Figure 1.1 A). We observed a decrease in the adhesion of BCR-ABL1^{+} BaF3 cells to the endothelium in mice pre-treated with GMI-1271 (P = 0.05, Figure 1.1B). This indeed proved the effect of GMI-1271 in reducing adhesion of leukaemia cells to E-selectin expressed on endothelial cells.

Figure 1.1

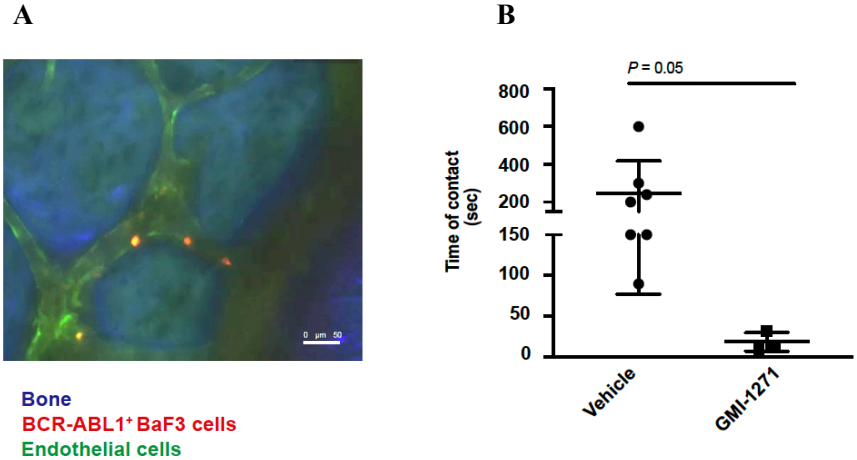

Figure 1.1: A) Representative 2 photon image of bone marrow calvarium of Tie2 GFP mice injected with cells labelled with CMTMR dye (orange). The bone is visualised in blue due to second harmonic generation (SHG). B) Time of contact (seconds) of BCR-ABL1$^+$ BaF3 cells labelled with CMTMR with calvarial endothelium 2 hours after injection in vehicle- or GMI-1271-pretreated unirradiated Tie2GFP mice by *in vivo* microscopy. The mice were treated with GMI-1271 2 hours before injection of cells.

2. GMI-1271 decreases the adhesion of primary CML cells to endothelium *in vivo*

After showing that GMI-1271 reduced adhesion of the leukaemic cell line BCR-ABL1$^+$ BaF3, we tested the effect of GMI-1271 on human CML cells obtained either from peripheral blood or bone marrow of CML patients. In order to test if we could recapitulate the findings observed above, we injected human CML cells and dextran-FITC (in order to visualise the vasculature) into un- irradiated Rag-2-/- / CD47-/- IL-2 receptor γ -/- mice pre-treated with vehicle or GMI-1271. The bone marrow vasculature was visualised similarly as described above (Figure 1.2 A). Treatment with GMI-1271 showed a significant reduction in adhesion of human CML cells to endothelium in 4 out of 5 patients (Figure 1.2 A, Figure 1.2 B-F).

Patient	Organ	Expression of BCR-ABL1
1	Bone marrow	Unknown
2	Peripheral blood	36%
3	Peripheral blood	74%
4	Peripheral blood	41%
5	Bone marrow	Unknown

Table 10: Patient samples used for the *in vivo* microscopy experiment.

These studies indicated that GMI-1271 leads to non-adhesion of BCR-ABL1$^+$ BaF3 and human CML cells to bone marrow endothelium *in vivo.*

Figure 1.2

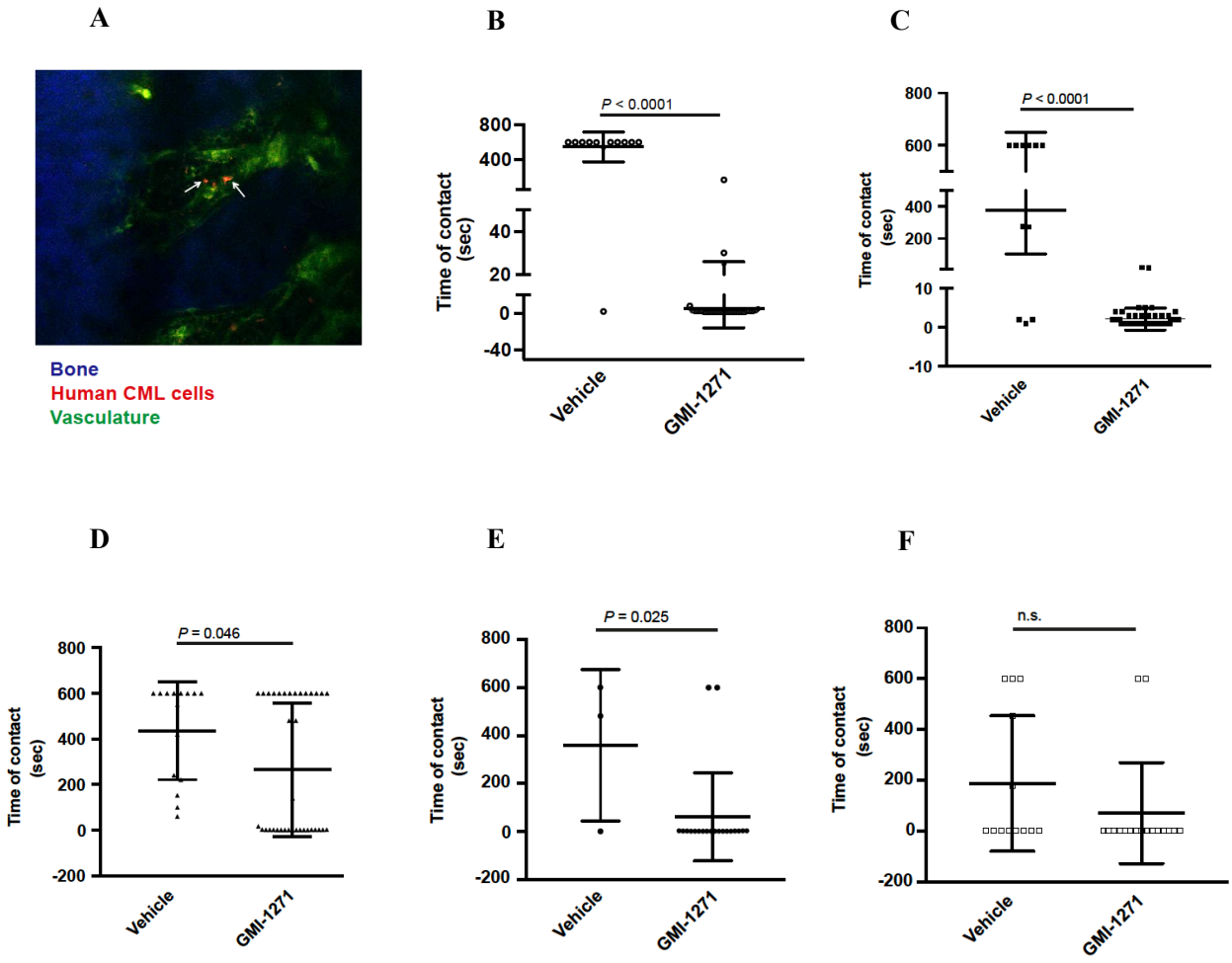

Figure 1.2: A) Representative image of bone marrow calvarium of Rag-2-/- / CD47-/- IL-2 receptor γ -/- mice injected with cells labelled with CMTMR dye (orange) and dextran FITC (green). The bone is visualised in blue due to second harmonic generation. B-F) Time of contact (seconds) of human CML cells labelled with CMTMR (cell membrane dye) to calvarial endothelium after 2 hours of injection in vehicle- or GMI-1271-treated unirradiated Rag-2-/- / CD47-/- IL-2 receptor γ -/- mice by *in vivo* microscopy.

3. Combination therapy of an E-selectin inhibitor with imatinib prolongs survival

The bone marrow microenvironment is known to protect leukaemia cells from chemotherapy by different mechanisms [1,2]. As mentioned in the introduction, the endothelium provides a protective niche and our experiments above show reduced adhesion of CML LSC to endothelium after treatment with GMI-1271 [160]. We then assessed targeting of the microenvironment by inhibiting E- selectin with GMI-1271 in combination with imatinib mesylate, a standard chemotherapeutic drug used in CML. Using a retroviral transduction/ transplantation model, we transduced 5- FU treated bone marrow with BCR-ABL1 expressing retrovirus and transplanted it into sub-lethally irradiated Balb/c recipients which had been randomized into 4 categories receiving different the following treatments: vehicle, imatinib, GMI-1271 and GMI-1271+imatinib. Treatments were started on day 10 after the engraftment of BCR-ABL1$^+$ cells in the bone marrow (Figure 2A). Treatment of murine recipients with CML with vehicle, GMI-1271, imatinib and the combination therapy imatinib + GMI-1271 led to significant prolongation of survival in mice treated with imatinib and GMI-1271 compared to vehicle or imatinib alone (P = 0.03, Figure 2B). All the mice developed CML and died of pulmonary infiltration by malignant myeloid cells, as described in this retroviral transplantation model [6]. We also assessed several parameters essential for detection of disease burden. Total leukocytes or WBCs (P = 0.0008, Figure 2C), spleen weight (P = 0.024, Figure 2D) measured at the time of sacrifice and BCR-ABL1$^+$ CD11b$^+$ myeloid cells (P = 0.031, Figure 2E) were significantly reduced in mice receiving imatinib + GMI-1271 compared to vehicle. However, we could only observe a trend towards reduction in WBCs, spleen weight and BCR-ABL1$^+$ CD11b$^+$ in mice receiving imatinib + GMI-1271 compared to imatinib alone. Interestingly, we could also observe a decrease in LIC, i.e. BCR-ABL1$^+$ Lin$^-$ cKit$^+$ cells in imatinib + GMI-1271- compared to vehicle treated mice (P = 0.001, Figure 2F), but only a trend in reduction when compared to imatinib only-

treated mice. In summary, combination treatment of CML mice with imatinib + GMI-1271 led to a significant prolongation in overall survival of mice compared to standard treatment with a concomitant reduction of tumour burden, spleen weights and leukocytes.

Figure 2

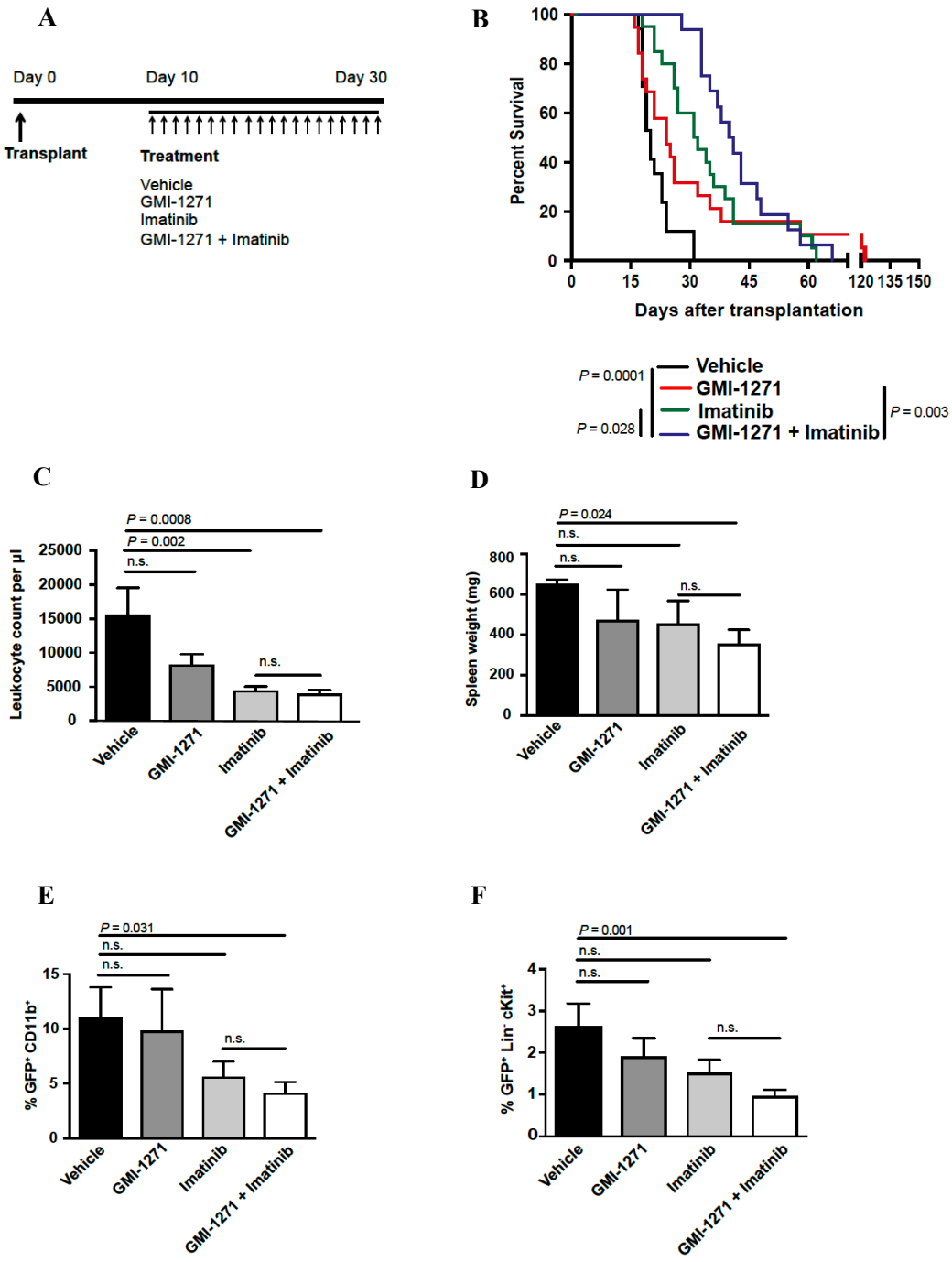

Figure 2: A) Treatment scheme for murine recipients with CML treated with vehicle, imatinib (100mg/kg), GMI-1271 (20 mg/kg) or a combination of imatinib and GMI-1271. Imatinib was administered once daily and GMI-1271 was administered twice a day. B) Kaplan-Meier-style survival curve for Balb/c recipients of BCR-ABL1-transduced BM treated with vehicle (black solid line), GMI-1271 i.p. (red), imatinib p.o. (green) and the combination of both imatinib and GMI-1271 (blue) beginning on day 10 after transplantation. The difference in survival between imatinib and imatinib and GMI-1271-treated mice was statistically significant (P = 0.028, Log-rank test, n=17). C-F) leukocytes per µl (ANOVA, Tukey test) (C), spleen weight (ANOVA, Tukey test) (D), BCR-ABL1$^+$ CD11b$^+$ (ANOVA, Tukey test) (E) and GFP$^+$ Lin$^-$ c-Kit$^+$ (ANOVA, Tukey test) (F) in bone marrow of Balb/c recipients of BCR-ABL1 transduced bone marrow treated with vehicle, GMI-1271, imatinib, imatinib and GMI-1271.

4. Inhibition to E-selectin leads to a decrease in homing and engraftment of leukaemia-initiating cells

Next, we assessed the short term homing after 18 hours of transplantation of BCR-ABL1$^+$ bone marrow, as described [5]. We observed a decrease in the percentage of BCR-ABL1$^+$ Lin$^-$ cKit$^+$ Sca1$^+$ cells which homed to the bone marrow (P = 0.03, Figure 3A) or spleen (P = 0.048, Figure 3A) of mice receiving GMI-1271 compared to vehicle. Long term engraftment of LIC was measured by Southern blot by probing the proviral integration events in splenic tissue of mice receiving vehicle, GMI-1271, imatinib or imatinib and GMI-1271 with a probe targeting GFP (Figure 3B). The number of leukaemia-initiating clones was significantly reduced in mice treated with imatinib and GMI-1271 compared to vehicle (P = 0.0002, Figure 3C) or imatinib alone (P = 0.007, Figure 3C).

This data suggests that inhibition of E-selectin with a combination of imatinib and GMI-1271 is beneficial and prolongs survival in mice with CML compared to imatinib alone. This might be due to a reduction in the homing of LIC after treatment with GMI-1271 and/or reduced long term engraftment of clones after treatment with GMI-1271and imatinib.

Figure 3

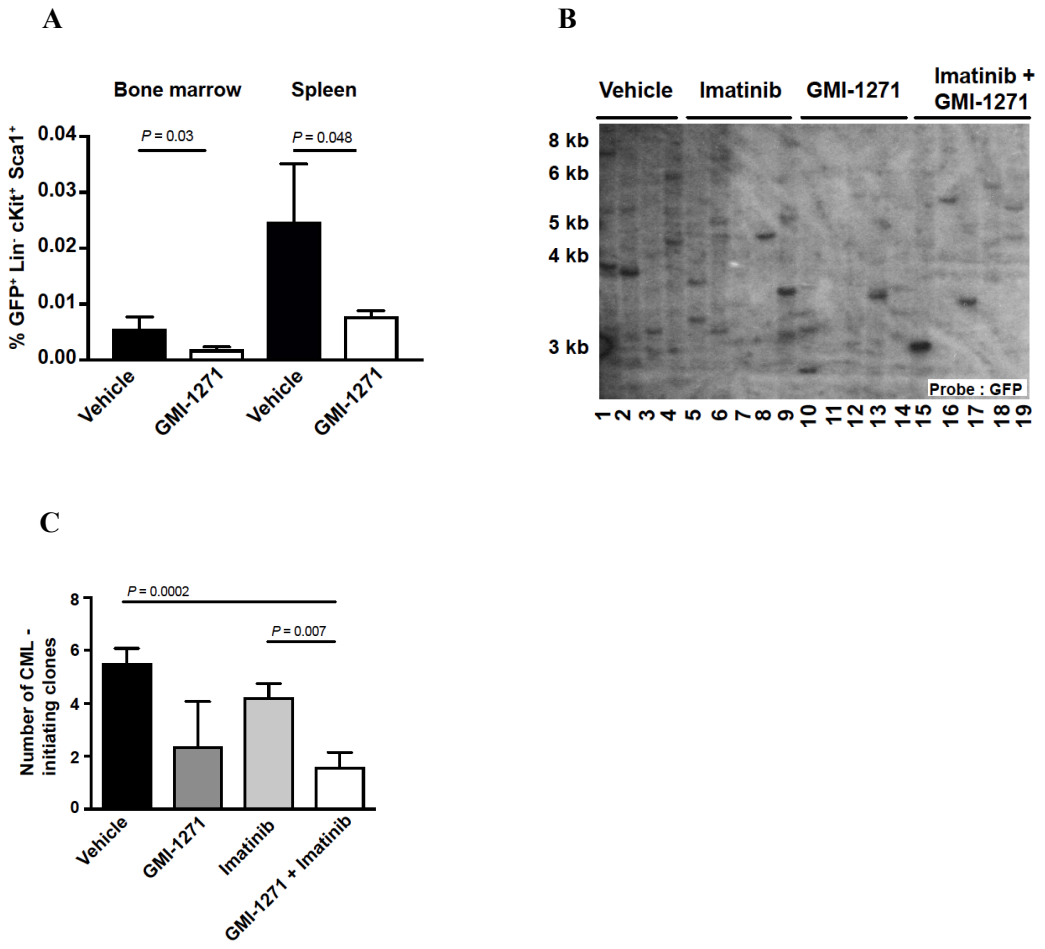

Figure 3: A) Percentage of BCR-ABL1^{+} Lin^{-} cKit^{+} Sca1^{+} cells that homed to bone marrow or spleen after 18 hours of transplantation (ANOVA, Tukey test, n=4). B) Southern blot with distant proviral integration sites, disease clonality in splenic tissues of mice receiving BCR-ABL1-transduced bone marrow and treated with vehicle (1-4), GMI-1271 (5-9), imatinib (10-14) or imatinib and GMI-1271 (17-21). C) Enumeration of clones as in B) (ANOVA, Tukey test, n=5).

5. Inhibition of E-selectin alters the localisation of leukaemic cells to endothelium

As we observed that treatment with GMI-1271 reduced the contact of cells to endothelium, we tested the localisation of LIC in the microenvironment. To study the localisation of leukaemia cells after treatment with GMI-1271 and imatinib, we performed *in vivo*

microscopy using 2 photon microscopy of leukaemia cells (BCR-ABL1$^+$ BaF3 or Lin$^-$ GFP$^+$ (BCR-ABL1$^+$)) injected into Tie2-GFP mice receiving treatment with vehicle, imatinib, GMI-1271 alone or imatinib + GMI-1271.

Interestingly, we observed a localisation of BCR-ABL1$^+$ BaF3 cells further away from endothelium in mice treated with imatinib + GMI-1271 compared to vehicle (P = 0.002, Figure 4A) and a trend towards localisation away from endothelium in mice treated with imatinib + GMI-1271 alone compared to imatinib (Figure 4A). However, the effect was more prominent in Lin$^-$ GFP$^+$ (BCR-ABL1$^+$) cells. In fact, the localisation of leukaemia cells was further away from endothelium in mice treated with imatinib + GMI-1271 compared to vehicle (P < 0.0001, Figure 4B) and imatinib alone (P = 0.001, Figure 4B). However, no significant changes in localisation of BCR-ABL1$^+$ BaF3 or Lin$^-$ GFP$^+$ (BCR-ABL1$^+$) cells were observed in relation to the bone (Figure 4C and 4D). This confirms again the role of GMI-1271 in specific inhibition of the interaction with the endothelium but not the osteoblastic niche.

Our results suggest that combination treatment with GMI-1271 + imatinib moves the leukaemia cells further away from endothelium.

Figure 4

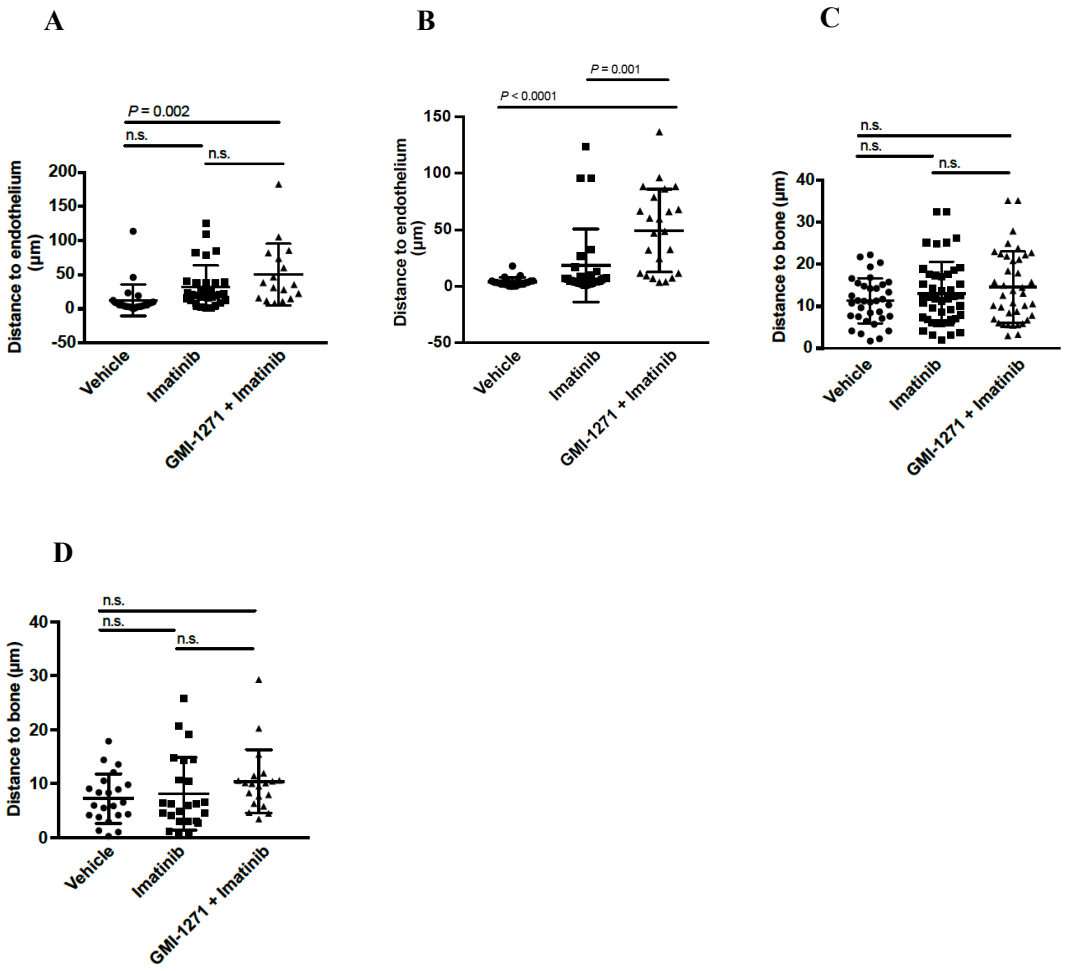

Figure 4: A-B) Shortest 3D distance (in µm) to endothelium of BCR-ABL1^{+} BaF3 cells (A) or Lin^{-} GFP^{+} (BCR-ABL1^{+}) cells (B) from FVB mice with established CML transplanted into Tie2-GFP mice (FVB background) and imaged by *in vivo* microscopy 20 hours after injection (ANOVA; Tukey Test, n=2). The imaging analysis was performed by ImageJ. C-D) Shortest 3D distance (in µm) to bone of BCR-ABL1^{+} BaF3 cells (C) or Lin^{-} GFP^{+} (BCR-ABL1^{+}) cells (D) from FVB mice with established CML transplanted into Tie2-GFP mice (FVB background) and imaged by *in vivo* microscopy 20 hours after injection (ANOVA; Tukey Test, n=2). The unirradiated recipient Tie2GFP mice were treated with vehicle (timepoints =0, 14 and 18 hours), imatinib (timepoints=0, 14 and 18 hours) and GMI-1271 and imatinib (timepoints=-2, 0, 14 and 18 hours).

6. Inhibition of E-selectin reduces adhesion of leukaemia cells and increase *Scl/Tal1* expression

Later, to understand the leukaemia cell-intrinsic mechanisms associated with non-adhesion to E-selectin we performed a set of *in vitro* adhesion assays using E-selectin- coated plates in attempt to recapitulate the *in vivo* findings. BCR-ABL1^{+} Lin^{-} cKit^{+} cells were plated on tissue culture wells pre-coated with recombinant E-selectin and treated with vehicle, GMI-1271, imatinib or imatinib and GMI-1271 for 6 hours (Figure 5A). We observed a significant reduction of adhesion to E-selectin after treatment with GMI-1271 alone (P = 0.02, Figure 5B) or in combination with imatinib (P = 0.03, Figure 5B) compared to vehicle, recapitulating our observations *in vivo* (Figure 1.1B, Figure 1.2 B-F). In order to more definitively prove specific interactions between E-selectin and GMI-1271, we performed a competitive inhibition assay by plating BCR-ABL1^{+} BaF3 cells on plates pre-coated with E-selectin. After incubation, soluble E-selectin in different concentrations was added to BCR-ABL1^{+} BaF3 with GMI-1271. This reversed the adhesion and led to an increase in the number of adherent cells to E-selectin in presence of 0.05 μg soluble E-selectin (P = 0.04, Figure 5C) or 0.1μg soluble E-selectin (P = 0.021, Figure 5C) suggesting specific interactions between E-selectin and GMI-1271.

Figure 5

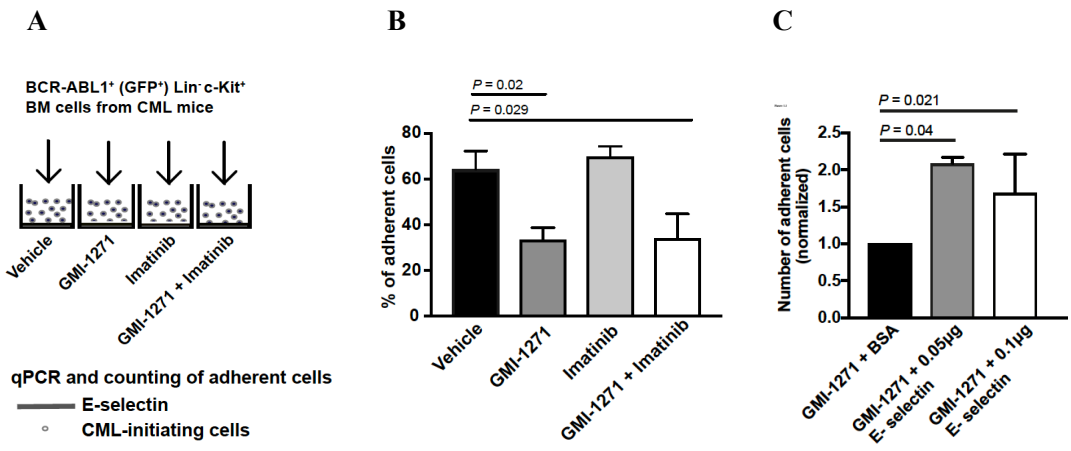

Figure 5: A) Schematic representation of an *in vitro* adhesion assay on wells pre-coated with E-selectin and addition of BCR-ABL1$^+$ Lin$^-$ cKit$^+$ or BCR-ABL1$^+$ BaF3 cells treated with vehicle, GMI-1271 (20μM), imatinib (10μM) or imatinib and GMI-1271 for 6 hours. B) Percentage of adherent BCR-ABL1$^+$ Lin$^-$ c-Kit$^+$ cells of total cells after a 6 hours incubation on recombinant E-selectin in the presence of vehicle (black), GMI-1271 (dark grey), imatinib (light grey) or imatinib plus GMI-1271 (white) normalized by the number of live cells. 20,000 cells per well had been plated in triplicate (ANOVA; Tukey Test, n=4). C) Number of adherent cells (normalised to BSA control) after a 6 hours incubation and addition of soluble E-selectin: 0.05 μg (dark grey) or 0.1 μg (white) (ANOVA; Tukey Test, n=3).

In order to see molecular changes associated due to non-adherence to E-selectin, we performed qPCR on BCR-ABL1$^+$ Lin$^-$ cKit$^+$ after adhesion as described in Figure 5A and 5B in non-adherent cells. We initially focused on *Scl/Tal1* due to its essential role as haematopoietic transcription factor involved in the regulation of haematopoietic stem cell and myeloid lineages [161,162]. Involvement of *Scl/Tal1* has also been reported in cell cycle, regulation of HSC and haematological malignancies [163]. In haematological malignancies like T-ALL, *Scl/Tal1* is reported to be overexpressed [164]. Interestingly, we observed an upregulation of the transcription factor and cell cycle regulator *Scl/Tal1* in presence of GMI-1271 alone (P = 0.017, Figure 6A). We recapitulated similar observations in K562 cells, a human BCR-ABL1$^+$ cell line, where treatment with GMI-1271 led to an increase of *SCL/TAL1* expression (P = 0.007, Figure 6B). In addition, to examine whether the observation was specific for *Scl/Tal1*, we tested several known defined and important regulatory genes involved in haematopoiesis like *MYC, GATA1, PU.1, KLF1* and *RUNX1* [15,165] in K562 cells after adhesion and inhibition of adhesion by GMI-1271 as in Figure 5A. However, we could not observe any changes in expression levels of *MYC, GATA1, PU.1, KLF1* or *RUNX1* (Figure 6C-G) after treatment with GMI-1271. We, thus, hypothesize that a connection may exist between E-selectin and *Scl/Tal1* and in order to prove it, we

performed another competitive adhesion assay as in Figure 5C by addition of soluble E-selectin to BCR-ABL1$^+$ BaF3 cells treated with GMI-1271 to neutralise the GMI-1271. Interestingly, addition of soluble E–selectin led to an increase in the adhesion of BCR-ABL1$^+$ BaF3 cells. Furthermore, qPCR showed a decrease of *Scl/Tal1* expression in adherent cells ($P = 0.028$, Figure 6 H).

Adhesion assays using human CD34$^+$ cells treated with our four drugs revealed no changes in expression patterns of *SCL/TAL1*, *MYC, GATA1, PU.1, KLF1* or *RUNX1* in non-adherent cells (Figure 7, A-F). This proves that an increase in *Scl/Tal1* expression might be specific for BCR-ABL1$^+$ cells.

To conclude, inhibition of E-selectin by GMI-1271 led to reduced adhesion of CML cells to E-selectin *in vitro* and *in vivo* accompanied by an increase in *Scl/Tal1* expression.

Figure 6

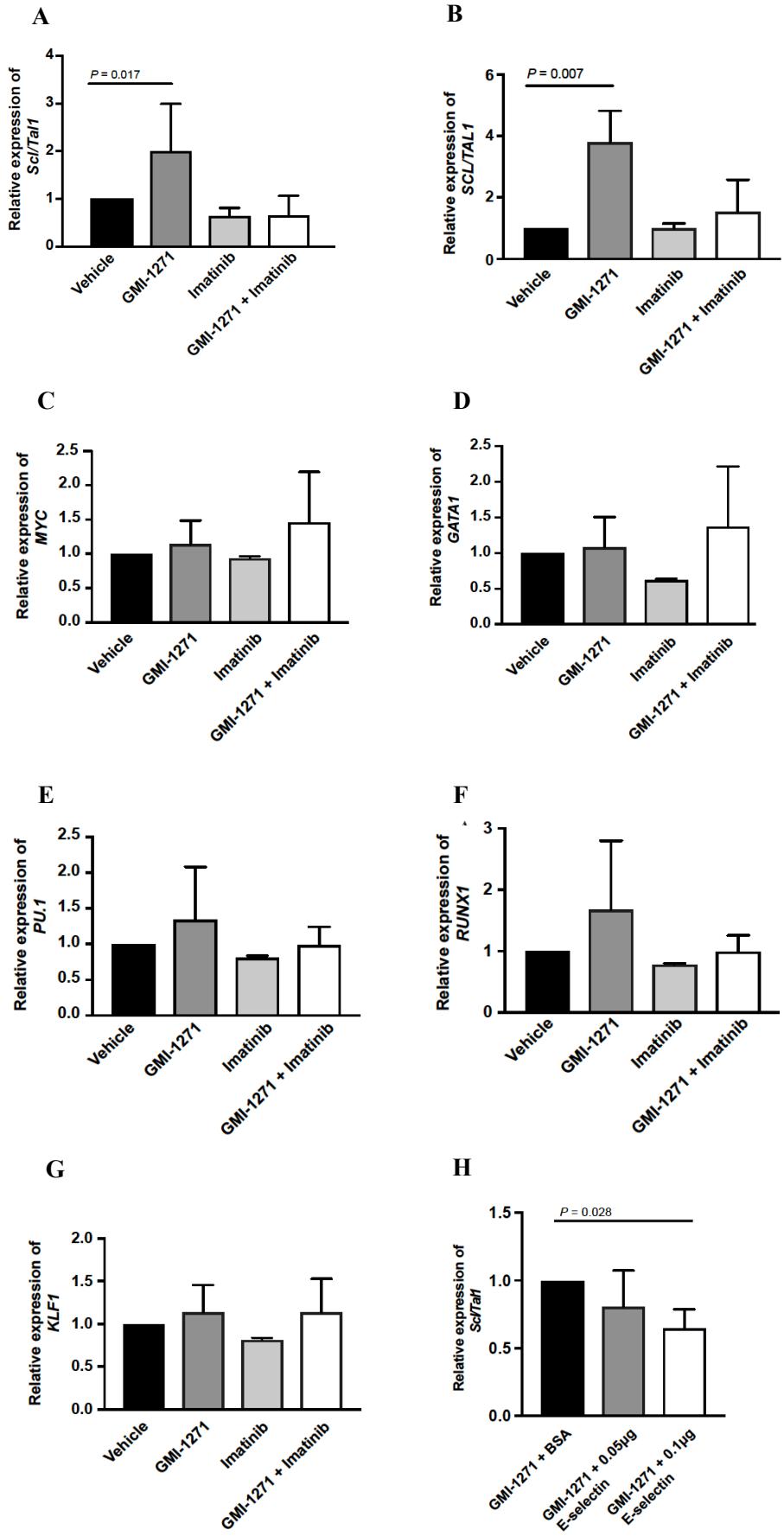
A
Relative expression of Scl/Tal1
P = 0.017
Vehicle
GMI-1271
Imatinib
GMI-1271 + Imatinib
B
Relative expression of SCL/TAL1
P = 0.007
C
Relative expression of MYC
D
Relative expression of GATA1
E
Relative expression of PU.1
F
Relative expression of RUNX1
G
Relative expression of KLF1
H
Relative expression of Scl/Tal1
P = 0.028
GMI-1271 + BSA
GMI-1271 + 0.05µg E-selectin
GMI-1271 + 0.1µg E-selectin

Figure 6 A) Relative expression of *Scl/Tal1* to GAPDH in BCR-ABL1^{+} Lin^{-} c-Kit^{+} cells plated on recombinant E-selectin as in Figure 5A) in the presence of vehicle (black), GMI-1271 (dark grey), imatinib (light grey) or imatinib plus GMI-1271 (white) (ANOVA; Tukey Test, n=3). B-G) Relative expression of *SCL/TAL1, MYC, GATA1, PU.1, KLF1* and *RUNX11* to *GAPDH* in K562 cells plated on human recombinant E-selectin in the presence of vehicle (black), GMI-1271 (dark grey), imatinib (light grey) or imatinib plus GMI-1271 (white) (ANOVA; Tukey Test, n=3). H) Relative expression of *Scl/Tal1* in BCR-ABL1^{+} BaF3 cells after a 6 hour incubation and addition of BSA or soluble E selectin 0.05 µg (dark grey) or 0.1 µg (white) and GMI-1271 (ANOVA; Tukey Test, n=3).

Figure 7

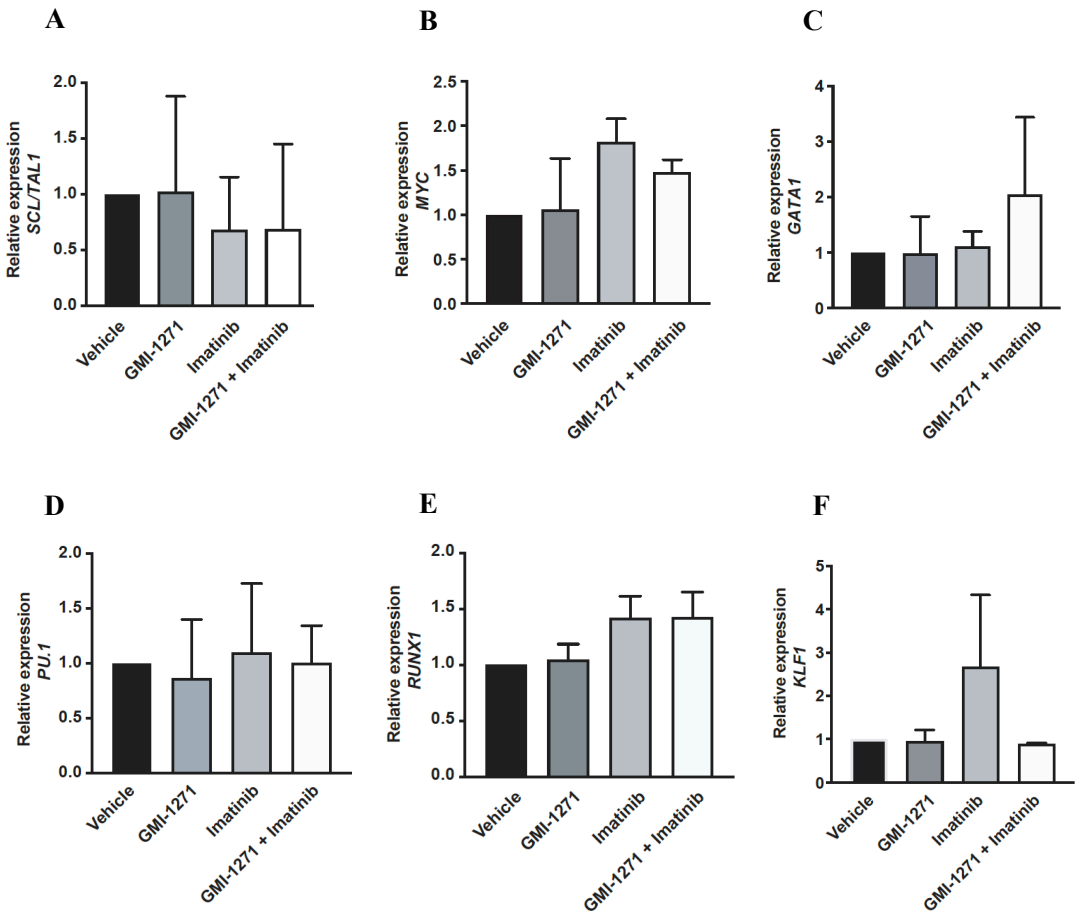

Figure 7 A-F) Relative expression of *SCL/TAL1, MYC, GATA1, PU.1, KLF1* and *RUNX11* in human CD34^{+} cells plated on human recombinant E-selectin in the presence of vehicle (black), GMI-1271 (dark grey), imatinib (light grey) or imatinib plus GMI-1271 (white) (ANOVA; Tukey Test, n=3).

7. *SCL/TAL1* regulates the expression of CD44

After the observation described in the adhesion assay in Figures 6A and 6B, we either silenced or overexpressed *SCL/TAL1* in K562 cells. In K562 cell lines, knockdown or overexpression of *SCL/TAL1* was confirmed by western blot analysis (Figure 8A and 8B). Consequently, a gene expression screen after knockdown of *SCL/TAL1* in K562 cells revealed an upregulation of CD44 (Figure 8C). CD44, an adhesion molecule, is known to bind E-selectin [166]. Moreover, CD44 and E-selectin are both known to be essential for homing and engraftment of BCR-ABL1$^+$ LIC cells in CML [5,6]. E-selectin is known to also bind other adhesion molecules on LIC such as PSGL-1, L-selectin and integrin. However, in the gene expression screen we could not observe differences in regulation of adhesion molecules other than CD44. Hence, we focused our work on CD44.

To further consolidate our findings, a qPCR analysis revealed that knockdown of *SCL/TAL1* led to upregulation of *CD44* (P = 0.0001, Figure 8D). Conversely, overexpression of *SCL/TAL1* in K562 or human CD34$^+$ cells led to downregulation of *CD44* (P = 0.0001, Figure 8E and 8F; P = 0.0001, Figure 8G).

Figure 8

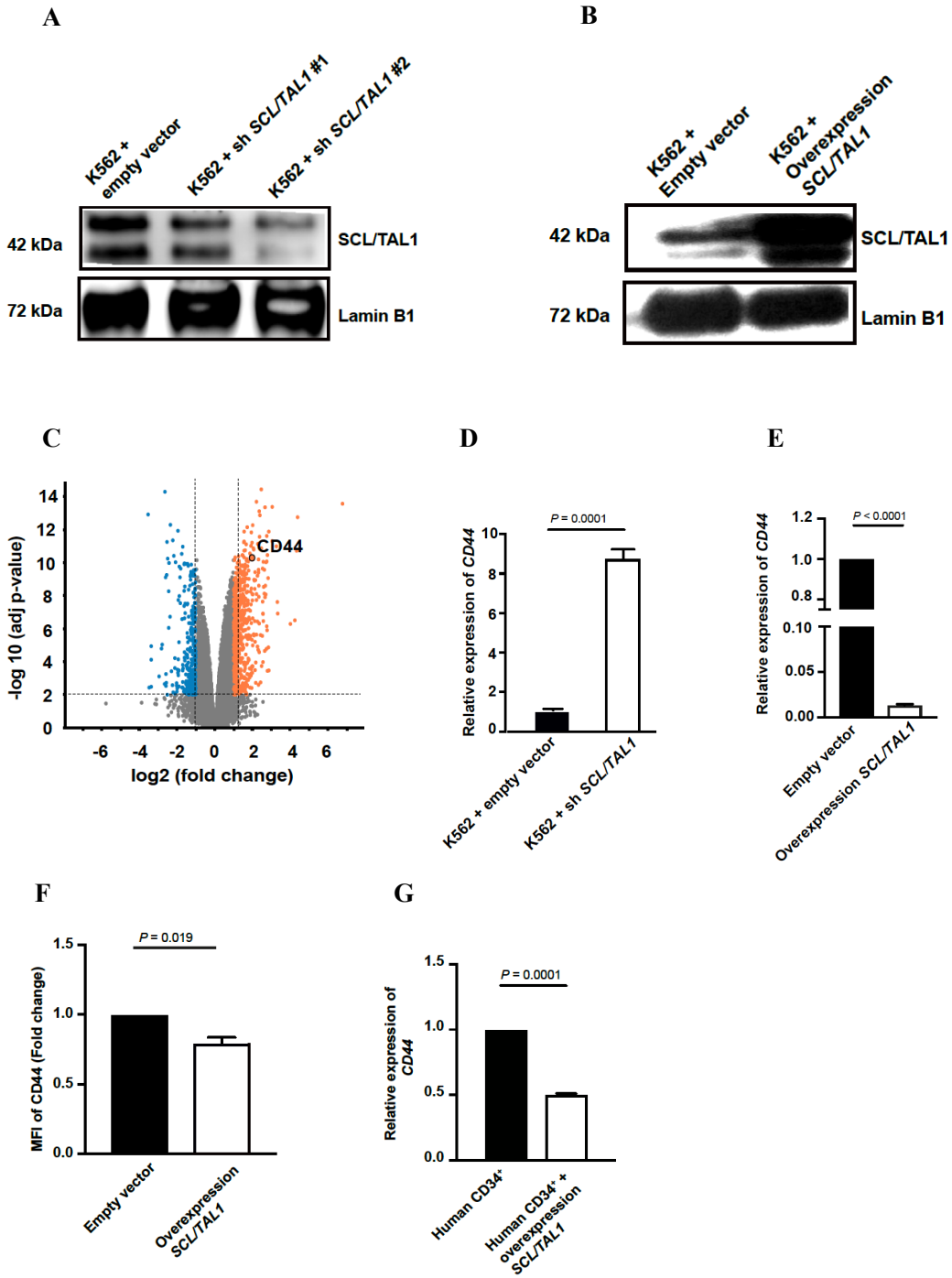
A
K562 + empty vector
K562 + sh SCL/TAL1 #1
K562 + sh SCL/TAL1 #2
42 kDa
SCL/TAL1
72 kDa
Lamin B1
B
K562 + Empty vector
K562 + Overexpression SCL/TAL1
42 kDa
SCL/TAL1
72 kDa
Lamin B1
C
-log 10 (adj p-value)
log2 (fold change)
CD44
D
P = 0.0001
Relative expression of CD44
K562 + empty vector
K562 + sh SCL/TAL1
E
P < 0.0001
Relative expression of CD44
Empty vector
Overexpression SCL/TAL1
F
P = 0.019
MFI of CD44 (Fold change)
Empty vector
Overexpression SCL/TAL1
G
P = 0.0001
Relative expression of CD44
Human CD34+
Human CD34+ + overexpression SCL/TAL1

Figure 8: A-B) Western blots showing knockdown or overexpression of SCL/TAL1 in K562 cells transduced with lentivirus expressing shRNA *scrambled* or *SCL/TAL1* or overexpressing *SCL/TAL1*. C) Volcano plot showing up- or downregulated genes in K562 cells after knockdown of *SCL/TAL1* relative to knockdown of lacZ as control. The x-axis indicates the fold change and the y-axis indicates the − log10 p value. The orange highlighted region shows a 2 fold up- and the blue region shows down-regulated genes with a P value < = 0.05. CD44 has been circled. D) Relative expression of *CD44* in K562 cells transduced with a *SCL/TAL1* shRNA-expressing or empty vector control (t-test, n=2). E) Relative expression of *CD44* in K562 cells transduced with a *SCL/TAL1*- overexpressing lentivirus or empty vector control (t-test, n=2). F) MFI (Median fluorescence intensity) of CD44 after infection with a *SCL/TAL1* overexpressing lentivirus or empty vector control (t-test, n=2). G) Relative expression of *CD44* in human $CD34^+$ cells transduced with a *SCL/TAL1* overexpressing lentivirus (t-test, n=3).

8. SCL/TAL1 regulates *CD44* expression at a transcriptional level

We hypothesized that SCL/TAL1 regulates the expression of *CD44* on CML cells, which is known to be overexpressed on CML cells [5]. In order to test whether SCL/TAL1 regulates CD44, we established a luciferase model using 293T or K562 cells which allows to assess the activity of CD44 by luciferase assay. Therefore, the CD44 regulatory element known to have *SCL/TAL1* binding sites (Figure 9A) was cloned into a vector containing a luciferase gene. Three different constructs containing different lengths of the CD44 regulatory element were obtained (Figure 9A). Individual transfection of these 3 constructs containing the same CD44 regulatory element regions into 293T cells led to a decrease in luciferase activity (CD44 activity) (Figure 9B). However, transfection of only construct 1 (short) in 293T cells significantly reduced luciferase activity (CD44 activity) compared to empty vector (P = 0.043, Figure 9B). Similar results were obtained after transfection in K562 cells, where construct 1 (short) significantly reduced CD44 activity (P = 0.03, Figure 9C). Therefore, we

performed further experiments only with construct 1(short). A luciferase assay on K562 cells transduced with either shRNA *scrambled*- or *SCL/TAL1*-expressing or *SCL/TAL1*-overexpressing lentivirus and transfection with control plasmid or CD44 regulatory element containing *SCL/TAL1* binding sites revealed decreased activity of CD44 when *SCL/TAL1* was overexpressed (P = 0.02, Figure 9D) and increased activity after knockdown of *SCL/TAL1* (P = 0.049, Figure 9D).

This confirms that SCL/TAL1 binds the CD44 regulatory element and controls its expression by reducing CD44 activity.

Figure 9

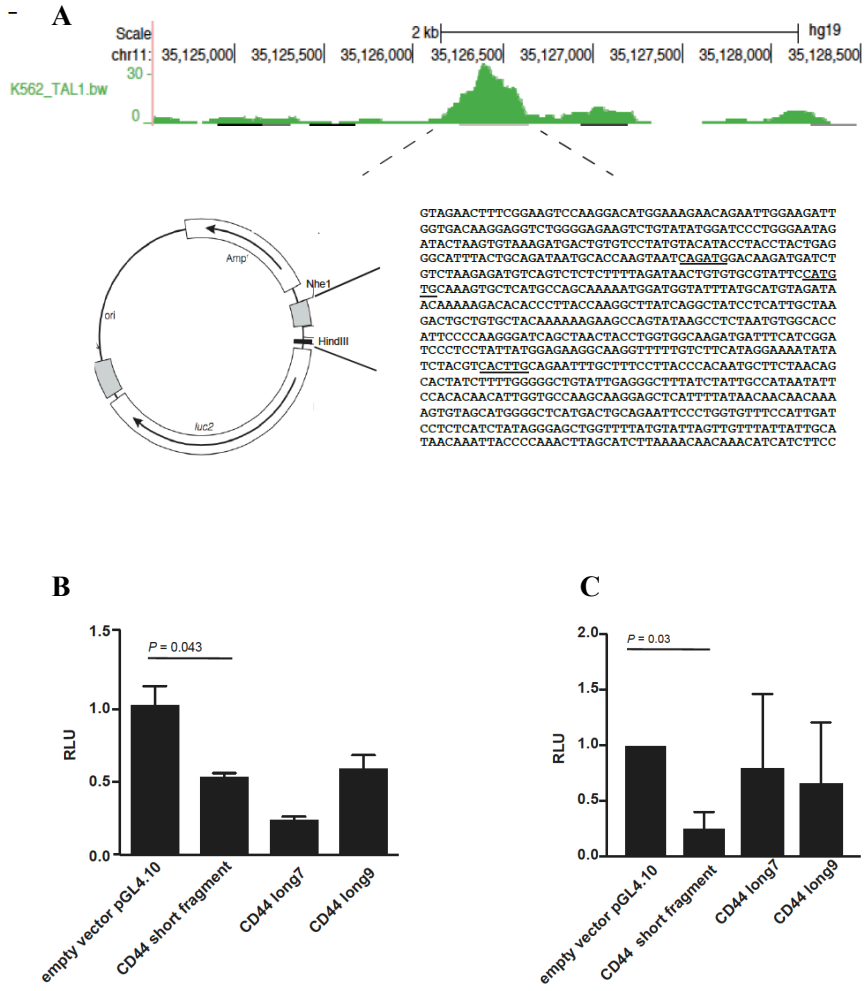

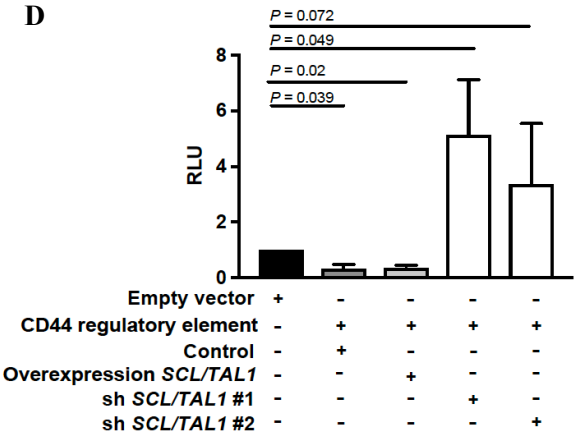

Figure 9 A) Cloning of a 700bp NheI - HindIII fragment from the human CD44 regulatory element containing SCL/TAL1 binding sites (underlined) into the pGL4.23 vector for use in the luciferase assays. SCL/TAL1 binding sites have the sequence CANNTG. B-C) Relative luminescence units (RLU) in the luciferase assay in 293T (B) and K562 cells (C) transfected with luciferase vector with fragments of 3 sizes, with each containing SCL/TAL1 binding sites (ANOVA; Tukey Test, n=3). D) Relative luminescence units (RLU) in a luciferase assay of K562 cells transfected with empty vector or a plasmid expressing the CD44 regulatory element alone in K562 cells transduced with a *SCL/TAL1*-overexpressing lentivirus (ANOVA; Tukey Test) or transduced with two different sh *SCL/TAL1*-expressing lentiviri (ANOVA; Tukey Test, n=4).

9. Imatinib increases the binding of SCL/TAL1 to the CD44 regulatory element

Next, we assessed the dependence of the regulation of CD44 expression on BCR-ABL1. To check the involvement of BCR-ABL1 for SCL/TAL1-dependent regulation of CD44, we designed a chromatin immunoprecipitation (ChIP) assay with 4 different primers binding to the CD44 regulatory element (Figure 10A). We treated K562 cells with vehicle or imatinib for 8 hours to block the kinase activity of BCR-ABL1 and performed a ChIP assay. This revealed an increase in the percent input or binding of SCL/TAL1 to the CD44 regulatory element, as tested by 4 different primers sets ($P = 0.001$, Figure 10B). As a negative control, we amplified regions in chromosome 18 and no profound differences was observed (Figure 10C). This experiment shows that imatinib abrogates BCR-ABL1 activity, as expected, and

in turn leads to an increase in the binding of SCL/TAL1 to the CD44 regulatory element resulting in decreased CD44 expression/activity.

Figure 10

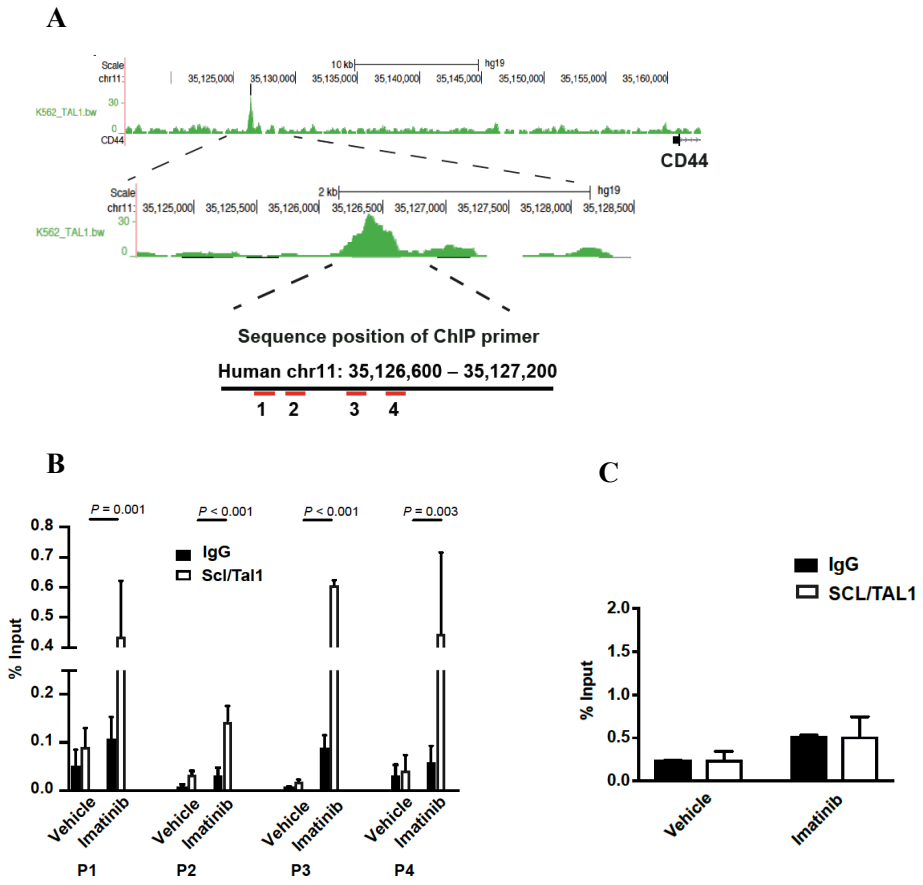

Figure 10 A) Genome from the UCGS genome browser representing human chromosome 11 and the sequence position of 4 primers binding to regions in the CD44 regulatory element for use in the ChIP assay. B) Graph representing the percent input of binding of SCL/TAL1 to the CD44 regulatory element using 4 different primer sets by qPCR in vehicle (black)- or imatinib (white)-treated K562 cells in the ChIP assay (n=3, t-test). C) Percent input of binding of SCL/TAL1 to chromosome 18 by qPCR in vehicle (black)- or imatinib (white)-treated K562 cells in the ChIP assay (n=2, t-test).

10. Overexpression of *Scl/Tal1* leads to prolongation of survival in murine CML

Our findings suggest that Scl/Tal1 negatively regulates the expression of *CD44*. Further, deficiency of CD44 is known to prolong the survival of mice with CML [5]. In order to identify the role of Scl/Tal1 *in vivo*, we aimed at overexpressing *Scl/Tal1* on LIC in murine studies of CML. Overexpression of *Scl/Tal1* in BCR-ABL1$^+$ BaF3 cells was confirmed by Western blot (Figure 11A). Consequently, we performed *in vivo* experiments having transduced LIC with a lentivirus overexpressing *Scl/Tal1* and transplanting these LIC into murine recipients. Overexpression of *Scl/Tal1* in BCR-ABL1$^+$ LIC led to a prolongation of survival of mice (P = 0.017, Figure 11B). The leukocyte count (P = 0.031, Figure 11 C) and tumour burden (P = 0.07, Figure 11D) were significantly reduced in mice with overexpressing *Scl/Tal1*, whereas spleen weights (Figure 11E) showed a trend towards reduction in mice transplanted with *Scl/Tal1* overexpressing LIC. The mean fluorescence intensity (MFI) of CD44 was reduced in mice with overexpressing *Scl/Tal1* (P = 0.031, Figure 11F). Southern blotting of spleen tissue from these mice showed a trend towards decreased clonality in mice which had received LIC overexpressing *Scl/Tal1* (Figure 11G). These data suggest that overexpression of *Scl/Tal1* leads to prolongation of survival of mice in CML via partial reduction of CD44 expression.

Figure 11

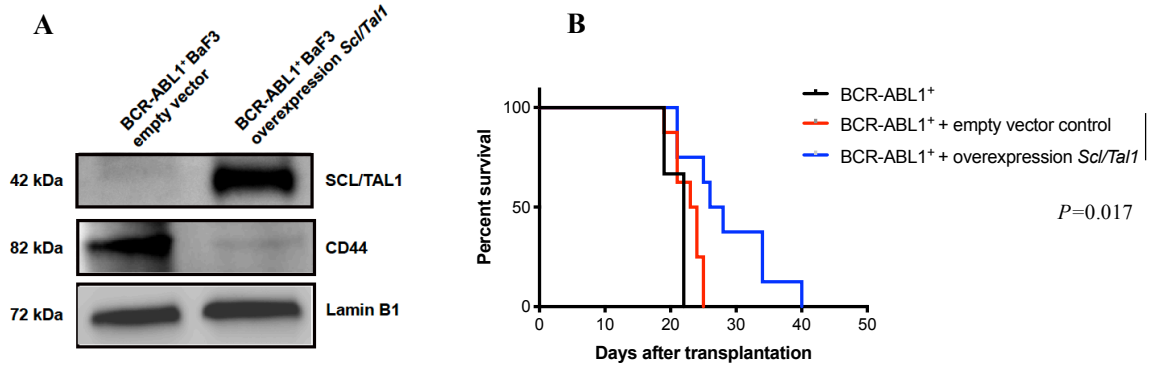

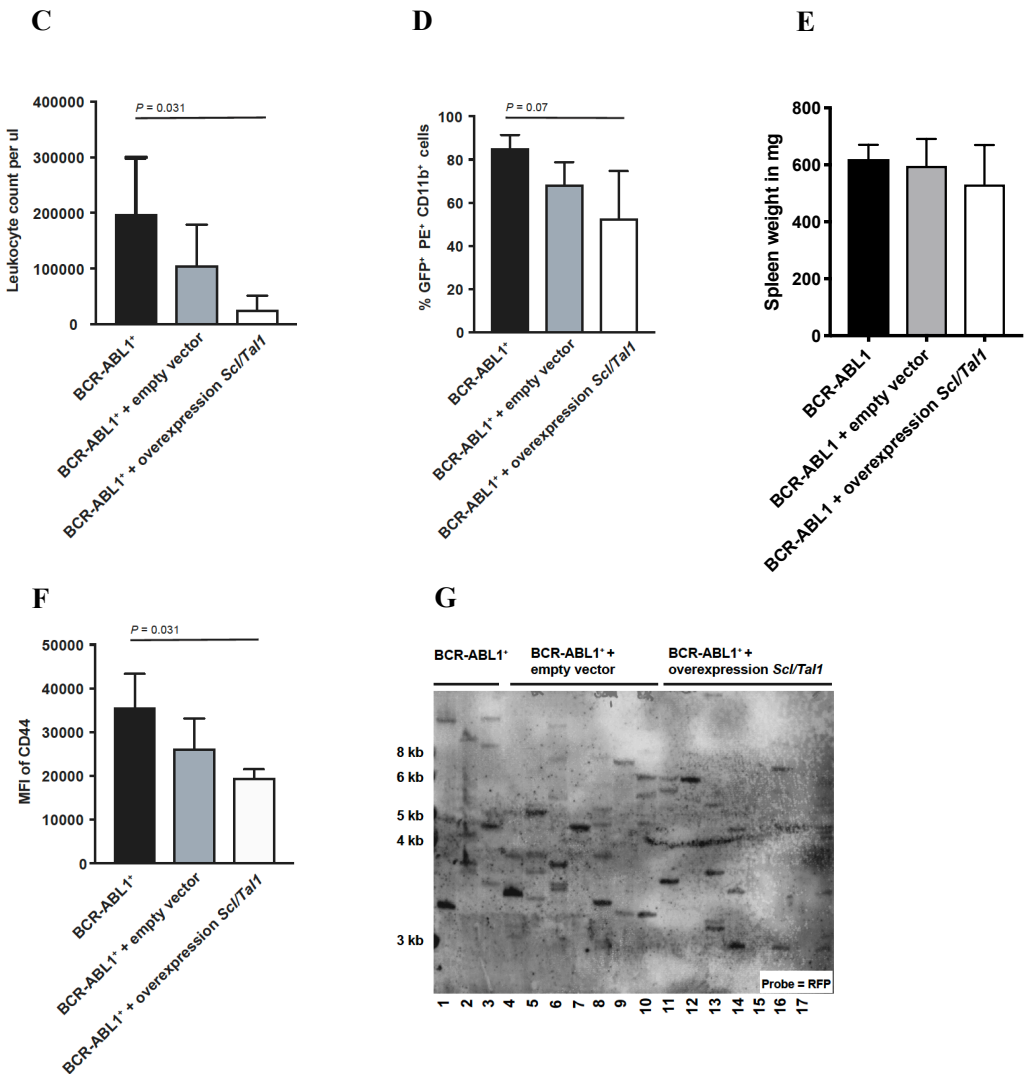

Figure 11 A) Western blot of the expression of SCL/TAL1 (42 kDa), CD44 (82 kDa) or Lamin B1 (72 kDa) in BCR-ABL1$^+$ BaF3 cells co-transduced with empty vector control- or the *Scl/Tal1*-overexpressing lentivirus. The immunoblot is representative of 2 independent experiments. B) Kaplan-Meier-style survival curve of Balb/c recipients with BCR-ABL1-transduced bone marrow (black) or BCR-ABL1-transduced bone marrow co-transduced with empty vector (red) or co-transduced with an *Scl/Tal1*-overexpressing lentivirus (blue) (Log-rank test, n=8). C-E) Leukocytes per µl (C), % GFP$^+$ PE$^+$ CD11b$^+$ cells (D) and spleen weights (E) in peripheral blood of recipients of BCR-ABL1-transduced bone marrow alone or co-transduced with empty vector or *Scl/Tal1*-overexpressing lentivirus (ANOVA; Tukey Test). F) Median fluorescence intensity (MFI) of CD44 in peripheral blood of recipients of BCR-ABL1-transduced bone marrow alone or co-transduced with empty vector or *Scl/Tal1*-overexpressing lentivirus (ANOVA; Tukey Test). G) Southern blot

showing distant proviral integration sites, representing disease clonality, in splenic tissues (taken at the time of death) of Balb/c recipients of bone marrow transduced with BCR-ABL1 alone (lanes 1-3), BCR-ABL1 plus empty vector control- (lanes 4-10) or BCR-ABL1 plus *Scl/Tal1*-overexpressing lentivirus (lanes 11-17).

11. Binding of CD44 to E-selectin might play a role in cell cycle regulation

In order to study the interaction between CD44 on leukaemia cells and the bone marrow microenvironment, we performed *in vivo* imaging using 2-photon microscopy. Imaging of the calvarium of Tie2GFP mice transplanted with BCR-ABL1$^+$ BaF3 or BCR-ABL1$^+$ BaF3 cells overexpressing CD44 showed an increased contact time of BCR-ABL1$^+$ BaF3 overexpressing CD44 to the endothelial layer suggesting an increase in adhesion ($P < 0.001$, Figure 12.1A).

Figure 12.1

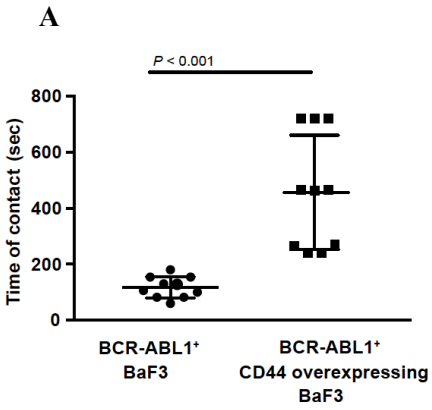

Figure 12.1 A) Time of contact of BCR-ABL1$^+$ BaF3 and BCR-ABL1$^+$ BaF3 cells overexpressing CD44 to endothelium in unirradiated Tie2GFP mice after 2 hours of injection (n=3, t-test).

It is well studied the involvement of SCL/TAL1 for the regulation of the cell cycle in haematopoietic progenitor cells [163]. As we observed above that the SCL/TAL1 – CD44 axis is of major importance in BCR-ABL1$^+$ cells, we tested the influence of CD44 on cell cycle in BCR-ABL1$^+$ cells. We performed an *in vitro* adhesion assay plating BCR-ABL1$^+$ BaF3 cells overexpressing CD44 on plates pre-coated with E-selectin or BSA in the presence of vehicle, GMI-1271, imatinib or GMI-1271 plus imatinib. After adhesion, we performed cell

cycle analysis with Ki67 and DAPI stains on the non-adherent fraction of cells (Figure 12.2 A). However, no significant changes in the G0, G1 or G2-S-M phases of the cell cycle between the different treatments on BSA (Figure 12.2 B) or E-selectin (Figure 12.2 C) coated plates were observed.

Figure 12.2

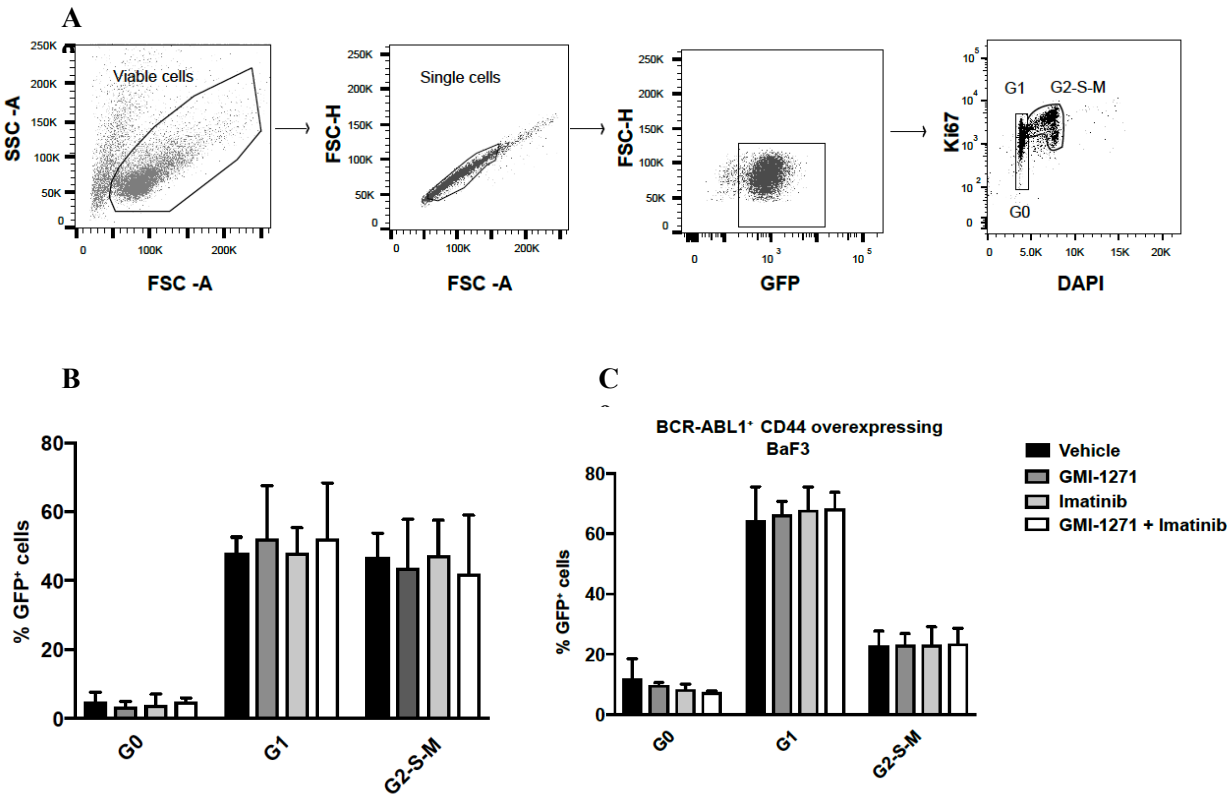

Figure 12.2 A) Gating strategy for cell cycle analysis with Ki67 and DAPI in the non-adherent or adherent fraction of BCR-ABL1$^+$ BaF3 or BCR-ABL1$^+$ BaF3 cells overexpressing CD44. B-C) Percentage of non-adherent BCR-ABL1$^+$ BaF3 overexpressing CD44 cells in the G0, G1 or G2-S-M phase of the cell cycle when plated on wells pre-coated with BSA (B) or E-selectin (C) and treated with vehicle, GMI-1271, imatinib or GMI-1271 plus imatinib (n=3, ANOVA; Tukey test).

12. Inhibition of E-selectin leads to an increase in cell cycle

We observed previously that inhibition of E-selectin with GMI-1271 led to an increase in *Scl/Tal1* expression, and SCL/TAL1 is shown to be correlated with an increase in cell cycle [163,167]. In order to address the effect of GMI-1271 on the cell cycle of the non-adherent and adherent fractions of BCR-ABL1$^+$ BaF3 cells following treatment with GMI-1271 and imatinib by adhesion assay, we plated these cells on plates pre-coated with BSA or E-selectin (Figure 13 A). Treatment of BCR-ABL1$^+$ BaF3 with GMI-1271 or imatinib did not show changes in G0, G1 or G2-S phase in non-adherent cells plated on a plate pre-coated with BSA (Figure 13B). However, on a plate pre-coated with E-selectin, an increase in the G2-S-M phase of the cell cycle and a decrease in G0 in the non-adherent fraction of BCR-ABL1$^+$ BaF3 cells were found after treatment with GMI-1271 only (P = 0.03, Figure 13C) or in combination with imatinib (P = 0.02, Figure 13C). Interestingly, the adherent fraction of cells in contact with E-selectin did not show any changes in cell cycle phases between treatments (Figure 13D). Based on our results *in vitro*, we performed a cell cycle analysis in an *in vivo* experiment as in Figure 2A. BCR-ABL1$^+$ Lin$^-$ c-Kit$^+$ leukaemia stem cells in CML mice treated with GMI-1271 only (P = 0.01, Figure 13 E) or with imatinib (P < 0.0001, Figure 13 E) had an increase in the fraction of cells in G2-S-M phase of the cell cycle, confirming the observations *in vitro*. These data suggest that treatment with GMI-1271 leads to non-adhesion and an increase in cell cycle specific to E-selectin *in vivo* and *in vitro*.

Figure 13

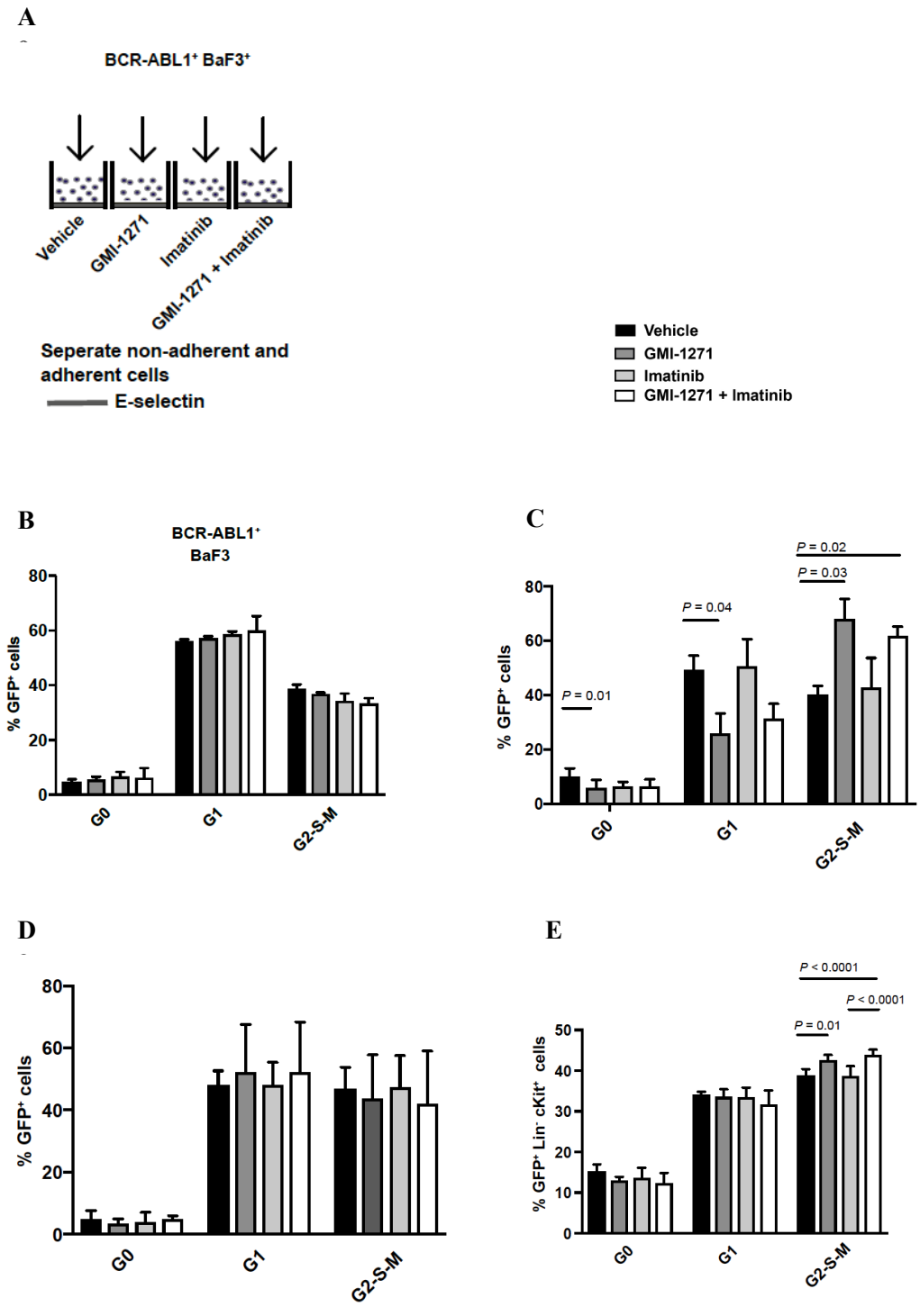
A
BCR-ABL1+ BaF3+
Vehicle
GMI-1271
Imatinib
GMI-1271 + Imatinib
Seperate non-adherent and adherent cells
E-selectin
Vehicle
GMI-1271
Imatinib
GMI-1271 + Imatinib
B
BCR-ABL1+ BaF3
% GFP+ cells
G0
G1
G2-S-M
C
P = 0.02
P = 0.03
P = 0.04
P = 0.01
% GFP+ cells
G0
G1
G2-S-M
D
% GFP+ cells
G0
G1
G2-S-M
E
P < 0.0001
P < 0.0001
P = 0.01
% GFP+ Lin- cKit+ cells
G0
G1
G2-S-M

Figure 13 A) Schematic representation of adhesion assay on pre-coated BSA or E-selectin wells and incubation of BCR-ABL1$^+$ BaF3 cells along with treatment - vehicle, GMI-1271, imatinib or GMI-1271 plus imatinib. B) Percentage of G0, G1 or G2-S-M phase of the cell cycle in non-adherent BCR-ABL1$^+$ BaF3 cells plated on pre-coated BSA. C-D) Percentage of G0, G1 or G2-S-M phases of the cell cycle in non-adherent (C) or adherent (D) BCR-ABL1$^+$ BaF3 cells plated on plates pre-coated with E-selectin. E) Percentage of BCR-ABL1$^+$ Lin$^-$ c-Kit$^+$ cells in recipients of bone marrow transduced with BCR-ABL1 and treated with vehicle, GMI-1271, imatinib or GMI-1271 plus imatinib as in Figure 2A in the G0, G1 or G2-S-M phases of the cell cycle.

13. Inhibition of E-selectin changes expression of cell cycle regulators

Cell cycling is tightly regulated by an interplay between different cyclin dependent kinases (CDK) and CDK inhibitors [168]. CDKs like CDK2, CDK4 and CDK6 and inhibitors like p16, p21 and p27 participate in regulation of the cell cycle. It is known that SCL/TAL1 is associated with an increase in cell cycle by acting as a repressor of p16 (a cell cycle inhibitor) and p21 [169] [124]. To understand whether CDKs are involved in an increase in cell cycle after treatment with GMI-1271 as in Figure 14 C, we performed immunofluorescence (IF) on BCR-ABL1$^+$ BaF3 cells after an adhesion assay on a plate pre-coated with E-selectin (Figure 13A). IF of non-adherent BCR-ABL1$^+$ BaF3 cells treated with GMI-1271 revealed changes in nuclear localisation of p16 (Figure 14A) and CDK4 (Figure 14B). Quantification of the fluorescence suggested a decrease in nuclear localisation of p16 ($P < 0.0001$, Figure 14C) and an increase in nuclear localisation of CDK4 ($P < 0.0001$, Figure 14D) after treatment with GMI-1271. Similarly, IF of non-adherent BCR-ABL1$^+$ BaF3 cells treated with GMI-1271 led to an increase in nuclear localisation of CDK4 (Figure 14E). However, quantification of the nuclear fluorescence did not reveal any significant changes (Figure 14F). p21 levels in the nucleus remained unaffected after treatment with GMI-1271 (Figure 14G).

Figure 14

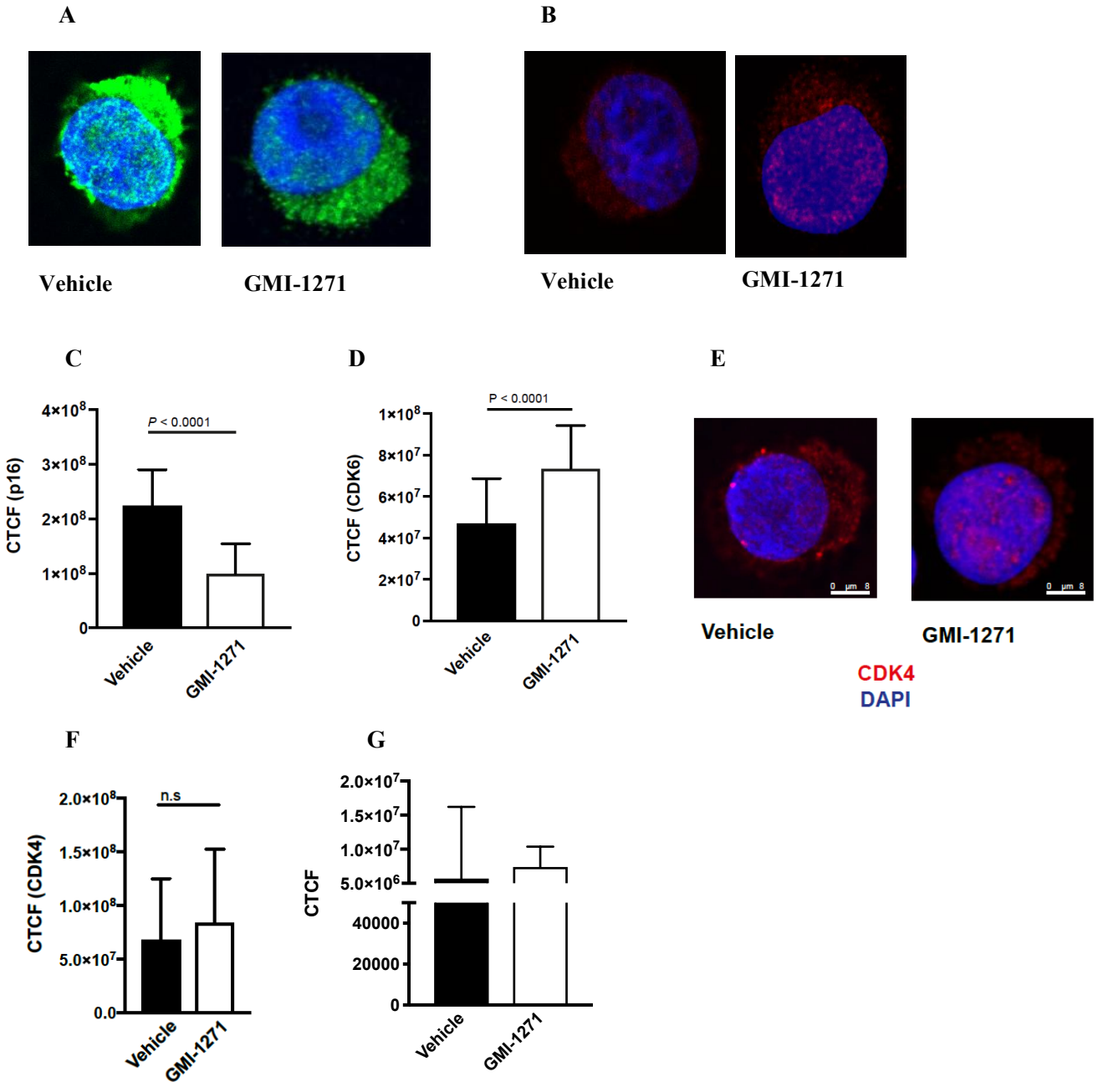

Figure 14 A-B) Representative immunofluorescence image of non-adherent BCR-ABL1^{+} BaF3 cells after performance of an adhesion assay showing the localisation of p16 (A) and CDK4 (B) in the nucleus or cytoplasm. C-D) CTCF (Corrected total fluorescence intensity) of p16 (C) and CDK4 (D) in the nucleus of BCR-ABL1^{+} BaF3 cells (n=3, t-test). E) Representative immunofluorescence image

of BCR-ABL1$^+$ BaF3 cells after an adhesion assay stained with anti-CDK4. F-G) CTCF of CDK4 (F) or p21 (G) in the nucleus of BCR-ABL1$^+$ BaF3 cells (n=3, t-test).

To confirm our findings in primary cells we performed immunofluorescence on Lin$^-$ BCR-ABL1$^+$ cells from CML mice following treatment with vehicle or GMI-1271 as in Figure 2A. Indeed, this revealed an increase in nuclear expression of SCL/TAL1 (P = 0.04, Figure 15B) and a decrease in the nuclear expression of p16 after treatment with GMI-1271 (P = 0.002, Figure 15C).

Figure 15

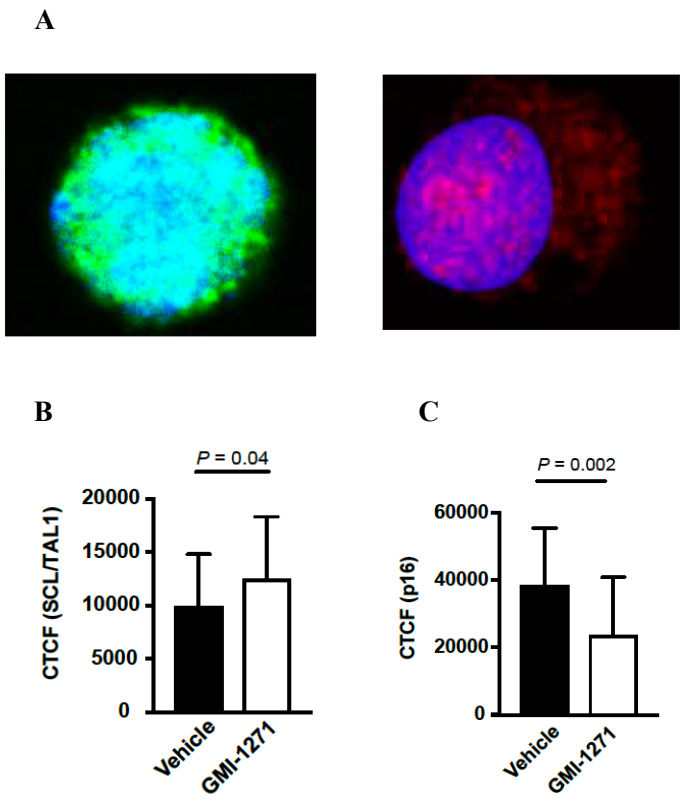

Figure 15 A) Representative immunofluorescence image of BCR-ABL1$^+$ Lin$^-$ cells from murine recipients receiving of BCR-ABL1$^+$ bone marrow treated with vehicle and GMI-1271. B-C) CTCF of nuclear SCL/TAL1 (B) and p16 (C) in BCR-ABL1$^+$ Lin$^-$ cells as in Figure 15A.

14. A synergistic effect of GMI-1271 and imatinib leads to decreased expression of CD44

In our ChIP studies, we had demonstrated that treatment of CML cells with imatinib leads to increased binding of SCL/TAL1 to the CD44 regulatory element. This resulted in a reduction of *CD44* transcription. In parallel, we showed that treatment with GMI-1271 led to an increase in SCL/TAL1 expression via non-adhesion to E-selectin. Starting from these observations, we hypothesised that there may be a synergistic effect of combination treatment of imatinib plus GMI-1271 on CD44 expression levels. To address this, we performed preliminary adhesion assays of BCR-ABL1$^+$ BaF3 or BaF3 cells on plates pre-coated with E-selectin. We observed an increase in the median fluorescence intensity (MFI) of CD44 in BCR-ABL1$^+$ BaF3 cells ($P < 0.0001$, Figure 16A) when plated on wells pre-coated with E-selectin. Additionally, treatment of BCR-ABL1$^+$ BaF3 or empty vector$^+$ BaF3 cells with imatinib plated on wells pre-coated with E-selectin led to a decrease of the MFI of CD44 in BCR-ABL1$^+$ BaF3 cells, but no effect was observed in empty vector$^+$ BaF3 cells ($P = 0.05$, Figure 16A and 16B). This confirms the specificity of the effect of imatinib in inhibiting BCR-ABL1 activity and reducing CD44 expression. In another adhesion assay with BCR-ABL1$^+$ BaF3 cells plated on wells pre-coated with E-selectin, treatment with imatinib led to a reduction of the MFI of CD44 ($P = 0.05$, Figure 16C). The effect was much more prominent in the non-adherent fraction of BCR-ABL1$^+$ BaF3 cells after combination treatment with imatinib and GMI-1271 ($P = 0.005$, Figure 16C). On the contrary, reduced levels of CD44 after combination treatment were only observed in non-adherent BCR-ABL1$^+$ BaF3 cells whereas no changes in CD44 expression were observed in adherent BCR-ABL1$^+$ BaF3 cells (Figure 16C).

These results indicate synergistic effects of GMI-1271 and imatinib on the reduction of CD44 expression in BCR-ABL1$^+$ cells. The results also implicate differential behaviour of BCR-ABL1$^+$ BaF3 cells, non-adherent or adherent to E-selectin, after treatment with GMI-1271 or imatinib in relation to CD44 expression.

Figure 16

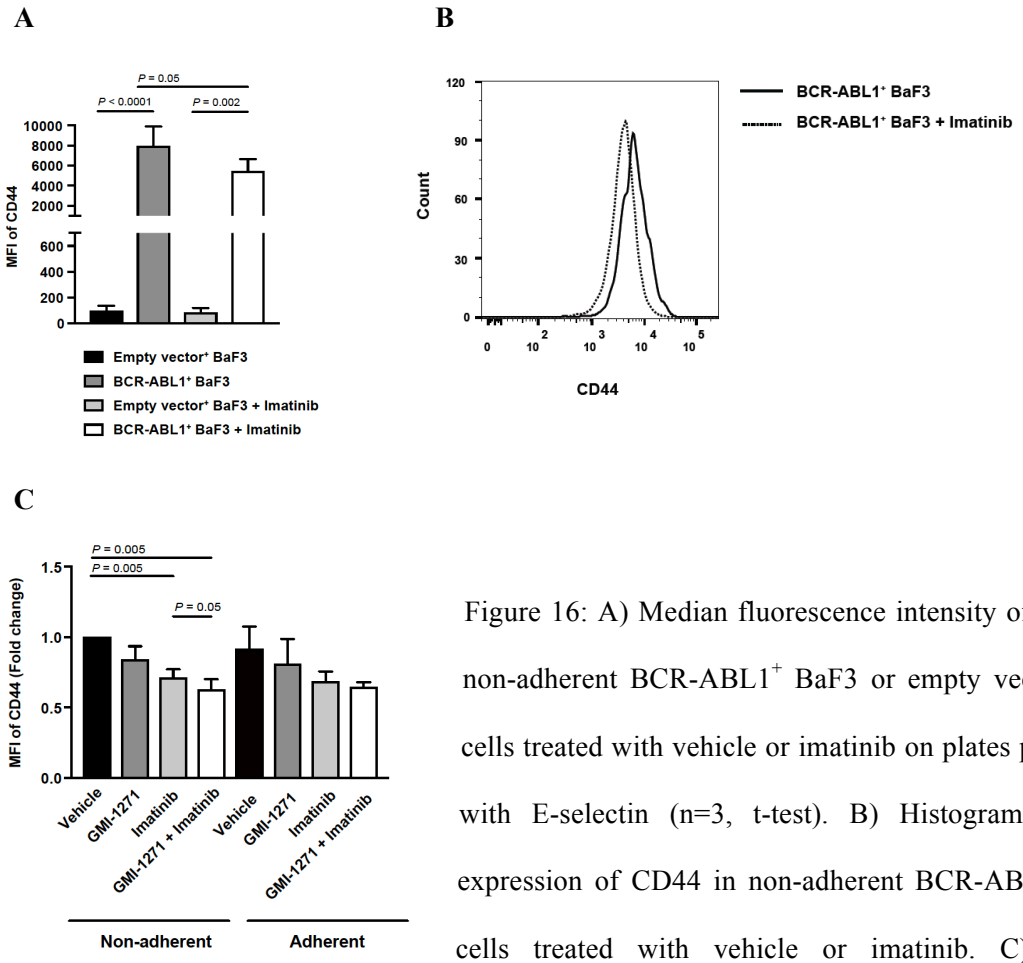

Figure 16: A) Median fluorescence intensity of CD44 in non-adherent BCR-ABL1$^+$ BaF3 or empty vector BaF3 cells treated with vehicle or imatinib on plates pre-coated with E-selectin (n=3, t-test). B) Histogram showing expression of CD44 in non-adherent BCR-ABL1$^+$ BaF3 cells treated with vehicle or imatinib. C) Median fluorescence intensity of CD44 in non-adherent or adherent BCR-ABL1$^+$ BaF3 plated on plates pre-coated with E-selectin and treated with vehicle, GMI-1271, imatinib or GMI-1271 plus imatinib (normalized to non-adherent vehicle-treated cells) (n=3, t-test).

15.BCR-ABL1 indirectly phosphorylates SCL/TAL1

The BCR-ABL1 fusion protein is an active tyrosine kinase, and it is known to phosphorylate multiple targets downstream [170], including the JAK-STAT pathway, the PI3K pathway and

the ERK pathway. Since SCL/TAL1 activity is regulated by phosphorylation at the T90 and S122 sites [171,172], we hypothesised that BCR-ABL1 may regulate the phosphorylation of SCL/TAL1. However, as SCL/TAL1 does not contain tyrosine phosphorylation sites, we hypothesised that AKT, phosphorylated by BCR-ABL1 [173], might act as an intermediate molecule phosphorylating SCL/TAL1 [171]. To test this hypothesis, we treated K562 cells with imatinib, wortmannin (a PI3K pathway inhibitor), MK-2226 (an AKT inhibitor) and performed Western blots on nuclear extracts. We observed that treatment with imatinib led to a decrease in the phosphorylation of SCL/TAL1 at the T90 and S122 sites (Figure 17A). Similarly, a prominent decrease in phosphorylation was observed at T90 and S122 sites after treatment with wortmannin (PI3K pathway inhibitor) and MK-2206 (AKT inhibitor). Indeed, treatment with imatinib, wortmannin (PI3K pathway inhibitor), MK-2206 (AKT inhibitor) also reduced phospho AKT levels. These observations indicated that phosphorylation of SCL/TAL1 is likely regulated via the PI3K/AKT pathway. To validate the results from the Western blot, we performed quantitative mass spectrometry by using triple stable isotope labelling with amino acids in cell culture (SILAC) of K562 cells treated with vehicle, imatinib or MK-2206. This demonstrated the mass increments from the medium (+6 Da) or heavy (+10 Da) SILAC-labeling on arginine on the pS122-bearing peptide “oxMVQLpSPPALAAPAAPGR” of SCL/TAL1 in MK-2206 treated cells at 2 and 4 hours (Figure 17B). Quantitative measurements by comparing the areas under the extracted ion chromatograms (XICs) of individual SILAC triplets revealed the decrease in relative abundance of phospho TAL1 S122 two and four hours after inhibition with MK-2206 (Figure 17C). Similarly, treatment with imatinib led to a decrease in relative abundance of phospho TAL1 S122 (Figure 17D). This confirmed that BCR-ABL1 phosphorylates pAKT, which in turn phosphorylates pTal1 T90 and pTal1 S122 sites.

Figure 17

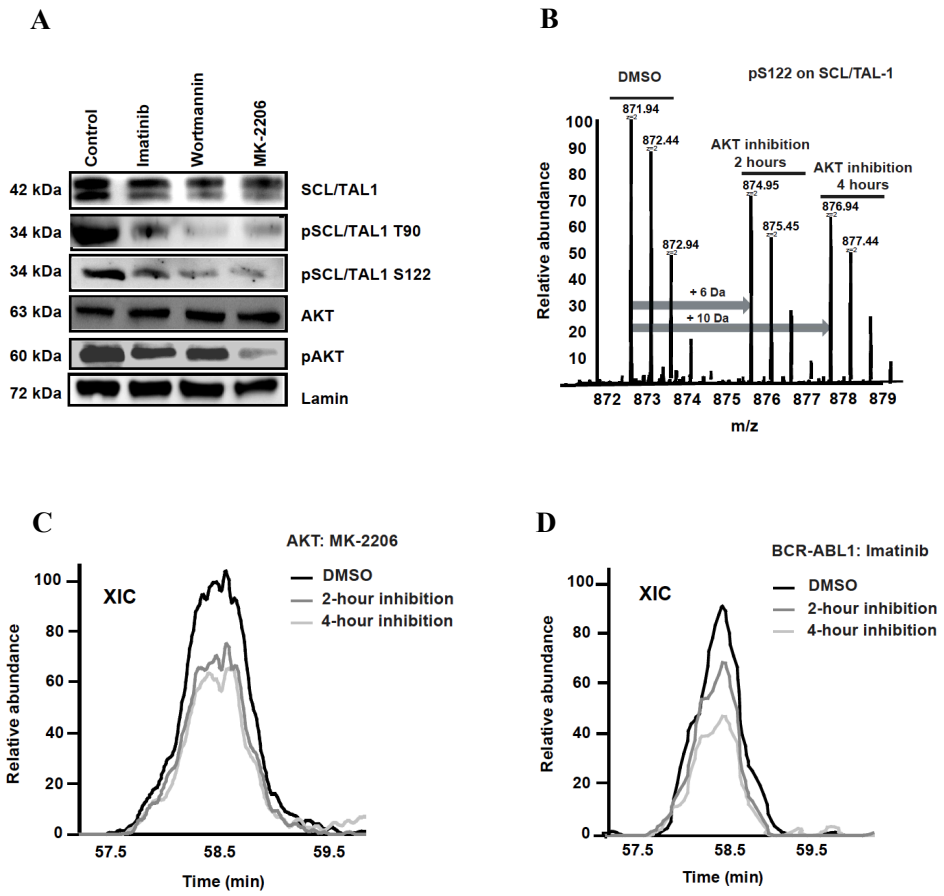

Figure 17 A) Western blot of nuclear lysates of K562 cells treated with vehicle, imatinib, the PI3-kinase inhibitor (wortmannin) or the AKT-inhibitor (MK-2206) and probed with antibodies to SCL/TAL1, pSCL/TAL1 T90, pSCL/TAL1S122, AKT, pAKT and Lamin B1. B to D) Quantitative mass spectrometry (MS) of K562 cells treated with vehicle, imatinib or MK-2206 for 0, 2 or 4 hours using triple SILAC-labelling and light-, medium- or heavy-labelled cells. After treatment, differently labelled cells were mixed and followed by MS analysis. B) An averaged MS1 spectrum showing the SILAC triplets of the pS122-bearing peptide "oxMVQLpSPPALAAPAAPGR" on SCL/TAL1 in AKT-inhibited cells. The arrows indicate the mass increments resulting from the medium (+6 Da) or heavy (+10 Da) SILAC-labelling on arginine. C to D) Areas under the extracted ion chromatogram (XIC) after mass spectrometry by triple SILAC labelling of the cells in (B) showing the relative abundance of pSCL/TAL1 S122 after inhibition with AKT inhibitor MK-2206 (C) and imatinib (D).

16. Molecular changes in the non-adherent and adherent fractions of the cells to E-selectin

As we observed difference in cell cycle (Figure 13 C) and expression of CD44 (Figure 16 C) in cells non-adherent and adherent to E-selectin, we performed a Western blot to check the phosphorylation status on SCL/TAL1 in non-adherent and adherent BCR-ABL1$^+$ BaF3 cells after an adhesion assay on E-selectin as in Figure 5A. Indeed, treatment with GMI-1271 alone or GMI-1271 plus imatinib increased the expression of SCL/TAL1 in non-adherent cells and decreased expression of SCL/TAL1 in adherent cells compared to vehicle (Figure 18A). Similarly, treatment with imatinib decreased pTAL1 T90 expression in non-adherent cells whilst the expression remained unchanged in adherent cells (Figure 18A). These results also correlate with previous observations of increased SCL/TAL1 expression in BCR-ABL1$^+$ cells after inhibition of E-selectin and reduction of phosphorylation only in non-adherent cells after treatment with imatinib. These studies also indicate the differences in behaviour of non-adherent and adherent cells after various treatment conditions.

Figure 18

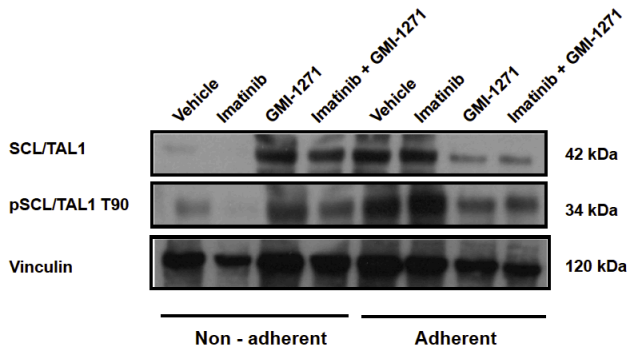

Figure 18 A) Western blot showing the expression of SCL/TAL1, pSCL/TAL1 T90 or vinculin in the non-adherent versus adherent fractions of BCR-ABL1$^+$ BaF3 cells plated on recombinant E-selectin in the presence of vehicle, GMI-1271, imatinib or imatinib + GMI-1271.

17. Secondary transplantation of CML-initiating cells from a GMI-1271- or imatinib-treated microenvironment increases aggressiveness of the disease

In order to assess possible changes associated with function of myeloid progenitors or CML stem cells after treatment with GMI-1271, we performed secondary transplantations from the bone marrow of CML mice treated with vehicle, GMI-1271, imatinib or imatinib and GMI-1271 into untreated wildtype recipients. Surprisingly, mice receiving bone marrow treated with imatinib and GMI-1271 had shorter survival compared to mice receiving bone marrow treated with imatinib (P = 0.045, Figure 19A), vehicle (P=0.03, Figure 19A) or GMI-1271 (P = 0.0004, Figure 19A). Consistently, we observed an increase in tumour burden (% BCR-ABL1$^+$ CD11b$^+$ cells) in the combination treatment (Figure 19B). Furthermore, spleen weights (Figure 19C) were higher in secondary recipient mice transplanted with bone marrow from a BMM treated with imatinib and GMI-1271 compared to vehicle (P=0.019, Figure 19C), imatinib (P=0.013, Figure 19C) or GMI-1271 (P=0.036, Figure 19C). In colony-forming assays, we observed a significantly higher number of colonies in bone marrow (P=0.033, Figure 19D) and spleen (Figure 19D) from mice treated with imatinib and GMI-1271 compared to mice treated with imatinib. In summary, these observations suggested that mice receiving bone marrow treated with GMI-1271 plus imatinib had a higher tumour burden, increased colony formation and shortened survival.

Taken together, these results suggest that although mice treated with GMI-1271 plus imatinib had prolonged survival in primary transplants, but if treatment is interrupted and the cells are exposed to new unconditioned environment, leukaemia cells can give rise to more aggressive disease as in secondary transplantation.

Figure 19

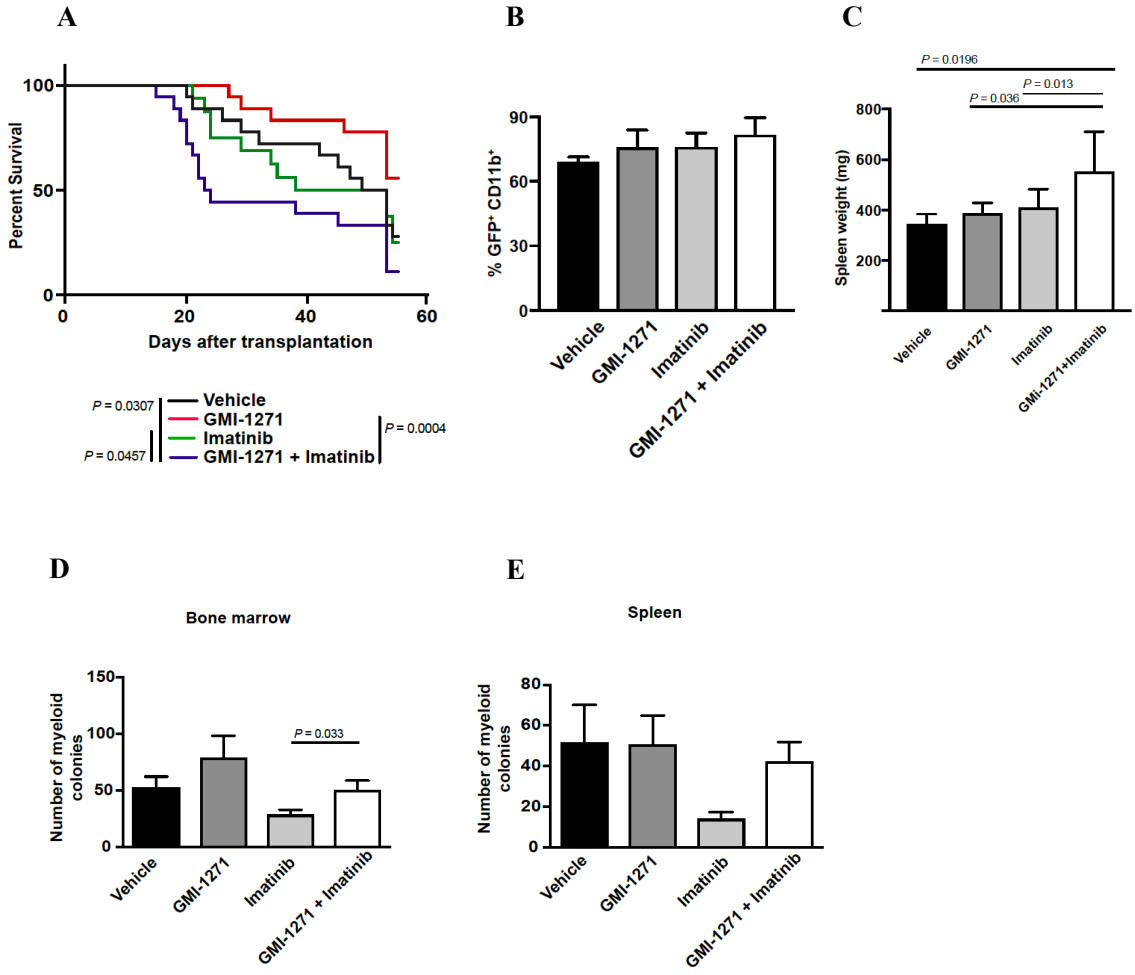

Figure 19 A) Kaplan-Meier-style survival curve for untreated secondary Balb/c recipients of bone marrow from CML mice treated with vehicle (black), GMI-1271 (red), imatinib (green) and the combination of imatinib and GMI-1271 (blue) (Log-rank test, n=18). B-C) % BCR-ABL1$^+$ CD11b$^+$ cells in bone marrow (B) or spleen weights (C) of secondary Balb/c recipients as in A). D-E) Number of myeloid colonies in methylcellulose from bone marrow (D) or spleen (E) cells from Balb/c recipients of BCR-ABL1-transduced BM treated with vehicle, GMI-1271, imatinib or imatinib plus GMI-1271 (n=8, ANOVA; Tukey test).

In order to explain the results obtained in Figure 19A, which may seem contradictory to the prolongation of survival observed in mice treated with GMI-1271 and imatinib in Figure 2A, we proposed two theories: 1. We hypothesized that differential behaviour of non-adherent

and adherent cells after primary transplant might be contributing to unexpected shortened survival in secondary recipients. 2. We also hypothesized that the cell cycle might be altered in secondary recipients, as GMI-1271 increases cell cycle in primary recipients. In order to test the first hypothesis, we performed colony formation assays on non-adherent and adherent cells. We performed an adhesion assay with BCR-ABL1$^+$ BaF3 plated on wells pre-coated with E-selectin and treated with vehicle, GMI-1271, imatinib or imatinib and GMI-1271. Non-adherent and adherent BCR-ABL1$^+$ BaF3 cells were separated and plated in methylcellulose. Interestingly, a higher number of colonies was observed from GMI-1271-treated non-adherent BCR-ABL1$^+$ BaF3 cells compared to GMI-1271- and imatinib-treated non-adherent BCR-ABL1$^+$ BaF3 cells. (P<0.0001, Figure 20A). Moreover, decreased colony formation was observed from GMI-1271- and imatinib-treated non-adherent BCR-ABL1$^+$ BaF3 cells compared to imatinib- or vehicle-treated non-adherent BCR-ABL1$^+$ BaF3 cells (P<0.0001, Figure 20A). These observations in non-adherent BCR-ABL1$^+$ BaF3 cells complement our previous findings that GMI-1271 might increase colony formation by increasing the cell cycle and co-treatment with imatinib reduces colony formation due to a decrease in leukaemia cells by imatinib.

However, GMI-1271-treated adherent BCR-ABL1$^+$ BaF3 cells have reduced colony numbers compared to GMI-1271-treated non-adherent BCR-ABL1$^+$ BaF3 cells (P<0.001, Figure 20A). In contrast, GMI-1271- plus imatinib-treated adherent BCR-ABL1$^+$ BaF3 cells give rise to increased colony numbers compared to GMI-1271- plus imatinib-treated non-adherent BCR-ABL1$^+$ BaF3 cells (P=0.05, Figure 20A). These results elucidate differential colony capacity formation in leukaemia cells non-adherent or adherent to E-selectin *in vitro* and possibly *in vivo*. However, while performing secondary transplantation we could not differentiate non-adherent and adherent cells from mice. The unknown ratio of non-adherent

to adherent cells transplanted into secondary recipients may have given rise to the unexpected aggressive survival.

In order to test our second hypothesis on the cell cycle status of leukaemia stem cells in secondary recipients, we performed cell cycle analysis in bone marrow cells of secondary recipients transplanted with bone marrow from mice treated with vehicle, imatinib, GMI-1271 or GMI-1271 plus imatinib on days 14 and 18 after transplantation. However, no differences were observed in G0, G1 and G2-S-M phases between the different conditions on day 14 (Figure 20B) or on day 18 (Figure 20C). The % BCR-ABL1^{+} Lin^{-} cKit^{+} Sca1^{+} cells (leukaemia-initiating cells) was also unaffected in bone marrow of secondary recipients transplanted with bone marrow treated with vehicle, imatinib, GMI-1271 or GMI-1271 plus imatinib (Figure 20D). Subsequently, we analyzed expression of CD44 as it is influenced by the presence of GMI-1271. However, no changes in the MFI of CD44 were observed in BCR-ABL1^{+} Lin^{-} cKit^{+} Sca1^{+}(Figure 20E) or BCR-ABL1^{+} Lin^{-} cKit^{+} (Figure 20F) bone marrow cells in secondary recipients on day 18.

These data suggest that secondary recipient mice transplanted with unconditioned/untreated CML-initiating cells might have different survival due to unknown changes in pathways/molecules occurring in leukaemia stem cells after treatment with the four different drugs/combinations.

Figure 20

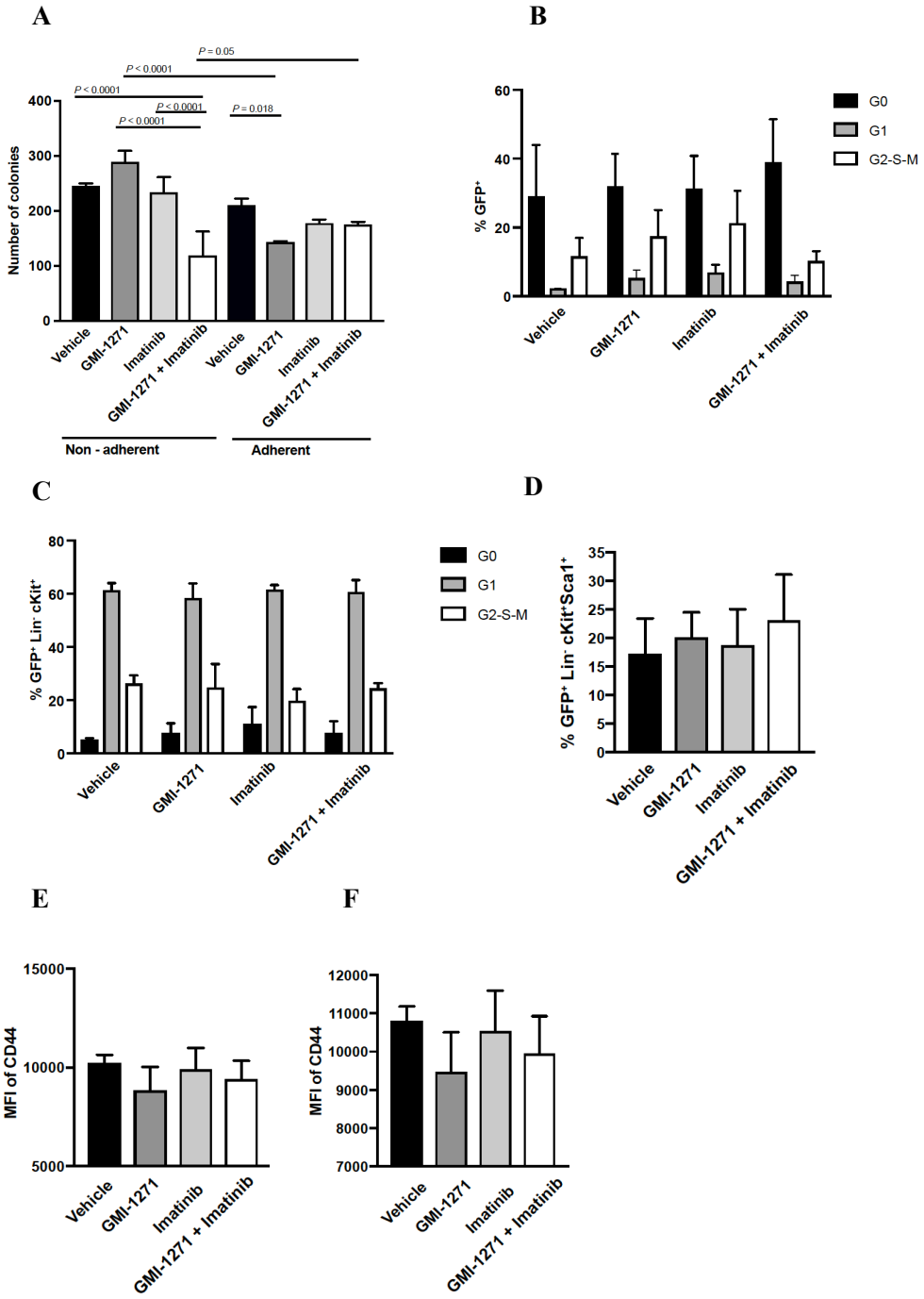
A
B
C
D
E
F
Number of colonies
P = 0.05
P < 0.0001
P < 0.0001
P < 0.0001
P < 0.0001
P = 0.018
Vehicle
GMI-1271
Imatinib
GMI-1271 + Imatinib
Non - adherent
Adherent
% GFP+
G0
G1
G2-S-M
% GFP+ Lin- cKit+
% GFP+ Lin- cKit+Sca1+
MFI of CD44

Figure 20 A) Number of colonies in methylcellulose from non-adherent and adherent BCR-ABL1$^+$ BaF3 cells plated on wells coated with E-selectin and treated with vehicle, GMI-1271, imatinib or imatinib and GMI-1271 (n=3, ANOVA; Tukey test). B-C) Cell cycle analysis by Ki67 and DAPI staining of BCR-ABL1$^+$ cells on day 14 (B) or in Lin$^-$ cKit$^+$ BCR-ABL1$^+$ cells on day 18 (C) from untreated secondary Balb/c recipients of bone marrow from CML mice treated with vehicle, GMI-1271, imatinib or the combination of imatinib and GMI-1271 (n=5, ANOVA; Tukey test). D) The percentage of BCR-ABL1$^+$ Lin$^-$ c-Kit$^+$ Sca1$^+$ cells in bone marrow from untreated secondary Balb/c recipients on day 18. E-F) Median fluorescence intensity (MFI) of CD44 in BCR-ABL1$^+$ Lin$^-$ c-Kit$^+$ cells (E) or in BCR-ABL1$^+$ Lin$^-$ cKit$^+$ Sca1$^+$ (F) on day 18.

18. Expression of *SCL/TAL1* can as prognostic factor in human patients with CML

Our observations in murine models and human CML cell lines suggested a negative correlation between *SCL/TAL1* and *CD44* expression. Hence, we correlated levels of *CD44* and *SCL/TAL1* in leukocytes from healthy individuals and CML patients. In healthy human leukocytes, we observed a lower expression for *CD44* and higher expression for *SCL/TAL1* ($P < 0.0001$, Figure 21A). However, in leukocytes from human CML patients we observed lower *SCL/TAL1* and higher *CD44* expression, the opposite from healthy patients ($P < 0.0001$, Figure 21B). These data suggest a negative correlation between expression of SCL/TAL1 and CD44 in healthy individuals and CML patients and an inverse link between healthy individuals and CML patients. To make stronger conclusion, we further examined the expression of *SCL/TAL1* and *CD44* in CD34$^+$ sorted samples from CP CML patients (n=59) [158]. We observed a significant negative correlation between *SCL/TAL1* and *CD44* expression ($P = 0.002$, correlation coefficient -0.40, Figure 21C).

These results indicate an inverse correlation between *SCL/TAL1* and *CD44* in CML patients similar to our murine studies.

Figure 21

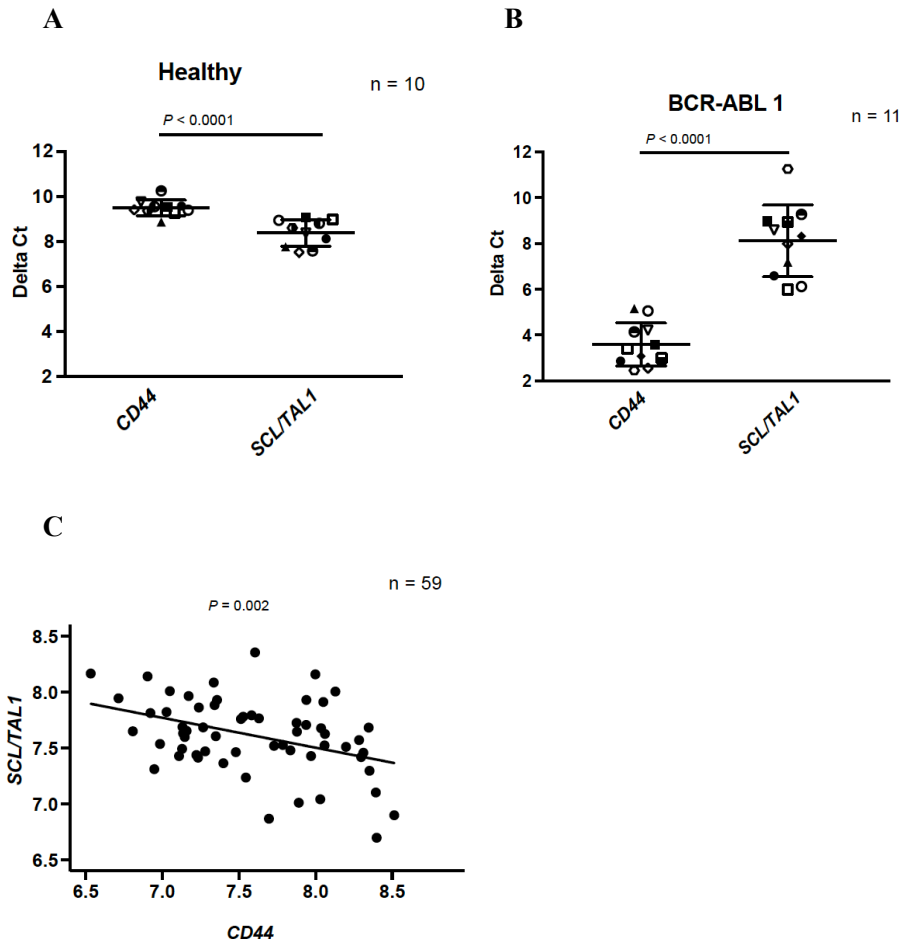

Figure 21 A-B) Delta Ct values for *CD44* and *SCL/TAL1* in peripheral blood leukocytes of healthy individuals (n=10) (A) or CML patients (n=11) (B). C) Negative correlation between *SCL/TAL1* and *CD44* expression in $CD34^+$ sorted samples from CP CML patients (n=59).

19. Significance of *SCL/TAL1* and *CD44* expression in the different phases of CML

In order to test the significance of *SCL/TAL1* and *CD44* gene expression in phases of CML, we obtained published data sets of SCL/TAL1 and CD44 in human CML samples [158,159]. We observed significantly higher *SCL/TAL1* levels in $CD34^+$ cells from healthy individuals compared to CML in chronic phase (P = 0.042, Figure 22A) or compared to CML in accelerated phase (P = 0.082, Figure 22A). Interestingly, *CD44* expression increased with

progression of CML disease from chronic phase to accelerated phase ($P < 0.0001$, Figure 22 B), while we found a trend towards lower expression of *CD44* in $CD34^+$ cells from healthy individuals compared to CML cells in blast crisis and accelerated phase (Figure 22 B).

We further examined a possible association in survival outcome between *SCL/TAL1* expression after allogenic transplantation in chronic phase CML patients (n=35). After dichotomization of *SCL/TAL1* into high and low expression groups at the third quartile, we observed that patients with lower *SCL/TAL1* expression had a significantly increased risk of relapse ($P = 0.033$, Figure 22C) and inferior relapse-free survival ($P = 0.033$, Figure 22D).

Together, these data suggest that expression of *SCL/TAL1* and *CD44* may correlate with disease progression in CML patients and SCL/TAL1 might be beneficial in providing a prognosis although larger cohorts are necessary to draw further conclusions.

Figure 22

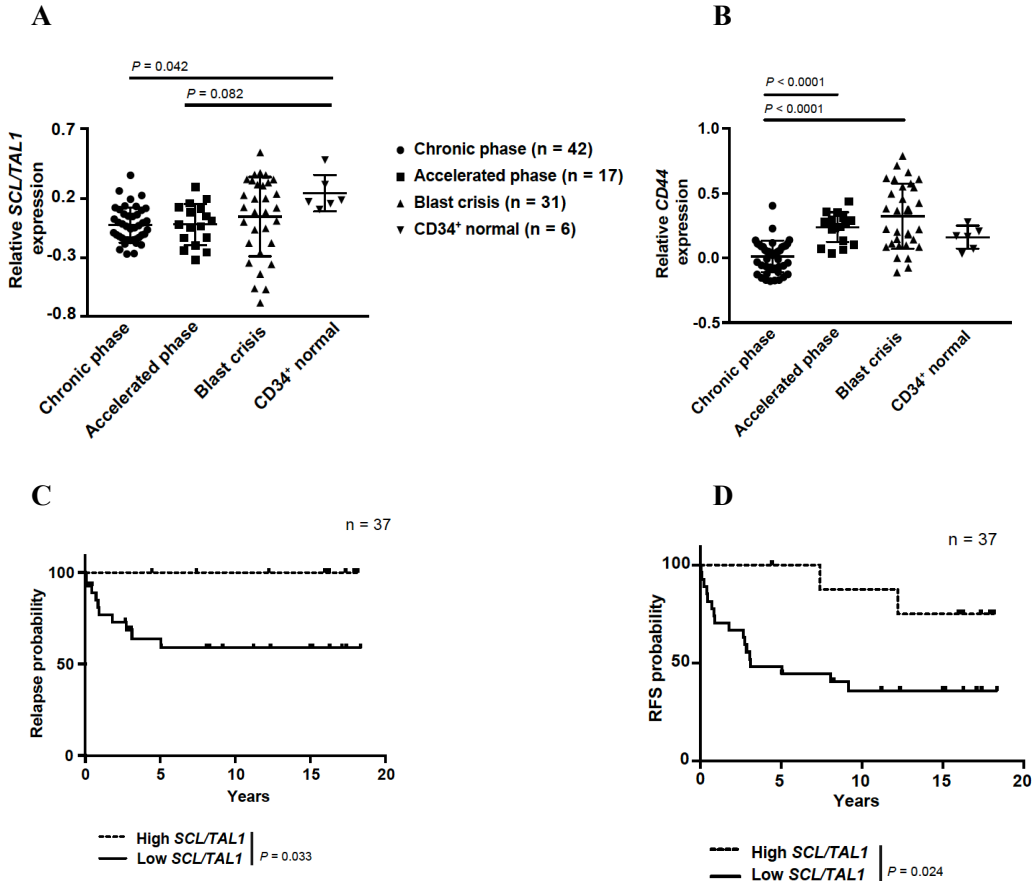

Figure 22 A-B) Relative *SCL/TAL1* (A) and *CD44* (B) expression in unsorted BM cells of patients in chronic phase (circles), accelerated phase (squares) or blast crisis (triangles) of CML versus normal human $CD34^+$ cells (upside down triangles). Gene expression for each individual sample is normalized to the mean expression in CP samples and is shown on a log10 scale (ANOVA, Tukey test). C-D) Kaplan-Meier-style curve of the probability of relapse (Log-rank test) (C) or relapse-free survival (Log-rank test) (D) of CML patients in chronic phase divided into low or high expression of *SCL/TAL1* (n=37).

20. Dual inhibition of CXCR4 and E-selectin

It is well studied that leukaemia cells, including CML cells, express C-X-C chemokine receptor type 4 (CXCR4) on its surface [174]. The CXCR4-CXCL12 axis promotes CML growth and various targeted therapies have been known to inhibit this axis [174] and targeting of CXCR4 with plerixafor (AMD3100) is known to reduce CML growth and survival [175]. A drug, GMI-1359, which is a dual inhibitor of E-selectin and CXCR4 is available. In order to study the dual inhibition of E-selectin and CXCR4, we performed retroviral transplantation as in Figure 2A. CML mice were treated with GMI-1359 to target E-selectin and CXCR4 and imatinib from day 10 after transplantation. Treatment of mice with CML with vehicle, GMI-1359, imatinib or imatinib + GMI-1359 led to a significant prolongation of survival of mice receiving imatinib + GMI-1359 compared to vehicle (P = 0.0009, Figure 23 A). However, mice treated with imatinib + GMI-1359 showed a trend towards prolongation of survival compared to imatinib alone (Figure 23 A). The percentage of BCR-$ABL1^+$ $CD11b^+$ myeloid cells of mice treated with imatinib + GMI-1359 was slightly reduced compared to mice treated with imatinib only on day 17 (Figure 23 B) and on day 29 (Figure 23 C). This experiment provided us with preliminary information on the possibility of simultaneously targeting CXCR4 and E-selectin with imatinib. However, further investigation is necessary.

Figure 23

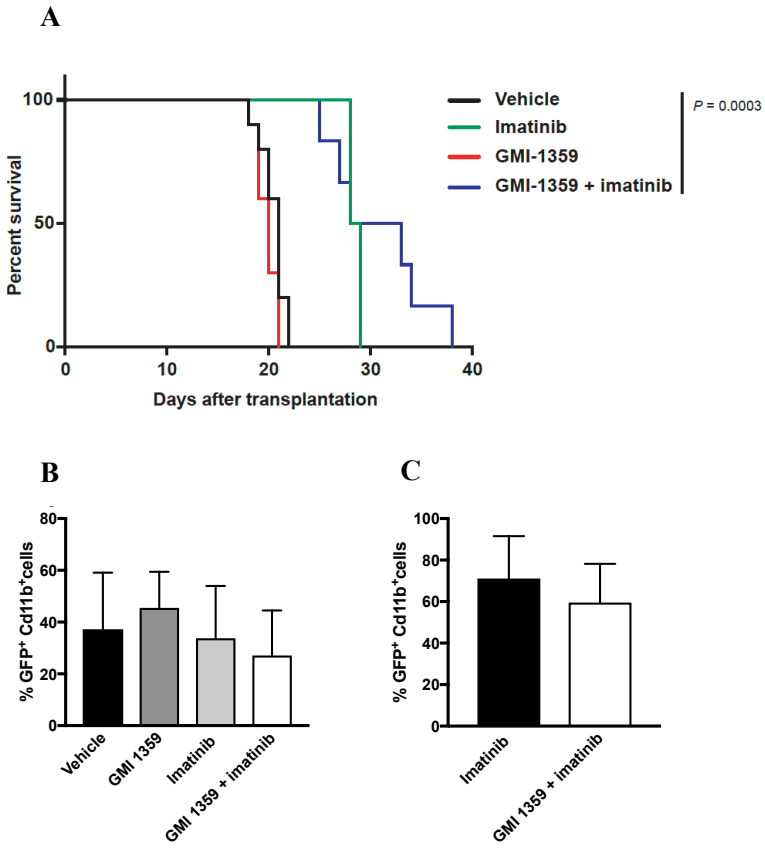

Figure 23 A) Kaplan-Meier-style survival curve for Balb/c recipients of BCR-ABL1-transduced BM treated with vehicle (black solid line), 20 mg/kg/dose GMI-1359 i.p. (green), 100 mg/kg imatinib p.o. (red) and the combination of both imatinib and GMI-1359 (blue) beginning on day 10 after transplantation (Log-rank test, n=10). B - C) The percentage of BCR-ABL1^{+} CD11b^{+} cells in the bone marrow of Balb/c recipients transplanted with BCR-ABL1 transduced bone marrow and treated with vehicle, GMI-1359, imatinib, imatinib and GMI-1359 on day 17(B) and day 29 (C).

Discussion:

The vascular niche offers chemo-protection to cancer stem cells

The concept of the contribution of the bone marrow microenvironment (BMM) to the regulation of hematopoietic stem and progenitor cells (HSPC) and their differentiation has been studied for the last decade [176] The BMM comprises of mesenchymal stromal cells (MSCs), osteolineage cells, neuronal and endothelial cells all of which govern and regulate HSPC function. The understanding of the interactions between HSCs and BMM and their alterations in malignant conditions can help to identify therapeutic strategies [177]. Experimental evidence suggests that the bone marrow microenvironment protects leukaemia cells from chemotherapy or tyrosine kinase inhibitor therapy, which may result in relapse of the disease [2]. In the vascular niche, the localisation of leukaemia cells near microvascular domains was associated with homing [178] [4]. The endothelium, a major component in the vascular niche expresses receptor molecules such as E-selectin and P-selectin. These receptors are recognised to play an essential role for the rolling and extravasation of neutrophils on or from endothelium during an injury or a stress response [101]. In different pathologies, like multiple myeloma, E-selectin offered resistance to multiple myeloma cells, and inhibition of E-selectin receptor and ligand improved survival of mice [103]. Breast cancer cells on the other hand are also known to depend on E-selectin for homing to the bone [179]. In malignant haematological diseases like CML, E-selectin on bone marrow endothelium was required for homing and engraftment of CML LICs, whereas P-selectin was dispensable [6]. Similarly, in AML mouse models, expression of E-selectin was upregulated in endothelial cells and protected AML cells from chemotherapy [180]. Recent studies in mouse models, on breast to bone metastasis suggest the essential role of E-selectin in the vascular niche for mesenchymal epithelial transition (MET) of cancer cells [181] [179]

In CML, imatinib mesylate, a tyrosine kinase inhibitor considered standard of care, is used as first line therapy for treatment which leads to a haematological remission in >90% of patients [182,183]. However, some patients may develop resistance to imatinib leading to disease relapse, possibly due to the occurrence of point mutations in the abl kinase domain or the persistence of leukaemia stem cells, harboured and supported by the BMM [184–186].

Targeting the vascular niche in haematological malignancies and solid tumours

Considering the chemoprotective nature of the BMM [2] and exclusive expression of E-selectin in the vascular niche and its role for engraftment of LSC in CML [4,6] , the emphasis of the current work was to analyse the involvement of E-selectin in the persistence of LSC in CML and how targeting this molecule may alter the disease course. GMI-1070, pan-selectin antagonist represented a novel therapeutic drug for sickle cell anaemia. However, recently, a specific E-selectin antagonist, GMI-1271 was used for the treatment of another haematological malignancy, acute myeloid leukaemia (AML), and has successfully completed phase1/2 clinical trials [104] with high remission rates and improved overall survival. Apart from haematological malignancies, treatment of breast cancer with GMI-1271 in mice reduced the metastatic behaviour of breast cancer cells to bone and lung [179]. In multiple myeloma studies, GMI-1271 sensitized the multiple myeloma cells to therapy [187] and, currently, a phase 1 clinical trial is being performed using GMI-1271 in multiple myeloma patients (clinicaltrials.gov: NCT02811822). In the current study, we have used GMI-1271 in combination with imatinib to understand the mechanism of protection of leukaemic cells from tyrosine kinase inhibitor therapy and how this may be targeted.

Targeting the BMM alters the localisation of CML stem cells in the BMM and influences the cell cycle status

Our data suggest that targeting the BMM by inhibition of the binding of BCR-ABL1^{+} CML cells to E-selectin by using the small molecule antagonist GMI-1271 and imatinib led to

prolongation of survival of CML *in vivo* (Figure 2B) compared to imatinib alone. Additionally, treatment with GMI-1271 also influenced the localisation of leukaemic initiating cells (LIC) in relation to the endothelium (Figure 4B) altering the cell cycle status (Figure 13E). It has been shown previously that endothelial cells can induce quiescence [188] and as imatinib can only target the cycling cells [189], our data suggest that non-binding to endothelium and, therefore, localisation of leukaemia cells further away from the endothelium might have caused better targeting of LIC with imatinib. Our Southern blot showing reduced clonality of disease also supports the idea of better targeting of LIC in the combination treatment [5].

However, our data on CML LSC and treatment with GMI-1271 contrasts with work in the normal HSC niche [7]. In normal haematopoiesis, E-selectin is known to support HSC proliferation [7] whereas our studies reports suggest that E-selectin helps to maintain the quiescence of CML LSC. However, it is worth noticing that studies on the normal HSC niche were performed using a precursor molecule to GMI-1271, named GMI-1070, which is a pan-selectin rather than an E-selectin-specific antagonist. Besides, previous studies also demonstrate that interactions with the BMM differ drastically between normal HSC [5] and LSC and even between oncogenes [142]. This might explain the difference of effects of GMI-1271 on normal HSC versus CML LSC.

SCL/TAL1 regulates the expression of CD44

Our results discovered the regulation of *CD44* by SCL/TAL1 on a transcriptional level. It is worth mentioning that besides CD44, there are other ligands of E-selectin including L-selectin and PSGL1, that are expressed on CML LICs [166] Interestingly, knockdown of *SCL/TAL1* only upregulated CD44 expression as shown by our mass spectrometry data whereas other ligands of E-selectin remained unaffected (Figure 8C, 8D). This suggested a

unique role of SCL/TAL1 in CML cells. A prominent role of SCL/TAL1 in pathological conditions has been reported before. In immature thymocytes aberrant expression of Scl/Tal1 leads to T-ALL [190]. It is reported that in T-ALL, SCL/TAL1 has occupancy at the regulatory regions of *CD69,* the *T-cell receptor α (TCRA)* enhancer*, NKX3-1*, and promoters of the *myeloblastosis* (*MYB)* and *triples homologues 2 (TRIB2)* genes [167,191–193] suggesting an important transcriptional role. Further studies indicate that TAL1 can act in a context-dependent manner as a bifunctional transcriptional regulator (activator or repressor) in T-ALL [194]. Our results further showed that SCL/TAL1 binds to the CD44 regulatory element and that there is increased occupancy at this site in the presence of imatinib (Figure 10B). The data suggest that the expression of *CD44* is controlled by SCL/TAL1 at the CD44 regulatory element by acting as a transcriptional repressor in BCR-ABL1$^+$ cells. However, it cannot be excluded that other transcriptional factors may also play a role in influencing CD44 expression [195,196].

Our work elaborates on the relevance of SCL/TAL1, that negatively regulates the expression of CD44, a cancer stem cell maker and essential ligand for E-selectin in CML. Conversely, we showed that over-expression of *Scl/Tal1* on LIC in our murine model of CML led to prolongation of survival of mice due to a decrease in expression of CD44 in CML cells (Figure 11B), as has been described [5]. Inhibition of E-selectin binding to CML cells with GMI-1271 led to an increase in the expression of CDK6 and a decrease in the expression of p16 which are known to be targets of Scl/Tal1 (Figure 14C, 14D) [191,197] Indeed, this supports our data that treatment with GMI-1271 increases the expression of Scl/Tal1 and, therefore, to a concomitant increase in the proliferation/cell cycle of LIC due to the upregulation of CDK6 and decreased expression of p16. This suggests the dual role of Scl/Tal1 in different haematological malignancies either behaving as an oncogene in T-ALL and probable tumour suppressor in CML. Our data and the published reports on the role of SCL/TAL1 in T-ALL

also sheds light on the diversity of molecular changes associated with lymphoid and myeloid malignancies [198]. However, a possible role of SCL/TAL1 in other myeloid malignancies like AML or its more specific involvement in CML has not been studied. CD44 and CD44v isoforms are considered cancer stem cell markers and critical regulators of stemness, tumour initiation and metastasis [199]. Evidence suggests that CD44 is associated as one of the cancer stem cell marker in solid cancers like lung cancer, breast cancer and colon cancer [200–202]. It would be interesting and relevant to study and explore the connection between SCL/TAL1 and CD44 in solid cancer, as CD44 also plays an important role in metastasis [203]. The study of this axis in other cancers might increase our insight into novel targets for treatment or prognostic markers.

BCR-ABL1 phosphorylates SCL/TAL1 via pAKT

Our work elaborates on a mechanistic crosstalk between the *BCR-ABL1* oncogene and CD44. BCR-ABL1, a constitutively active tyrosine kinase, regulates components of via phosphorylation, several signalling pathways like the MAPK kinase, PI3K/Akt signalling and JAK-STAT pathways etc. BCR-ABL1 can phosphorylate PI3K by more than one pathway and once PI3K is active, it activates AKT kinase [204]. Phosphorylation of AKT can affect the phosphorylation of several other downstream targets [170]. Our data suggest that BCR-ABL1 activity is associated with phosphorylation of SCL/TAL1 at pT90 and pS122 but this occurs via the phosphorylation ability of AKT, which itself is phosphorylated by BCR-ABL1 (Figure 17A). Active AKT is known to phosphorylate SCL/TAL1, and this causes inhibition of its activity due to lack of distribution in the nucleus [171]. Our data complement this published study, that phosphorylation of SCL/TAL1 by pAKT may inhibit its function which, as shown in our study, results in regulation of CD44 expression. Concomitantly, treatment with imatinib (leading to inhibition of BCR-ABL1) decreases the phosphorylation of AKT and, therefore, also the phosphorylation of SCL/TAL1.

Consequently, SCL/TAL1 activity is decreased. Our data connect the previously unknown mechanistic interaction between CD44, a ligand for E-selectin (and extracellular matrix proteins) on BCR-ABL1$^+$ cells and its transcriptional regulation by SCL/TAL1 with its involvement in binding to E-selectin in the vascular niche and LIC cell cycle.

Our results also illustrate differences in cell cycle and possibly other factors between non-adherent leukaemia cells and adherent cells that possibly maintain contact with the niche (Figure 16C, Figure 18A). These data give us preliminary results stating that non-adherent cells and adherent cells may differ mechanistically and that adhesion between leukaemia stem cells and the niche may play a role in chemo-protection.

Exposure of leukaemia cells treated with GMI-1271 and imatinib to a new microenvironment increases the aggressiveness of the disease

In order to assess the frequency and function of BCR-ABL1$^+$ myeloid progenitors and CML stem cells in mice treated with vehicle, imatinib, GMI-1271 or imatinib and GMI-1271, we performed secondary transplantations. The shortened survival in secondary recipients of bone marrow from an imatinib- and GMI-1271-treated (Figure 19A) was unexpected given the increased survival observed in imatinib- and GMI-1271-treated primary recipients (Figure 2B) and the decreased disease clonality by Southern blotting (Figure 3C). This may be partially explained by the fact that DNA for Southern blotting was obtained from spleen rather than bone marrow due to insufficient number of DNA which can be obtained from bone marrow. Also, the DNA obtained for Southern blotting was taken at the time of death, when the number of LIC may be low and quite different between treatment groups. In contrast, for the secondary transplantations the primary mice were sacrificed on a specific day early on during the course of disease, when the effects of treatment on LIC number and function may have been the most prominent. The number of myeloid colonies obtained from bone marrow (Figure 19D) or spleen (Figure 19E) was higher in the combined treatment of

imatinib plus GMI-1271, because GMI-1271 induces cell cycling and, thereby, possibly increased colony formation capacity. Although the number of LIC are reduced by the combination treatment, they might be functionally altered due to an increase in cycling induced by GMI-1271 and, therefore, lead to shortened survival. An alternative explanation might be the possible differential properties of BCR-ABL1^{+} cells non-adhering or adhering to E-selectin as observed for the cell cycle (Figure 13C and D), the formation of myeloid colonies (Figure 20A), molecular changes in SCL/TAL1 (Figure 18A) and effects on CD44 expression (Figure 16C). The observations in the secondary transplantation experiment may also be due to the simultaneous transplantation of adhering and non-adhering cells which cannot be separated *in vivo*. The lack of effect on cell cycle or expression of CD44 in CML stem/progenitor cells in secondary recipients (Figure 20E, 20F) points to the fact that multiple other mechanisms may be involved in secondary recipients independent of the observations in studies of primary recipients treated with the four different drugs or their combinations. The co-treatment with imatinib and GMI-1271 in primary recipients is beneficial due to the mechanisms explained above. However, it cannot be excluded that certain other molecular targets may have been affected also; for example, the deregulation of the apoptotic pathway due to the presence of imatinib or activation of other signalling cascades. These factors may have contributed to the results observed in the secondary transplants.

Targeting E-selectin and CXCR4 in combination with BCR-ABL1 inhibition may provide a better targeting strategy for CML

Like E-selectin, chemokine receptor CXCR4 has been predominantly studied in HSCs and also in CML, CML cells expressing CXCR4 have better migration and adhesion to niche [174]. The CXCR4 pathway contributes to chemo-resistance, metastatic diseases and lower survival in solid cancers [205]. Studies targeting CXCR4 with AMD3100 were successful *in*

vitro and *in vivo* in CML overcoming the protective nature of stroma [206] [174] Other studies report that AMD3100 with TKIs result in CNS infiltration of leukaemia cells [175]. GMI-1359, a successor compound of GMI-1271, is known to target E-selectin and CXCR4 in combination. In AML, GMI-1359 and sorafenib, a protein kinase inhibitor, demonstrated anti-leukaemic activity in the *FLT3* – ITD AML model compared to sorafenib alone with a concomitant improvement of normal haematopoiesis [207]. In multiple myeloma, GMI-1359, similar to GMI-1271, decreased adhesion and chemotaxis of multiple myeloma cells re-sensitizing them to therapy [187]. Currently, GMI-1359 is being evaluated in phase 1 clinical trials in healthy volunteers (clinicaltrials.gov: NCT02931214). Taking into account the above-mentioned studies, our data in CML indicates that the inhibition of E-selectin and CXCR4 may be beneficial in CML also. It will be of great importance to understand the molecular mechanisms involved in the combined action of dual inhibition of E-selectin and CXCR4 in combination with tyrosine kinase inhibitor therapy for survival studies in CML and how these may differ from treatment with GMI-1271 alone. Additionally, it might be interesting to delineate whether the SCL/TAL1-CD44 axis is involved in the effect of treatment of CML with GMI-1359 given the modest prolongation of survival. However, more experiments need to be conducted to confirm the results observed here, but targeting only E-selectin along with an inhibitor of BCR-ABL1 might serve as a new therapeutic strategy.

Correlation between SCL/TAL1 and CD44 in human patients

The human data complements the *in vivo* studies, where an inverse correlation between *SCL/TAL1* and *CD44* in healthy and CML patients was observed (Figure 21A, 21B). The *SCL/TAL1* expression was found to be higher in healthy human $CD34^+$ cells considered as stem/progenitor cells in than in leukocytes from CML patients [208] (Figure 22A). Increasing expression of *CD44* was observed in advanced phases of the disease. Gene ontology studies

have reported that certain genes are differentially expressed in the various phases of CML. For example, genes involved in structural integrity, immune and inflammatory response were decreased and WNT signalling was higher in blast crisis compared to chronic phase [158]. Therefore, the differences in *CD44* expression which we observe might be phase-specific and it would be interesting to study if the correlation between *SCL/TAL1* and *CD44* is phase-specific. We also observed that patients expressing lower *SCL/TAL1* levels had an increased risk of relapse and inferior relapse-free survival (Figure 22C, 22D). Summarizing the observations in our human data, the expression of *SCL/TAL1* might also add value as a prognostic marker in CML.

Conclusion

In our work, we show that inhibition of binding of BCR-ABL1$^+$ cells to E-selectin in the vascular niche increases cell cycle progression and improves the response to imatinib therapy. Furthermore, our data shows that SCL/TAL1 is a transcriptional regulator of CD44 expression, whereby phosphorylation of SCL/TAL1 is controlled by AKT which is downstream of the BCR-ABL1 tyrosine kinase. The regulation of the expression of CD44, a cancer stem cell marker, via the BCR-ABL1-AKT-SCL/TAL1 pathway, as well as the regulation of cell cycle of LSC due to non-adhesion to the niche, suggest a novel concept of the dislocation of leukaemic cells from the niche leading to an increase in proliferation and an improved response to tyrosine kinase inhibitor therapy.

List of abbreviations

5-FU	5-fluorouracil
A-MuLV	Abelson murine leukemia virus
AGM	Aorta gonad mesoderm
ALL	Acute lymphoblastic leukaemia
AML	Acute myelogenous leukaemia
BAD	BCL2 associated agonist of cell death
BCL	B-cell lymphoma
BCR	Breakpoint cluster region
BMM	Bone marrow microenvironment
BMP	Bone morphogenetic proteins
BTK	Bruton tyrosine kinase
CAR	CXCL-12 abundant reticular cells
CCL3	C-C motif chemokine ligand
CDK	Cyclin-dependent kinase
CDKN1A	CDK inhibitor 1A
CEBP α	CCAAT enhancer binding protein alpha
CLL	Chronic lymphocytic leukaemia
CLP	Common lymphoid progenitors
CML	Chronic myeloid leukaemia
CMP	Common myeloid progenitors
CRKL	Crk like protein
CTCF	Corrected total cell fluorescence
CXCL12	C-X-C ligand
CXCR4	C-X-C chemokine receptor type 4
DNMT3A	DNA methyltransferase 3A
DR3	Death receptor 3
E2A	Transcriptional factor 3
ECM	Extracellular matrix
EMAPII	Endothelial monocyte activating polypeptide II
EPO	Erythropoietin
ERM	Ezrin, Radixin and Moesin
ESL-1	E-selectin ligand 1
FGF2	Fibroblast growth factor
FITC	Fluorescein isothicyanate
G-CSF	Granulocyte colony forming factor
GAPDH	Glyceraldehyde phosphate dehydrogenase
GAS6	Growth specific arrest 6
GATA1	GATA binding protein 1
GFP	Green florescent protein
GMP	Granulocyte macrophages progenitors
HA	Hyaluronic acid
HSC	Hematopoietic stem cells
HSPC	Hematopoietic stem and progenitor cells
ICAM	Intercellular Adhesion Molecule
IDH	Isocitrate dehydrogenase
IKZF1	Ikaros family zinc finger 1

IL2RG	Interleukin 2receptor gamma
IL3	Interleukin 3
ITD	Internal tandem duplications
IVM	Intravital microscope
KLF	Krueppel like factor
LAMP1/2	Lysosomal associated membrane protein 1/2
LIC	Leukaemia initiating cell
LMO2	LIM domain only
LPS	Bacterial lipopolysaccharide
LSC	Leukaemia stem cells
LSK	Lin^{-} $Sca1^{+}$ $cKit^{+}$
MDS	Myelodysplasia syndrome
MET	Mesenchymal epithelial transition
MFI	Median fluorescence intensity
MPN	Myeloproliferative neoplasia
MPP	Multipotent progenitors
MSC	Mesenchymal stem cells
NG2	Neural-glial antigen
NO	Nitric oxide
NPM1	Nucleophosmin 1
OTC	Carboxyamidotrizole/orotate
PFA	Paraformaldehyde
Ph	Philadelphia
PIGF	Placental growth factor
PSGL1	P-selectin glycoprotein ligand 1
PTH	Parathyroid hormone
RAG2	Recombinant activating gene 2
RAR γ	Retinoic acid receptor gamma
RBC	Red blood cells
ROS	Reactive oxygen species
RUNX	Runt-related transcription factor
SCF	Stem cell factor
SCL	Stem cell leukemia
SHG	Second harmonic generation
T-ALL	T cell acute lymphoblastic leukaemia
TAL1	T-cell acute lymphoblastic leukaemia protein 1
TCRA	T-cell receptor α
TET2	Ten–eleven translocation oncogene family member 2
TF	Transcription factors
TKD	Tyrosine kinase domain
TNFα	Tumor necrosis factor
TPO	Thrombopoietin
TRIB2	Triples homologues 2
VCAM	Vascular cell adhesion molecule
VEGF	Vascular endothelial growth factor
XIC	Extracted ion chromotogram
YAP	Yes associated protein

References

1. Kumar, R., Godavarthy, P. S. & Krause, D. S. The bone marrow microenvironment in health and disease at a glance. *J. Cell Sci.* **131**, (2018).
2. Ishikawa, F. *et al.* Chemotherapy-resistant human AML stem cells home to and engraft within the bone-marrow endosteal region. *Nat. Biotechnol.* **25**, 1315–21 (2007).
3. Deininger, M. W. N., Goldman, J. M. & Melo, J. V. The molecular biology of chronic myeloid leukemia The molecular biology of chronic myeloid leukemia. *Structure* **96**, 3343–3356 (2009).
4. Sipkins, D. A. *et al.* In vivo imaging of specialized bone marrow endothelial microdomains for tumour engraftment. *Nature* **435**, 969–73 (2005).
5. Krause, D. S., Lazarides, K., von Andrian, U. H. & Van Etten, R. A. Requirement for CD44 in homing and engraftment of BCR-ABL-expressing leukemic stem cells. *Nat. Med.* **12**, 1175–80 (2006).
6. Krause, D. S., Lazarides, K., Lewis, J. B., von Andrian, U. H. & Van Etten, R. A. Selectins and their ligands are required for homing and engraftment of BCR-ABL1+ leukemic stem cells in the bone marrow niche. *Blood* **123**, 1361–1371 (2014).
7. Winkler, I. G. *et al.* Vascular niche E-selectin regulates hematopoietic stem cell dormancy, self renewal and chemoresistance. *Nat. Med.* **18**, 1651–7 (2012).
8. Palis, J. & Yoder, M. C. Yolk-sac hematopoiesis: the first blood cells of mouse and man. *Exp. Hematol.* **29**, 927–36 (2001).
9. Orkin, S. H. & Zon, L. I. Hematopoiesis: An Evolving Paradigm for Stem Cell Biology. *Cell* **132**, 631–644 (2008).
10. Ottersbach, K. & Dzierzak, E. The murine placenta contains hematopoietic stem cells within the vascular labyrinth region. *Dev. Cell* **8**, 377–87 (2005).
11. Gekas, C., E. Rhodes, K. & K. A. Mikkola, H. Isolation and Analysis of Hematopoietic Stem Cells from the Placenta. *J. Vis. Exp.* (2008). doi:10.3791/742
12. Yang, L. *et al.* Identification of Lin(-)Sca1(+)kit(+)CD34(+)Flt3- short-term hematopoietic stem cells capable of rapidly reconstituting and rescuing myeloablated transplant recipients. *Blood* **105**, 2717–23 (2005).
13. Akashi, K., Traver, D., Miyamoto, T. & Weissman, I. L. A clonogenic common myeloid progenitor that gives rise to all myeloid lineages. *Nature* **404**, 193–197 (2000).
14. MANZ, M. G. *et al.* Dendritic Cell Development from Common Myeloid Progenitors. *Ann. N. Y. Acad. Sci.* **938**, 167–174 (2006).
15. Zhu, J. & Emerson, S. G. Hematopoietic cytokines, transcription factors and lineage commitment. *Oncogene* **21**, 3295–3313 (2002).
16. Tabbara, I. A. & Robinson, B. E. Hematopoietic growth factors. *Anticancer Res.* **11**, 81–90
17. McMahon, K. A. *et al.* Mll Has a Critical Role in Fetal and Adult Hematopoietic Stem Cell Self-Renewal. *Cell Stem Cell* **1**, 338–345 (2007).
18. Rodrigues, N. P. *et al.* Haploinsufficiency of GATA-2 perturbs adult hematopoietic stem-cell homeostasis. *Blood* **106**, 477–484 (2005).
19. van Galen, P. *et al.* Reduced lymphoid lineage priming promotes human hematopoietic stem cell expansion. *Cell Stem Cell* **14**, 94–106 (2014).
20. Cheng, H., Zheng, Z. & Cheng, T. New paradigms on hematopoietic stem cell differentiation. *Protein Cell* (2019). doi:10.1007/s13238-019-0633-0
21. Pietras, E. M. *et al.* Functionally Distinct Subsets of Lineage-Biased Multipotent Progenitors Control Blood Production in Normal and Regenerative Conditions. *Cell Stem Cell* **17**, 35–46 (2015).
22. Wilson, A. *et al.* Hematopoietic stem cells reversibly switch from dormancy to self-renewal during homeostasis and repair. *Cell* **135**, 1118–29 (2008).
23. Velten, L. *et al.* Human haematopoietic stem cell lineage commitment is a continuous process. *Nat. Cell Biol.* **19**, 271–281 (2017).
24. Karamitros, D. *et al.* Single-cell analysis reveals the continuum of human lympho-myeloid progenitor cells. *Nat. Immunol.* **19**, 85–97 (2018).

25. Krause, D. S. & Scadden, D. T. *A hostel for the hostile: The bone marrow niche in hematologic neoplasms*. *Haematologica* **100**, 1376–1387 (2015).
26. Adams, G. B. & Scadden, D. T. The hematopoietic stem cell in its place. *Nat. Immunol.* **7**, 333–337 (2006).
27. Calvi, L. M. *et al.* Osteoblastic cells regulate the haematopoietic stem cell niche. *Nature* **425**, 841–846 (2003).
28. Ding, L. & Morrison, S. J. Haematopoietic stem cells and early lymphoid progenitors occupy distinct bone marrow niches. *Nature* **495**, 231–235 (2013).
29. Kiel, M. J. *et al.* SLAM Family Receptors Distinguish Hematopoietic Stem and Progenitor Cells and Reveal Endothelial Niches for Stem Cells. *Cell* **121**, 1109–1121 (2005).
30. Lo Celso, C. *et al.* Live-animal tracking of individual haematopoietic stem/progenitor cells in their niche. *Nature* **457**, 92–96 (2009).
31. Morrison, S. J. & Scadden, D. T. The bone marrow niche for haematopoietic stem cells. *Nature* **505**, 327–334 (2014).
32. Kunisaki, Y. *et al.* Arteriolar niches maintain haematopoietic stem cell quiescence. *Nature* **502**, 637–43 (2013).
33. Ludin, A. *et al.* Reactive Oxygen Species Regulate Hematopoietic Stem Cell Self-Renewal, Migration and Development, As Well As Their Bone Marrow Microenvironment. *Antioxid. Redox Signal.* **21**, 1605–1619 (2014).
34. Itkin, T. *et al.* Distinct bone marrow blood vessels differentially regulate haematopoiesis. *Nature* **532**, 323–328 (2016).
35. Gur-Cohen, S. *et al.* PAR1 signaling regulates the retention and recruitment of EPCR-expressing bone marrow hematopoietic stem cells. *Nat. Med.* **21**, 1307–1317 (2015).
36. Méndez-Ferrer, S. *et al.* Mesenchymal and haematopoietic stem cells form a unique bone marrow niche. *Nature* **466**, 829–834 (2010).
37. Ding, L., Saunders, T. L., Enikolopov, G. & Morrison, S. J. Endothelial and perivascular cells maintain haematopoietic stem cells. *Nature* **481**, 457–462 (2012).
38. Chen, Q. *et al.* Fate decision of mesenchymal stem cells: adipocytes or osteoblasts? *Cell Death Differ.* **23**, 1128–1139 (2016).
39. Kramer, A. C. *et al.* Dermatopontin in Bone Marrow Extracellular Matrix Regulates Adherence but Is Dispensable for Murine Hematopoietic Cell Maintenance. *Stem cell reports* **9**, 770–778 (2017).
40. Riccio, I. *et al.* Musculoskeletal problems in pediatric acute leukemia. *J. Pediatr. Orthop. B* **22**, 264–269 (2013).
41. Davis, A. S., Viera, A. J. & Mead, M. D. Leukemia: An overview for primary care. *Am. Fam. Physician* **89**, 731–738 (2014).
42. Bowman, R. L., Busque, L. & Levine, R. L. Clonal Hematopoiesis and Evolution to Hematopoietic Malignancies. *Cell Stem Cell* **22**, 157–170 (2018).
43. Byrd, J. C. *et al.* Pretreatment cytogenetic abnormalities are predictive of induction success, cumulative incidence of relapse, and overall survival in adult patients with de novo acute myeloid leukemia: results from Cancer and Leukemia Group B (CALGB 8461). *Blood* **100**, 4325–36 (2002).
44. Gaidzik, V. & Döhner, K. Prognostic Implications of Gene Mutations in Acute Myeloid Leukemia With Normal Cytogenetics. *Semin. Oncol.* **35**, 346–355 (2008).
45. Cancer Genome Atlas Research Network *et al.* Genomic and epigenomic landscapes of adult de novo acute myeloid leukemia. *N. Engl. J. Med.* **368**, 2059–74 (2013).
46. Falini, B., Nicoletti, I., Martelli, M. F. & Mecucci, C. Acute myeloid leukemia carrying cytoplasmic/mutated nucleophosmin (NPMc+ AML): biologic and clinical features. *Blood* **109**, 874–85 (2007).
47. Cheng, K. *et al.* The cytoplasmic NPM mutant induces myeloproliferation in a transgenic mouse model. *Blood* **115**, 3341–3345 (2010).
48. Ley, T. J. *et al. DNMT3A* Mutations in Acute Myeloid Leukemia. *N. Engl. J. Med.* **363**, 2424–2433 (2010).
49. Marcucci, G. *et al.* Age-related prognostic impact of different types of DNMT3A mutations in adults with primary cytogenetically normal acute myeloid leukemia. *J. Clin. Oncol.* **30**,

742–50 (2012).
50. Shlush, L. I. *et al.* Identification of pre-leukaemic haematopoietic stem cells in acute leukaemia. *Nature* **506**, 328–333 (2014).
51. Kelly, L. M. FLT3 internal tandem duplication mutations associated with human acute myeloid leukemias induce myeloproliferative disease in a murine bone marrow transplant model. *Blood* **99**, 310–318 (2002).
52. Marcucci, G., Haferlach, T. & Döhner, H. Molecular Genetics of Adult Acute Myeloid Leukemia: Prognostic and Therapeutic Implications. *J. Clin. Oncol.* **29**, 475–486 (2011).
53. Chou, W.-C. *et al.* TET2 mutation is an unfavorable prognostic factor in acute myeloid leukemia patients with intermediate-risk cytogenetics. *Blood* **118**, 3803–3810 (2011).
54. Shah, A., John, B. M. & Sondhi, V. Acute lymphoblastic leukemia with treatment--naive Fanconi anemia. *Indian Pediatr.* **50**, 508–10 (2013).
55. Chessells, J. M. *et al.* Down's syndrome and acute lymphoblastic leukaemia: clinical features and response to treatment. *Arch. Dis. Child.* **85**, 321–325 (2001).
56. Mullighan, C. G. *et al.* Rearrangement of CRLF2 in B-progenitor– and Down syndrome–associated acute lymphoblastic leukemia. *Nat. Genet.* **41**, 1243–1246 (2009).
57. Shahjahani, M. *et al.* Molecular basis of chronic lymphocytic leukemia diagnosis and prognosis. *Cell. Oncol.* **38**, 93–109 (2015).
58. GROFFEN, J. *et al.* Philadelphia chromosomal breakpoints are clustered within a limited region, bcr, on chromosome 22. *Cell* **36**, 93–99 (1984).
59. Rowley, J. D. Letter: A new consistent chromosomal abnormality in chronic myelogenous leukaemia identified by quinacrine fluorescence and Giemsa staining. *Nature* **243**, 290–3 (1973).
60. Laneuville, P. Abl tyrosine protein kinase. *Semin. Immunol.* **7**, 255–266 (1995).
61. Lewis, J. M. & Schwartz, M. A. Integrins regulate the association and phosphorylation of paxillin by c-Abl. *J. Biol. Chem.* **273**, 14225–30 (1998).
62. Sawyers, C. L., McLaughlin, J., Goga, A., Havlik, M. & Witte, O. The nuclear tyrosine kinase c-abl negatively regulates cell growth. *Cell* **77**, 121–131 (1994).
63. Melo, J. V. The diversity of BCR-ABL fusion proteins and their relationship to leukemia phenotype. *Blood* **88**, 2375–84 (1996).
64. Carpino, N. *et al.* p62(dok): a constitutively tyrosine-phosphorylated, GAP-associated protein in chronic myelogenous leukemia progenitor cells. *Cell* **88**, 197–204 (1997).
65. Oda, T. *et al.* Crkl is the major tyrosine-phosphorylated protein in neutrophils from patients with chronic myelogenous leukemia. *J. Biol. Chem.* **269**, 22925–8 (1994).
66. Levitzki, A. & Gazit, A. Tyrosine kinase inhibition: an approach to drug development. *Science* **267**, 1782–8 (1995).
67. Druker, B. J. & Lydon, N. B. Lessons learned from the development of an abl tyrosine kinase inhibitor for chronic myelogenous leukemia. *J. Clin. Invest.* **105**, 3–7 (2000).
68. Casolari, D. A. & Melo, J. V. Chronic myeloid leukaemia. *Chromosom. Translocat. Genome Rearrange. Cancer* **385**, 107–138 (2015).
69. Skorski, T. *et al.* Phosphatidylinositol-3 kinase activity is regulated by BCR/ABL and is required for the growth of Philadelphia chromosome-positive cells. *Blood* **86**, 726–36 (1995).
70. Sattler, M. *et al.* The proto-oncogene product p120CBL and the adaptor proteins CRKL and c-CRK link c-ABL, p190BCR/ABL and p210BCR/ABL to the phosphatidylinositol-3' kinase pathway. *Oncogene* **12**, 839–46 (1996).
71. Skorski, T. *et al.* Transformation of hematopoietic cells by BCR/ABL requires activation of a PI-3k/Akt-dependent pathway. *EMBO J.* **16**, 6151–61 (1997).
72. del Peso, L., González-García, M., Page, C., Herrera, R. & Nuñez, G. Interleukin-3-induced phosphorylation of BAD through the protein kinase Akt. *Science* **278**, 687–9 (1997).
73. Frisch, B. J. *et al.* Functional inhibition of osteoblastic cells in an in vivo mouse model of myeloid leukemia. *Blood* **119**, 540–550 (2012).
74. Welner, R. S. *et al.* Treatment of Chronic Myelogenous Leukemia by Blocking Cytokine Alterations Found in Normal Stem and Progenitor Cells. *Cancer Cell* **27**, 671–681 (2015).
75. Schepers, K. *et al.* Myeloproliferative Neoplasia Remodels the Endosteal Bone Marrow

Niche into a Self-Reinforcing Leukemic Niche. *Cell Stem Cell* **13**, 285–299 (2013).
76. Walkley, C. R. *et al.* A microenvironment-induced myeloproliferative syndrome caused by retinoic acid receptor gamma deficiency. *Cell* **129**, 1097–110 (2007).
77. Walkley, C. R., Shea, J. M., Sims, N. A., Purton, L. E. & Orkin, S. H. Rb Regulates Interactions between Hematopoietic Stem Cells and Their Bone Marrow Microenvironment. *Cell* **129**, 1081–1095 (2007).
78. Raaijmakers, M. H. G. P. *et al.* Bone progenitor dysfunction induces myelodysplasia and secondary leukaemia. *Nature* **464**, 852–857 (2010).
79. Dong, L., Zheng, H. & Qu, C.-K. CCL3 is a key mediator for the leukemogenic effect of *Ptpn11* -activating mutations in the stem-cell microenvironment. *Blood* **130**, 1471–1474 (2017).
80. Agarwal, P. *et al.* Mesenchymal Niche-Specific Expression of Cxcl12 Controls Quiescence of Treatment-Resistant Leukemia Stem Cells. *Cell Stem Cell* **24**, 769-784.e6 (2019).
81. Chien, S. *et al.* A Novel Small Molecule E-Selectin Inhibitor GMI-1271 Blocks Adhesion of AML Blasts to E-Selectin and Mobilizes Blood Cells in Nodscid IL2Rgc−/− Mice Engrafted with Human AML. *Blood* **120**, (2012).
82. Hawkins, E. D. *et al.* T-cell acute leukaemia exhibits dynamic interactions with bone marrow microenvironments. *Nature* **538**, 518–522 (2016).
83. Ponta, H., Sherman, L. & Herrlich, P. A. CD44: From adhesion molecules to signalling regulators. *Nat. Rev. Mol. Cell Biol.* **4**, 33–45 (2003).
84. Jin, L., Hope, K. J., Zhai, Q., Smadja-Joffe, F. & Dick, J. E. Targeting of CD44 eradicates human acute myeloid leukemic stem cells. *Nat. Med.* **12**, 1167–1174 (2006).
85. Yi, H. *et al.* Integrin alphavbeta3 enhances β-catenin signaling in acute myeloid leukemia harboring Fms-like tyrosine kinase-3 internal tandem duplication mutations: implications for microenvironment influence on sorafenib sensitivity. *Oncotarget* **7**, 40387–40397 (2016).
86. Bajaj, J. *et al.* CD98-Mediated Adhesive Signaling Enables the Establishment and Propagation of Acute Myelogenous Leukemia. *Cancer Cell* **30**, 792–805 (2016).
87. Lundell, B., McCarthy, J., Kovach, N. & Verfaillie, C. Activation of β1 integrins on CML progenitors reveals cooperation between β1 integrins and CD44 in the regulation of adhesion and proliferation. *Leukemia* **11**, 822–829 (1997).
88. Veiga, J. P., Costa, L. F., Sallan, S. E., Nadler, L. M. & Cardoso, A. A. Leukemia-stimulated bone marrow endothelium promotes leukemia cell survival. *Exp. Hematol.* **34**, 610–621 (2006).
89. Hatfield, K. *et al.* Primary human acute myeloid leukaemia cells increase the proliferation of microvascular endothelial cells through the release of soluble mediators. *Br. J. Haematol.* **144**, 53–68 (2009).
90. Zhang, B. *et al.* Microenvironmental protection of CML stem and progenitor cells from tyrosine kinase inhibitors through N-cadherin and Wnt–β-catenin signaling. *Blood* **121**, 1824–1838 (2013).
91. Jacamo, R. *et al.* Reciprocal leukemia-stroma VCAM-1/VLA-4-dependent activation of NF-κB mediates chemoresistance. *Blood* **123**, 2691–702 (2014).
92. Yang, R. Y. *et al.* Expression of galectin-3 modulates T-cell growth and apoptosis. *Proc. Natl. Acad. Sci.* **93**, 6737–6742 (1996).
93. Fei, F. *et al.* Galectin-3 in pre-B acute lymphoblastic leukemia. *Leukemia* **27**, 2385–2388 (2013).
94. Graves, B. J. *et al.* Insight into E-selectin/ligand interaction from the crystal structure and mutagenesis of the lec/EGF domains. *Nature* **367**, 532–538 (1994).
95. Kunkel, E. J. & Ley, K. Distinct phenotype of E-selectin-deficient mice. E-selectin is required for slow leukocyte rolling in vivo. *Circ. Res.* **79**, 1196–204 (1996).
96. Gout, S., Tremblay, P.-L. & Huot, J. Selectins and selectin ligands in extravasation of cancer cells and organ selectivity of metastasis. *Clin. Exp. Metastasis* **25**, 335–344 (2008).
97. Walz, G., Aruffo, A., Kolanus, W., Bevilacqua, M. & Seed, B. Recognition by ELAM-1 of the sialyl-Lex determinant on myeloid and tumor cells. *Science (80-.).* **250**, 1132–1135 (1990).

98. Hidalgo, A., Peired, A. J., Wild, M. K., Vestweber, D. & Frenette, P. S. Complete Identification of E-Selectin Ligands on Neutrophils Reveals Distinct Functions of PSGL-1, ESL-1, and CD44. *Immunity* **26**, 477–489 (2007).
99. Leeuwenberg, J. F. *et al.* E-selectin and intercellular adhesion molecule-1 are released by activated human endothelial cells in vitro. *Immunology* **77**, 543–9 (1992).
100. Frenette, P. S., Mayadas, T. N., Rayburn, H., Hynes, R. O. & Wagner, D. D. Susceptibility to infection and altered hematopoiesis in mice deficient in both P- and E-selectins. *Cell* **84**, 563–74 (1996).
101. Zhong, L. *et al.* E-Selectin-Mediated Adhesion and Extravasation in Cancer. *Encycl. Cancer* 1618–1624 (2014). doi:10.1007/978-3-662-46875-3_1781
102. Barthel, S. R. *et al.* Definition of molecular determinants of prostate cancer cell bone extravasation. *Cancer Res.* **73**, 942–52 (2013).
103. Natoni, A. *et al.* E-selectin ligands recognised by HECA452 induce drug resistance in myeloma, which is overcome by the E-selectin antagonist, GMI-1271. *Leukemia* **31**, 2642–2651 (2017).
104. DeAngelo, D. J. *et al.* Uproleselan (GMI-1271), an E-Selectin Antagonist, Improves the Efficacy and Safety of Chemotherapy in Relapsed/Refractory (R/R) and Newly Diagnosed Older Patients with Acute Myeloid Leukemia: Final, Correlative, and Subgroup Analyses. *Blood* **132**, 331–331 (2018).
105. Screaton, G. R. *et al.* Genomic structure of DNA encoding the lymphocyte homing receptor CD44 reveals at least 12 alternatively spliced exons. *Proc. Natl. Acad. Sci. U. S. A.* **89**, 12160–4 (1992).
106. Goldstein, L. A. *et al.* A human lymphocyte homing receptor, the Hermes antigen, is related to cartilage proteoglycan core and link proteins. *Cell* **56**, 1063–1072 (1989).
107. Stamenkovic, I., Amiot, M., Pesando, J. M. & Seed, B. A lymphocyte molecule implicated in lymph node homing is a member of the cartilage link protein family. *Cell* **56**, 1057–1062 (1989).
108. Naor, D., Wallach-Dayan, S. B., Zahalka, M. A. & Sionov, R. V. Involvement of CD44, a molecule with a thousand faces, in cancer dissemination. *Semin. Cancer Biol.* **18**, 260–267 (2008).
109. Goldstein, L. A. & Butcher, E. C. Identification of mRNA that encodes an alternative form of H-CAM(CD44) in lymphoid and nonlymphoid tissues. *Immunogenetics* **32**, 389–97 (1990).
110. Konstantopoulos, K. & Thomas, S. N. Cancer Cells in Transit: The Vascular Interactions of Tumor Cells. *Annu. Rev. Biomed. Eng.* **11**, 177–202 (2009).
111. Ishii, S. *et al.* CD44 participates in the adhesion of human colorectal carcinoma cells to laminin and type IV collagen. *Surg. Oncol.* **2**, 255–64 (1993).
112. Greenfield, B. *et al.* Characterization of the heparan sulfate and chondroitin sulfate assembly sites in CD44. *J. Biol. Chem.* **274**, 2511–7 (1999).
113. Bajorath, J., Greenfield, B., Munro, S. B., Day, A. J. & Aruffo, A. Identification of CD44 Residues Important for Hyaluronan Binding and Delineation of the Binding Site. *J. Biol. Chem.* **273**, 338–343 (1998).
114. Mori, T. *et al.* Structural basis for CD44 recognition by ERM proteins. *J. Biol. Chem.* **283**, 29602–12 (2008).
115. Lokeshwar, V. B., Fregien, N. & Bourguignon, L. Y. Ankyrin-binding domain of CD44(GP85) is required for the expression of hyaluronic acid-mediated adhesion function. *J. Cell Biol.* **126**, 1099–109 (1994).
116. Fedorchenko, O. *et al.* CD44 regulates the apoptotic response and promotes disease development in chronic lymphocytic leukemia. *Blood* **121**, 4126–4136 (2013).
117. Xu, Y., Stamenkovic, I. & Yu, Q. CD44 attenuates activation of the hippo signaling pathway and is a prime therapeutic target for glioblastoma. *Cancer Res.* **70**, 2455–64 (2010).
118. Takahashi, E. *et al.* Tumor Necrosis Factor-α Regulates Transforming Growth Factor-β-dependent Epithelial-Mesenchymal Transition by Promoting Hyaluronan-CD44-Moesin Interaction. *J. Biol. Chem.* **285**, 4060–4073 (2010).

119. Jin, L., Hope, K. J., Zhai, Q., Smadja-Joffe, F. & Dick, J. E. Targeting of CD44 eradicates human acute myeloid leukemic stem cells. *Nat. Med.* **12**, 1167–74 (2006).
120. Zöller, M., Rajasagi, M., Vitacolonna, M. & Luft, T. Thymus repopulation after allogeneic reconstitution in hematological malignancies. *Exp. Hematol.* **35**, 1891–1905 (2007).
121. Begley, C. G. *et al.* Chromosomal translocation in a human leukemic stem-cell line disrupts the T-cell antigen receptor delta-chain diversity region and results in a previously unreported fusion transcript. *Proc. Natl. Acad. Sci. U. S. A.* **86**, 2031–5 (1989).
122. Robb, L. *et al.* Absence of yolk sac hematopoiesis from mice with a targeted disruption of the scl gene. *Proc. Natl. Acad. Sci. U. S. A.* **92**, 7075–9 (1995).
123. Shivdasani, R. A., Mayer, E. L. & Orkin, S. H. Absence of blood formation in mice lacking the T-cell leukaemia oncoprotein tal-1/SCL. *Nature* **373**, 432–4 (1995).
124. Lacombe, J. *et al.* Scl regulates the quiescence and the long-term competence of hematopoietic stem cells. *Blood* **115**, 792–803 (2010).
125. Benyoucef, A. *et al.* The SCL/TAL1 Transcription Factor Represses the Stress Protein DDiT4/REDD1 in Human Hematopoietic Stem/Progenitor Cells. *Stem Cells* **33**, 2268–79 (2015).
126. Wu, W. *et al.* Dynamic shifts in occupancy by TAL1 are guided by GATA factors and drive large-scale reprogramming of gene expression during hematopoiesis. *Genome Res.* **24**, 1945–1962 (2014).
127. Massari, M. E. & Murre, C. Helix-loop-helix proteins: regulators of transcription in eucaryotic organisms. *Mol. Cell. Biol.* **20**, 429–40 (2000).
128. Correia, N. C., Arcangeli, M.-L., Pflumio, F. & Barata, J. T. Stem Cell Leukemia: how a TALented actor can go awry on the hematopoietic stage. *Leukemia* **30**, 1968–1978 (2016).
129. Ferrando, A. A. *et al.* Biallelic transcriptional activation of oncogenic transcription factors in T-cell acute lymphoblastic leukemia. *Blood* **103**, 1909–11 (2004).
130. Ferrando, A. A. *et al.* Gene expression signatures define novel oncogenic pathways in T cell acute lymphoblastic leukemia. *Cancer Cell* **1**, 75–87 (2002).
131. Aplan, P. D. *et al.* An scl gene product lacking the transactivation domain induces bony abnormalities and cooperates with LMO1 to generate T-cell malignancies in transgenic mice. *EMBO J.* **16**, 2408–19 (1997).
132. Gerby, B. *et al.* SCL, LMO1 and Notch1 Reprogram Thymocytes into Self-Renewing Cells. *PLoS Genet.* **10**, e1004768 (2014).
133. Bendall, L. J. & Bradstock, K. F. G-CSF: From granulopoietic stimulant to bone marrow stem cell mobilizing agent. *Cytokine Growth Factor Rev.* **25**, 355–367 (2014).
134. Löwenberg, B. *et al.* Effect of Priming with Granulocyte Colony-Stimulating Factor on the Outcome of Chemotherapy for Acute Myeloid Leukemia. *N. Engl. J. Med.* **349**, 743–752 (2003).
135. Liu, S.-H. *et al.* A novel CXCR4 antagonist IgG1 antibody (PF-06747143) for the treatment of hematologic malignancies. *Blood Adv.* **1**, 1088–1100 (2017).
136. Nervi, B. *et al.* Chemosensitization of acute myeloid leukemia (AML) following mobilization by the CXCR4 antagonist AMD3100. *Blood* **113**, 6206–6214 (2009).
137. Hoellenriegel, J. *et al.* The Spiegelmer NOX-A12, a novel CXCL12 inhibitor, interferes with chronic lymphocytic leukemia cell motility and causes chemosensitization. *Blood* **123**, 1032–9 (2014).
138. Kariolis, M. S. *et al.* Inhibition of the GAS6/AXL pathway augments the efficacy of chemotherapies. *J. Clin. Invest.* **127**, 183–198 (2017).
139. Byrd, J. C. *et al.* Targeting BTK with Ibrutinib in Relapsed Chronic Lymphocytic Leukemia. *N. Engl. J. Med.* **369**, 32–42 (2013).
140. Corrado, C. *et al.* Carboxyamidotriazole-Orotate Inhibits the Growth of Imatinib-Resistant Chronic Myeloid Leukaemia Cells and Modulates Exosomes-Stimulated Angiogenesis. *PLoS One* **7**, e42310 (2012).
141. Passaro, D. *et al.* Increased Vascular Permeability in the Bone Marrow Microenvironment Contributes to Disease Progression and Drug Response in Acute Myeloid Leukemia. *Cancer Cell* **32**, 324-341.e6 (2017).
142. Krause, D. S. *et al.* Differential regulation of myeloid leukemias by the bone marrow

microenvironment. *Nat. Med.* **19**, 1513–7 (2013).
143. Copland, M. *et al.* Dasatinib (BMS-354825) targets an earlier progenitor population than imatinib in primary CML but does not eliminate the quiescent fraction. *Blood* **107**, 4532–4539 (2006).
144. Chu, S. *et al.* Detection of BCR-ABL kinase mutations in CD34+ cells from chronic myelogenous leukemia patients in complete cytogenetic remission on imatinib mesylate treatment. *Blood* **105**, 2093–2098 (2005).
145. Maeda, T. Transforming property of TEL-FGFR3 mediated through PI3-K in a T-cell lymphoma that subsequently progressed to AML. *Blood* **105**, 2115–2123 (2005).
146. Jiao, P. *et al.* MK-2206 induces cell cycle arrest and apoptosis in HepG2 cells and sensitizes TRAIL-mediated cell death. *Mol. Cell. Biochem.* **382**, 217–24 (2013).
147. Mohr, J. *et al.* The cell fate determinant Scribble is required for maintenance of hematopoietic stem cell function. *Leukemia* **32**, 1211–1221 (2018).
148. Celso, C. Lo, Wu, J. W. & Lin, C. P. *In vivo* imaging of hematopoietic stem cells and their microenvironment. *J. Biophotonics* **2**, 619–631 (2009).
149. Van Etten, R. A. Retroviral transduction models of Ph+ leukemia: advantages and limitations for modeling human hematological malignancies in mice. *Blood Cells. Mol. Dis.* **27**, 201–5 (2001).
150. Wolff, N. C. & Ilaria, R. L. Establishment of a murine model for therapy-treated chronic myelogenous leukemia using the tyrosine kinase inhibitor STI571. *Blood* **98**, 2808–16 (2001).
151. Kuvardina, O. N. *et al.* RUNX1 represses the erythroid gene expression program during megakaryocytic differentiation. *Blood* **125**, 3570–9 (2015).
152. Li, S. *et al.* The P190, P210, and P230 forms of the BCR/ABL oncogene induce a similar chronic myeloid leukemia-like syndrome in mice but have different lymphoid leukemogenic activity. *J. Exp. Med.* **189**, 1399–412 (1999).
153. Göllner, S. *et al.* Loss of the histone methyltransferase EZH2 induces resistance to multiple drugs in acute myeloid leukemia. *Nat. Med.* **23**, 69–78 (2017).
154. Kolodziej, S. *et al.* PADI4 acts as a coactivator of Tal1 by counteracting repressive histone arginine methylation. *Nat. Commun.* **5**, 3995 (2014).
155. McCloy, R. A. *et al.* Partial inhibition of Cdk1 in G $_2$ phase overrides the SAC and decouples mitotic events. *Cell Cycle* **13**, 1400–1412 (2014).
156. Burgess, A. *et al.* Loss of human Greatwall results in G2 arrest and multiple mitotic defects due to deregulation of the cyclin B-Cdc2/PP2A balance. *Proc. Natl. Acad. Sci. U. S. A.* **107**, 12564–9 (2010).
157. Kohrs, N. *et al.* MiR144/451 Expression Is Repressed by RUNX1 During Megakaryopoiesis and Disturbed by RUNX1/ETO. *PLoS Genet.* **12**, e1005946 (2016).
158. Radich, J. P. *et al.* Gene expression changes associated with progression and response in chronic myeloid leukemia. *Proc. Natl. Acad. Sci. U. S. A.* **103**, 2794–9 (2006).
159. McWeeney, S. K. *et al.* A gene expression signature of CD34+ cells to predict major cytogenetic response in chronic-phase chronic myeloid leukemia patients treated with imatinib. *Blood* **115**, 315–325 (2010).
160. Poulos, M. G. *et al.* Activation of the vascular niche supports leukemic progression and resistance to chemotherapy. *Exp. Hematol.* **42**, 976-986.e3 (2014).
161. de la Grange, P. B. *et al.* Low SCL/TAL1 expression reveals its major role in adult hematopoietic myeloid progenitors and stem cells. *Blood* **108**, 2998–3004 (2006).
162. Hall, M. & Curtis, D. SCL/Tal1 and lymphoid versus myeloid lineage assignment. *Blood* **105**, 1365; author reply 1365-6 (2005).
163. Dey, S., Curtis, D. J., Jane, S. M. & Brandt, S. J. The TAL1/SCL transcription factor regulates cell cycle progression and proliferation in differentiating murine bone marrow monocyte precursors. *Mol. Cell. Biol.* **30**, 2181–92 (2010).
164. Sanda, T. & Leong, W. Z. TAL1 as a master oncogenic transcription factor in T-cell acute lymphoblastic leukemia. *Exp. Hematol.* **53**, 7–15 (2017).
165. Rothenberg, E. V, Hosokawa, H. & Ungerbäck, J. Mechanisms of Action of Hematopoietic Transcription Factor PU.1 in Initiation of T-Cell Development. *Front. Immunol.* **10**, 228

(2019).
166. Dimitroff, C. J., Lee, J. Y., Rafii, S., Fuhlbrigge, R. C. & Sackstein, R. CD44 is a major E-selectin ligand on human hematopoietic progenitor cells. *J. Cell Biol.* **153**, 1277–86 (2001).
167. Kusy, S. *et al.* NKX3.1 is a direct TAL1 target gene that mediates proliferation of TAL1-expressing human T cell acute lymphoblastic leukemia. *J. Exp. Med.* **207**, 2141–56 (2010).
168. Lim, S. & Kaldis, P. Cdks, cyclins and CKIs: roles beyond cell cycle regulation. *Development* **140**, 3079–93 (2013).
169. Shank-Calvo, J. A., Draheim, K., Bhasin, M. & Kelliher, M. A. p16Ink4a or p19Arf loss contributes to Tal1-induced leukemogenesis in mice. *Oncogene* **25**, 3023–3031 (2006).
170. Cilloni, D. & Saglio, G. Molecular pathways: BCR-ABL. *Clin. Cancer Res.* **18**, 930–7 (2012).
171. Palamarchuk, A. *et al.* Akt phosphorylates Tal1 oncoprotein and inhibits its repressor activity. *Cancer Res.* **65**, 4515–9 (2005).
172. Cheng, J. T., Cobb, M. H. & Baer, R. Phosphorylation of the TAL1 oncoprotein by the extracellular-signal-regulated protein kinase ERK1. *Mol. Cell. Biol.* **13**, 801–8 (1993).
173. Bibi, S. *et al.* Co-operating STAT5 and AKT signaling pathways in chronic myeloid leukemia and mastocytosis: possible new targets of therapy. *Haematologica* **99**, 417–29 (2014).
174. Weisberg, E. *et al.* Inhibition of CXCR4 in CML cells disrupts their interaction with the bone marrow microenvironment and sensitizes them to nilotinib. *Leukemia* **26**, 985–90 (2012).
175. Agarwal, A. *et al.* Effects of plerixafor in combination with BCR-ABL kinase inhibition in a murine model of CML. *Blood* **120**, 2658–2668 (2012).
176. Zon, L. I. Intrinsic and extrinsic control of haematopoietic stem-cell self-renewal. *Nature* **453**, 306–13 (2008).
177. Passegue, E., Jamieson, C. H. M., Ailles, L. E. & Weissman, I. L. Normal and leukemic hematopoiesis: Are leukemias a stem cell disorder or a reacquisition of stem cell characteristics? *Proc. Natl. Acad. Sci.* **100**, 11842–11849 (2003).
178. Colmone, A. *et al.* Leukemic Cells Create Bone Marrow Niches That Disrupt the Behavior of Normal Hematopoietic Progenitor Cells. *Science* **322**, 1861–1865 (2008).
179. Price, T. T. & Sipkins, D. A. E-Selectin and SDF-1 regulate metastatic trafficking of breast cancer cells within the bone. *Mol. Cell. Oncol.* **4**, e1214771 (2017).
180. Winkler, I. G. *et al.* Vascular Niche E-Selectin Protects Acute Myeloid Leukaemia Stem Cells from Chemotherapy. *Blood* **124**, (2014).
181. Esposito, M. *et al.* Bone vascular niche E-selectin induces mesenchymal-epithelial transition and Wnt activation in cancer cells to promote bone metastasis. *Nat. Cell Biol.* **21**, 627–639 (2019).
182. Hehlmann, R., Hochhaus, A., Baccarani, M. & European LeukemiaNet. Chronic myeloid leukaemia. *Lancet (London, England)* **370**, 342–50 (2007).
183. Soverini, S. *et al.* BCR-ABL kinase domain mutation analysis in chronic myeloid leukemia patients treated with tyrosine kinase inhibitors: recommendations from an expert panel on behalf of European LeukemiaNet. *Blood* **118**, 1208–1215 (2011).
184. Kumar, A., Bhattacharyya, J. & Jaganathan, B. G. Adhesion to stromal cells mediates imatinib resistance in chronic myeloid leukemia through ERK and BMP signaling pathways. *Sci. Rep.* **7**, 9535 (2017).
185. Puissant, A. *et al.* Imatinib triggers mesenchymal-like conversion of CML cells associated with increased aggressiveness. *J. Mol. Cell Biol.* **4**, 207–20 (2012).
186. Tamai, M. *et al.* T315I mutation of BCR-ABL1 into human Philadelphia chromosome-positive leukemia cell lines by homologous recombination using the CRISPR/Cas9 system. *Sci. Rep.* **8**, 9966 (2018).
187. Muz, B. *et al.* Inhibition of E-Selectin (GMI-1271) or E-selectin together with CXCR4 (GMI-1359) re-sensitizes multiple myeloma to therapy. *Blood Cancer J.* **9**, 68 (2019).
188. Cogle, C. R. *et al.* Functional integration of acute myeloid leukemia into the vascular niche. *Leukemia* **28**, 1978–1987 (2014).
189. Corbin, A. S. *et al.* Human chronic myeloid leukemia stem cells are insensitive to imatinib

despite inhibition of BCR-ABL activity. *J. Clin. Invest.* **121**, 396–409 (2011).
190. Tan, T. K., Zhang, C. & Sanda, T. Oncogenic transcriptional program driven by TAL1 in T-cell acute lymphoblastic leukemia. *Int. J. Hematol.* **109**, 5–17 (2019).
191. Sanda, T. *et al.* Core transcriptional regulatory circuit controlled by the TAL1 complex in human T cell acute lymphoblastic leukemia. *Cancer Cell* **22**, 209–21 (2012).
192. Bernard, M. *et al.* Helix-loop-helix (E2-5, HEB, TAL1 and Id1) protein interaction with the TCRalphadelta enhancers. *Int. Immunol.* **10**, 1539–49 (1998).
193. Palii, C. G. *et al.* Differential genomic targeting of the transcription factor TAL1 in alternate haematopoietic lineages. *EMBO J.* **30**, 494–509 (2011).
194. Palomero, T. *et al.* Transcriptional regulatory networks downstream of TAL1/SCL in T-cell acute lymphoblastic leukemia. *Blood* **108**, 986–92 (2006).
195. Zhang, W. *et al.* ETS-1-mediated transcriptional up-regulation of CD44 is required for sphingosine-1-phosphate receptor subtype 3-stimulated chemotaxis. *J. Biol. Chem.* **288**, 32126–37 (2013).
196. Feng, C. *et al.* Regulatory factor X1 is a new tumor suppressive transcription factor that acts via direct downregulation of CD44 in glioblastoma. *Neuro. Oncol.* **16**, 1078–1085 (2014).
197. Hansson, A., Manetopoulos, C., Jönsson, J. I. & Axelson, H. The basic helix-loop-helix transcription factor TAL1/SCL inhibits the expression of the p16INK4A and pTalpha genes. *Biochem. Biophys. Res. Commun.* **312**, 1073–81 (2003).
198. Chen, J. *et al.* Identification of similarities and differences between myeloid and lymphoid acute leukemias using a gene-gene interaction network. *Pathol. - Res. Pract.* **211**, 789–796 (2015).
199. Wang, L., Zuo, X., Xie, K. & Wei, D. The Role of CD44 and Cancer Stem Cells. *Methods Mol. Biol.* **1692**, 31–42 (2018).
200. Ricardo, S. *et al.* Breast cancer stem cell markers CD44, CD24 and ALDH1: expression distribution within intrinsic molecular subtype. *J. Clin. Pathol.* **64**, 937–46 (2011).
201. Roudi, R. *et al.* Clinical significance of putative cancer stem cell marker CD44 in different histological subtypes of lung cancer. *Cancer Biomark.* **14**, 457–67 (2014).
202. Hong, I. *et al.* Expression of the Cancer Stem Cell Markers CD44 and CD133 in Colorectal Cancer: An Immunohistochemical Staining Analysis. *Ann. Coloproctol.* **31**, 84–91 (2015).
203. Li, W. *et al.* Unraveling the roles of CD44/CD24 and ALDH1 as cancer stem cell markers in tumorigenesis and metastasis. *Sci. Rep.* **7**, 13856 (2017).
204. Kim, J. H. *et al.* Activation of the PI3K/mTOR pathway by BCR-ABL contributes to increased production of reactive oxygen species. *Blood* **105**, 1717–23 (2005).
205. Mukherjee, D. & Zhao, J. The Role of chemokine receptor CXCR4 in breast cancer metastasis. *Am. J. Cancer Res.* **3**, 46–57 (2013).
206. Beider, K. *et al.* Combination of imatinib with CXCR4 antagonist BKT140 overcomes the protective effect of stroma and targets CML in vitro and in vivo. *Mol. Cancer Ther.* **13**, 1155–69 (2014).
207. Zhang, W. *et al.* Dual E-Selectin/CXCR4 Antagonist GMI-1359 Exerts Efficient Anti-Leukemia Effects in a FLT3 ITD Mutated Acute Myeloid Leukemia Patient-Derived Xenograft Murine Model. *Blood* **128**, (2016).
208. Jiang, X. *et al.* Properties of CD34+ CML stem/progenitor cells that correlate with different clinical responses to imatinib mesylate. *Blood* **116**, 2112–21 (2010).

Acknowledgments

I express my gratitude and respect to my supervisor Prof. Daniela S. Krause who encouraged me to pursue this project with her expertise, consistent guidance and advices helping me to gain immense experience in the field. I would like extend my acknowledgment to Rahul and Valentina who contributed to critical discussions and suggestions that helped me to shape my PhD thesis.

My sincere thanks to Dr. Jorn Lausen and Stefanie Herkt who contributed scientific input to this project. I would like to acknowledge Djamel Aggoune who provided preliminary experimental data which contributed significantly to my PhD work. Additionally, I would like to thank Kuan Ting Pan and Thomas Oellreich for helping us with the mass spectrometry experiments, Jenna Voutsinas and Vivian Oehler for providing us the human data sets and analysis.

I would like to acknowledge my colleagues and friends: Raquel, Costy, Christina, Nina, Divij, Joscha, Julian and Pablo. I truly enjoyed working with them in a research environment that stimulates help, ideas, humor, care and innovative thinking and ideas. It was great pleasure working with them and I appreciate their support and encouragements.

My thanks to Prof. Marschalek who supervised me and consistently guided during the PhD procedure.

My special thanks to my husband Vikram, for his patience, encouragement and understanding during the course of my work. Last but not the least, my deepest thanks to my parents and family and friends who supported and encouraged me to pursue PhD career.

Parimala Sonika Godavarthy

Date of Birth : 11th June, 1992
Nationality : Indian
Address : Apartment 73, Schifferstrasse 38, 60594, Frankfurt am Main
Mobile Number : 004917684700839
Email Address : sonika1127@gmail.com, godavarthy@gsh.uni-frankfurt.de

Education

January 2016 until Present	PhD Student in Hematology/Oncology Georg Speyer Haus, Frankfurt am Main, Germany
2012 - 2015	Master of Science in Life Sciences (M.Sc) Friedrich Schiller University, Jena, Germany Score: 2.3/5
2009-2012	Bachelor of Science in Biotechnology (B.Sc) Fergusson College, University of Pune, Pune, India Score: 70.86 %
2009	High School Certificate Score: 81.5 %
2007	Secondary School Certificate Score: 86.76%

Research Experience

January 2016 until Present	PhD in Hematology/Oncology **Prof. Dr. Daniela. S. Krause**, Georg-Speyer-Haus Title: "Involvement of vascular bone marrow niche in Chronic Myeloid Leukemia via TAL1 and CD44"
June 2016 until December 2016	Research Internship **Dr. Jörn Lausen**, Georg Speyer Haus Title: "The involvement of PRMT6 in hematopoiesis"
November 2014 until April 2015	Research Assistant University hospital, Jena
October 2013 until November 2014	Master Thesis **Dr. Helen Morrison**, Leibniz Institute on Ageing Title: "Role of tumor suppressor *Nf2* in regulation of Spermatogonial stem cell proliferation by niche dependent manner"

May 2011 until February 2012	Bachelor Thesis **Dr. Vasudevan Seshadri**, National Centre for Cell Sciences, India Title: "Binding activity of PABP individual domains on 5' UTR of insulin regulating glucose metabolism"

Trainings and Awards

- Short industrial training to Serum Institute of India, Pune for development of vaccines (2010)
- Bioinformatics course to learn phylogenetic analysis
- Scholarship awarded by exploratory program funded by Jamshetji Tata Trust (2011)
- Poster presentation in Retreat and annual research oral presentation of Georg Speyer Haus
- Head of Organization committee of inter departmental Fest in University (2011)

Laboratory/Technical Skills

- Advanced live imaging by Intravital Microscope/ 2 Photon microscope
- Expertise in Confocal Imaging
- Molecular Biology and Cell biology /Biochemistry Techniques /Cell Culture: Western Blots, qPCR, Cloning, ChIP, Luciferase assay
- Mouse Bone marrow transduction/Transplantations
- *In vivo* mouse models
- Retrovirus /lentivirus production
- Flow Cytometry and sorting
- Seahorse
- Bioinformatics: Python (Intermediate level)
- ELISA
- Handling of human patient materials
- Isolation of mesenchymal stromal cells (MSC), endothelial cells
- **Softwares/Programs**: Fiji Image analysis, FlowJo, Adobe Illustrator, Prism, MS office

Courses

- IELTS
- FELASA-B certificate- Animal handling experience
- Goethe Institute- A1 and A2 (German)

Languages: English, Hindi, Telugu, Marathi, German

Invited published Reviews

1. Kumar R, **Godavarthy PS**, Krause DS . "The bone marrow microenvironment and disease at a glance". *J Cell Sci. 2018 Feb 22;131(4)*.PMID :29472498

2. Karantanou C, **Godavarthy PS**, Krause DS . "Targeting the bone marrow microenvironment in acute leukemia". *Leukemia Lymphoma. 2018 Feb 12:1-11*.PMID: 29431560

Publications

1. **Godavarthy PS**, Kumar R, Herkt SC, Pereira RS, Hayduk N, Weissenberger ES, Aggoune D, Manavski Y, Lucas T, Pan KT, Voutsinas JM, Wu Q, Müller MC, Saussele S, Oellerich T, Oehler VG, Lausen J, Krause DS. "The vascular bone marrow niche influences outcome in chronic myeloid leukemia via the E-selectin - SCL/TAL1 - CD44 axis". *Haematologica. 2019 Apr 24*. PMID:31018977

2. Hoang VT*, Verma D*, **Godavarthy PS**, Llavona P, Steiner M, Gerlach K, Michels BE, Bohnenberger H, Wachter A, Oellerich T, Müller-Kuller U, Weissenberger E, Voutsinas JM, Oehler VG, Farin HF, Zörnig M, Krause DS. "The transcriptional factor FUBP1 influences disease outcome in murine and human myeloid leukemia". *Leukemia. 2018 Jan 11*. PMID: 30635626

3. Dash BP, Mohr J, Weinert S, Herzog C, **Godavarthy PS**, Zanetti C, Perner F, Braun-Dullaeus R, Hartleben B, Huber TB, Walz G, Naumann M, Ellis S, Vasioukhin V, Kähne T, Krause DS, Heidel FH. "Diverging impact of cell fate determinants Scribble and Llgl1 on adhesion and migration of hematopoietic stem cells" . *J Cancer Res Clin Oncology. 2018. Oct;144(10):1933-1944* PMID: 30083817.

4. Mohr J, Dash BP, Schnoeder TM, Wolleschak D, Herzog C, Tubio Santamaria N, Weinert S**, Godavarthy S**, Zanetti C, Naumann M, Hartleben B, Huber TB, Krause DS, Kähne T, Bullinger L, Heidel FH . "The cell fate determinant Scribble is required for maintenance of hematopoietic stem cell function". *Leukemia. 2018 May;32(5):1211-1221*. PMID: 29467485

5. Divij Verma*, Costanza Zanetti*, **Parimala Sonika Godavarthy***, Rahul Kumar, Barbara Burroni, Michaela Fontenay, Daniela S. Krause. "Bone marrow niche-derived extracellular matrix-degrading enzymes influence the progression of B-cell acute lymphoblastic leukemia" (In revision)

Posters and Oral presentation

1. **Sonika Godavarthy**, Stefanie Herkt, Eva Weissenberger, Djamel Aggoune, Thomas Oellerich, Vivian Oehler, Richard Van Etten, Joern Lausen, Daniela S. Krause. "Involvement of the vascular niche in the regulation of murine chronic myeloid Leukemia".
   Poster presentation at European Society of Hematology (ESH) on Tumour Environment in Hematological Malignancies and its therapeutic targeting, April 2017, Berlin, Germany.

2. **Sonika Godavarthy**, Stefanie Herkt, Eva Weissenberger, Djamel Aggoune, Kuan-Ting Pan, Jenna M. Voutsinas, Qian Wu, Thomas Oellerich, Martin C. Müller, Vivian Oehler, Richard Van Etten, Joern Lausen, Daniela S. Krause. "Involvement of the vascular niche in the regulation of murine Chronic Myeloid Leukemia".
   Teaser oral presentation and poster presentation at International Society for Experimental Hematology (ISEH), August 2017, Frankfurt, Germany.
3. **Parimala Sonika Godavarthy**, Stephanie C. Herkt, Nina Hayduk, Eva S.Weissenberger, Yosif Manavski , Tina Lucas , Kuan-Ting Pan , Jenna M. Voutsinas[5], Qian Wu , Martin C. Müller , Thomas Oellerich , Vivian G. Oehler , Joern Lausen , Daniela S. Krause. "The vascular bone marrow niche influences outcome in Chronic Myeloid Leukemia" **Poster presentation** at American Society of Hematology (ASH), December 2018, San Diego, USA.

Abstracts

1. **Sonika Godavarthy**, Stefanie Herkt, Eva Weissenberger, Djamel Aggoune, Kuan-Ting Pan, Jenna M. Voutsinas, Qian Wu, Thomas Oellerich, Martin C. Müller, Vivian Oehler, Richard Van Etten, Joern Lausen, Daniela S. Krause. "Involvement of the vascular niche in the regulation of murine chronic myeloid leukaemia".
   Oral presentation at European Society of Hematology (ESH) on Chronic Myeloid Leukemia: Biology and Therapy, September 2017, Portugal.

Professional experience and activities

- Member of Systems-based Therapy of AML Stem Cells (SyTASC) (2016- until now)

- Yearly oral presentation in SyTASC, Dresden committee. "The role of bone marrow microenvironment in relapse of DNMT3a mutated patient samples".